THEORETICAL AND EXPERIMENTAL INVESTIGATION OF A THREE-DIMENSIONAL MAGNETIC-SUSPENSION BALANCE FOR DYNAMIC STABILITY RESEARCH IN WIND TUNNELS

TECHNICAL ANNUAL STATUS REPORT

1 MARCH 1967 TO 1 MARCH 1968

National Aeronautics and Space Administration

Grant No. NGR-47-005-029

Submitted by:

H. M. Parker, R. N. Zapata, G. B. Matthews
Principal Investigators

Prepared with the Cooperation of:

F. E. Moss, Senior Staff

R. A. Smoak, Senior Staff

I. D. Jacobson, Senior Staff

R. E. Russell, Senior Staff

D. S. Wood, Graduate Assistant

Division of Aerospace Engineering and Engineering Physics

RESEARCH LABORATORIES FOR THE ENGINEERING SCIENCES

SCHOOL OF ENGINEERING AND APPLIED SCIENCE

UNIVERSITY OF VIRGINIA

CHARLOTTESVILLE, VIRGINIA

Report No. AST-4030-105-68U

March 1968

Copy No.__

TABLE OF CONTENTS

LIST OF FIGURES

List of Figures (Continued)

SECTION I
INTRODUCTION

The current, rather large Cold Magnetic Wind Tunnel balance project at University of Virginia has grown out of an initially small NASA study grant which began in December 1964. After two short extensions in time without additional funds and one short extension with small additional funds, in January 1967 a new and the present phase of the project began. At that time a large NASA grant (unexpectedly as a supplementary grant to the then current grant and with a formal starting date of 1 September 1966) for a small prototype cold magnetic wind tunnel balance came into being. This fact reflects both the expectation of probable success and the estimate of usefulness, if successful, of the University of Virginia 3-D magnetic balance which the University of Virginia group and the NASA sponsors had acquired at that time. The authors of this report believe that these expectations and estimates have not significantly changed.

The most significant features of magnetic wind tunnel balances, when compared with conventional balances, are 1) the absence of a physical connection to the model under test (the conventional sting) and 2) the wide range and types of interaction between the balance and the model, and consequent influences on the position and/or motion of the model, which can be arranged. Thus one envisions the removal of sting effects from wind tunnel testing and the possibility of investigating in the wind tunnel dynamic aerodynamic effects.

There are two magnetic wind tunnel balance systems currently under rather intensive investigation and development: 1) the MIT/French 5-D system and 2) the University of Virginia 3-D system. The two are so different in the basic principle and mode of operation that one must consider them as complementary rather than competitive. The MIT balance basically supports a rod-like element of magnetic material of reasonable

fineness ratio, holds it at a desired orientation in the tunnel and measures fivecomponents of forces and moments (roll control and rolling moment measurement can be added), and has the ability of commanding simple motions of the model and the ability in principle to measure the additional forces and moments due to the motion (the frequency and accuracy limitations in such dynamic modes have yet, to the authors' knowledge, to be demonstrated). The University of Virginia balance basically supports a sphere of magnetic material, holds the sphere center fixed (in principle) or commands simple translational motions of the sphere center, and (ideally) allows the model complete rotational freedom or imposes simple and adjustable influences on the rotational motion. Of course, neither system imposes an inherent limitation on the kind of non-magnetic model which may be built around the magnetically supported element, provided an adequate position sensing system may be arranged. The MIT system, especially with roll control added, appears to be admirably suited for static measurements (fixed orientation); the University of Virginia system with roll control added could in principle operate in a static lifting configuration with the use of suitable techniques. The MIT system can operate in dynamic modes, corresponding to simple commanded motions, and, in principle, measure the dynamic contributions to the aerodynamic force and moments. The approach to dynamic stability investigations for the University of Virginia system is significantly different. Basically or ideally, the model is allowed complete rotational freedom and translational freedom in certain frequency ranges (or is subjected to adjustable and measureable balance induced restraints in rotation and translation), then the observation of the model motion with the use of the equations of motion allows the determination of the aerodynamic forces and moments, dynamic as well as static components. Thus the University of Virginia system approach to dynamic stability is quite analogous to the gun range and free flight techniques with, one can speculate, improvements on both. An inherent and perhaps

undesirable characteristic of the University of Virginia system corresponds to the difficulty, with fixed model geometry, of reducing the complexity of the model motion. For larger tunnels and models, one can and does envision externally commanded aerodynamic control. An investigator may one day "fly his model" in a wind tunnel equipped with a University of Virginia magnetic balance.

On approaching the problem of scaling a magnetic balance to larger sizes, the same inherent difficulty is encountered by both the MIT and the University of Virginia balance systems. Using conventional water cooled copper coils, the necessity of producing the magnetic fields and gradients from further away results in the joulian losses (I^2R), power, and mass of copper increasing to unacceptable values for the sizes desirable. The obvious alternative corresponds to the use of some combination of superconductor and high purity supercooled normal conductor coils, i.e. cryogenic systems, or the cold magnetic balance. The University of Virginia cold prototype magnetic balance project may be viewed as a first step in the development of a cryogenic magnetic wind tunnel balance of a size suitable for wind tunnel dynamic stability investigations, the size of which from the magnetic balance viewpoint is rather large, i.e. perhaps 4 to 8 feet diameter tunnels.

The objectives of the University of Virginia cold prototype magnetic balance project are:

1. The identification and hopefully the solution, of the engineering and marriage-induced problems encountered in the tunnel, model, cryogenic magnetic balance complex.
2. Demonstrative operation of such a system.
3. The demonstration of the feasibility of significant quantitative dynamic stability investigations with such a system.
4. The accumulation of sufficient experience and knowledge so that the design may be extrapolated to larger sizes with maximum and good confidence.

It should be noted that objective 4) establishes what one may call the philosophy of the project. On the assumption that the other objectives will be met, and all other factors being the same, a choice of alternate methods would be made on the basis of suitability in a larger size balance. Indeed, the philosophy is that a moderate penalty would be accepted to gain scalableness.

Currently the project is approximately at the end of the prototype design stage. The details of the earlier developments are chronicled in the previous proposals and status reports [1-5]. During the present reporting period (1 March 1967 to 1 March 1968) significant modifications in the balance design and operation modes have been made (See Section II). Section III details the essentially frozen present design status of the various components and their construction status. Section IV outlines the plans and prospects for the immediate future. Section V outlines current thoughts on the longer range plans and prospects, including some speculations on perhaps exotic and probably far down the road modifications and techniques. Finally, Section VI details the budgetary considerations.

It is likely to be obvious to the reader that various portions of this report have been written by various different people. That fact is also evidenced by the list of authors on the cover. It is hoped that the sequence and coverage of topics is reasonably smooth and logical, however little or no effort has been devoted to harmonizing the styles of the authors. Hopefully, there is not too much redundancy.

SECTION II

MODIFICATIONS IN BALANCE DESIGN AND OPERATION MODE

During the present reporting period, significant modifications of the balance design and operation modes have occurred. This section presents details of these modifications and the factors and reasoning involved in them. Generally involved were 1) the increase in understanding of specific aspects of the total problem and their influence on the total system as study proceeded, 2) the trading off of specific uncertainties, perhaps coupled with small changes in risk versus reward acceptability, and 3) an increased appreciation of the realistic costs of the various subsystems. It should be made clear that, while the more realistic cost estimates coupled with general budgetary considerations have played an important role in the modifications, the University of Virginia group believes that neither the objectives of the prototype project nor the expectations of accomplishing them have been degraded significantly. To the contrary, it is believed that the modifications have increased the technical expectation of success.

The significant modifications that have occurred in the last year may be grouped as follows: The left member of a pair is the older item, the right member is the new, modified item.

1. Balance
   a. High Purity Al Coils -- Stabilized, Superconductor Coils
   b. Cold (~ 20°K) Helium Gas Refrigerant -- Liquid Helium (~ 4°K) Refrigerant
   c. Symmetrical About Zero Gradient Coil Current Mode -- Uni-directional Gradient Coil Current Mode.
2. Model Mode
   a. 3 Degree of Freedom Model Motion -- Quasi-6 Degree of Freedom Model Motion.

3. Independent

   a. Precision Aerodynamic Data Acquisition System -- Non-precision Aerodynamic Data Acquisition System

Items 1a), 1b), and 1c) are essentially dependent on each other, and this balance group interacts strongly with item 2a). Item 3a) is unrelated to the others.

The balance group of modifications, especially item 1a), essentially occurred because of three reasons, and partially resulted from a trading-off of uncertainties. First, high purity aluminum performance turns out to be not as good and certain as had been expected. Various people had encountered strong performance degrading stress-resistivity effects (NASA-Lewis magnet group was very helpful here), and the effect is difficult to predict for a complicated configuration. Secondly, the accumulating experience of superconductor groups with highly stabilized superconductor magnets in unsteady current modes indicated somewhat better and more certain performance than had been recognized. Thus these two factors indicated less advantage of the aluminum route over the superconductor route than had been assumed. Thirdly, our opinion, and that of other magnet groups, was that the superconductor approach would eventually prove to be the better of the two for a large balance and thus it is better to gain experience with the superconductor system in the prototype. The modification 1b) resulted from the necessity of refrigerating to 4°K for the superconductor system, and significant advantages are the larger conductor to liquid heat transfer rates and the ease of providing large total cooling by reservoiring the liquid helium. Even though a watt of refrigeration at 4°K is several times more costly than a watt at 20°K and even though decreasing the temperature to 4°K from 20°K does not increase the performance of practical purity aluminum, the liquid helium system might have been seriously considered due to the advantage to be gained from the ease of reservoiring liquid helium and the increased maximum heat transfer rates.

The modification 1c) is slightly more involved. The use of Al coils, coupled with 20°K helium gas refrigerant and limited gas heat transfer rates, dictated the symmetrical-about-zero gradient coil current operation for minimum heat production rates. Bi-directional (symmetrical) operation of the gradient coil power supply system increases quite significantly their cost and complexity over uni-directional operation. For stabilized superconductor coils the losses (heat production) are dependent on the current variation (to first order proportional to rate of current change) and within certain ranges are independent of the DC current component. Thus the necessity of bi-directional gradient coil power supply operation disappears. An additional input to the current mode modification is that the model motion mode modification 2a) results in less variable force demand capacity and hence less variable gradient coil current demand capacity.

The model motion mode modification 2a) resulted from a deeper understanding and appreciation of the model motion problem, coupled with balance system "facts of life." Much of the early thinking had been based on the simplifying assumption that the center of the magnetic sphere embedded in the model would be held fixed with only casual thoughts that the translational motion of the sphere in actual practice would be non-zero and that corrections to the analysis and data reduction procedure would be made for it. After all, the translational equations of motion are simple, the balance system to operate must use readily available sphere position information, and the balance forces exerted on the sphere are easily and accurately outputted! Careful consideration of model size, configuration, and characteristics (in the process of choosing a group of specific first trial models) and estimates of approximate model motions to be expected and desirable led to a rather important conclusion. To hold the sphere center fixed to within a negligible fraction of the sphere diameter (for a reasonable range of model configurations, oscillation frequencies, etc.) would require a

balance frequency response and force capacity which seemed entirely unrealistic. Rough, initial power supply system cost and complexity estimates, based on these rather unrealistic frequency and force capacity requirements, confirmed the non-feasibility of scaling such a system to an eight foot tunnel.

Once it is accepted, for a model in an interesting and desirable oscillatory rotational mode of motion (especially a high lift configuration model), that it is not practical to hold the sphere position fixed, even in the engineering sense, then it is a small step to consider the possibilities when minimal restraints are placed on the sphere position. Accepting the fact that appreciable translational motion will occur, and hence must be taken into account in the information reduction, there seems to be no really significant difference between a given translational amplitude and an amplitude twice or four times as large, provided only that the model is still retained in the tunnel. Thus the original and simplified notion of a purely rotational, 3-D model motion mode was replaced with the concept of the quasi-6 degree of freedom mode. The word quasi is used to indicate that it is only the high frequency oscillation translation modes that are free and that the low frequency and DC translational modes are restrained by the balance in order to retain the model in the tunnel.

As best as can be presently foreseen there is one nearly certain and two fairly probable disadvantages of the Quasi-6 mode as compared to the idealistic 3-D model mode. The advantages are rampant!

1. Disadvantages

    a. The problem of aerodynamic data acquisition (model linear and angular displacements, velocities, and accelerations) by methods so far studied, and presumably any method, is rendered somewhat more difficult (less precision, all else the same) as the translational motion increases. Though

this effect is nearly certain, firm estimates of its magnitude (dependent on the method) are not yet available.

b. In the general problem of extracting aerodynamic information, it may be a disadvantage not to be able to exert high-frequency large forces on the sphere. One could imagine that a forced translation at frequencies around a natural aerodynamic frequency could create a more favorable information extraction situation. [It may be noted that an effort to retain some (small) force capacity at higher frequencies is being made. This corresponds to a small amplitude, linear mode of the control system, as distinct from the minimum time (bang-bang) large amplitude mode.]

c. It is possible, even fairly probable, that the precision with which certain kinds of stability information can be extracted will be reduced as the translational motion increases. No example of this can be cited at present.

2. Advantages

a. It is possible, even likely, that the precision with which certain other kinds of stability information can be extracted will be enhanced as the translational motion increases. For example, the classic problem of separating C_{m_q} and $C_{m_{\dot{\alpha}}}$ is almost certainly aided, though perhaps to still poor accuracy, by increased translation.

b. The Quasi-6 mode certainly seems to be the closest approach to free flight obtainable in a ground-fixed installation, since the restraints are the minimum required to retain the model in the tunnel. Thus the "fly the model" qualitative approach to stability is enhanced. As another example, it seems clear that a more realistic simulation of the roll-pitch resonance phenomenon for missile configurations

(including the non-linear aspects) could be achieved.

c. The ability to introduce a disturbance on the model is retained. The range of input disturbances possible is reduced, primarily due to the reduced balance frequency response, but is likely to be adequate for most cases.

d. As compared to the idealized 3-D mode, the Quasi-6 mode results in drastically reduced requirements on balance frequency response and gradient coil force capacity. The latter is reflected immediately in reduced balance size, weight, power, and cost.

e. The gradient coil power supply systems cost and complexity are drastically reduced.

f. It would appear that the Quasi-6 mode both enhances the probability that the superconductor coil system will perform satisfactorily and will reduce the AC losses (hence the He boil-off rate and total boil-off for a run). In short, the Quasi-6 mode should give the superconductor approach a better chance.

To summarize the 3-D to Quasi-6 mode modification, it appears that the Quasi-6 mode is, in the first place, equivalent to accepting a realistic view of the total problem, and that the probability of achieving the objectives of the project has increased, perhaps significantly.

The last modification listed above, 3a), corresponds in the large view to deferring to a later time the time and effort involved in incorporating a really precise aerodynamic data acquisition sub system into the total system. The dominant justification is that it seems highly likely that a reasonably optimum method for, say, an 8' tunnel system would be quite different from the method for the 6" prototype, and thus the objective of ~~scalableness~~ scalableness is not aided. It should be noted that one

may expect that, when the prototype phase is concluded, the 6" system will remain as a basic research tool (hopefully) at the University of Virginia. At that time the addition of a reasonably optimum data acquisition sub system to the complex is to be expected. For the prototype phase a fairly crude, but still quantitative, data acquisition system is contemplated. An incidental advantage of this order of priorities is that the eventual design of the precision data system can be based on the accumulated experience with the cold balance system.

SECTION III

PRESENT DESIGN AND CONSTRUCTION STATUS

A. GENERAL DESCRIPTION OF THE COMPLETE SYSTEM

From the arguments advanced in section 2 is should be clear that the design and construction of the cold balance system represents a much more difficult technological task than was anticipated at the time the original proposal was written. The correspondingly higher demands of time, manpower and hardware expenditures make it imperative that the essential objectives of the project be always kept as a point of reference. In terms of functions to be performed by the cold balance these objectives can be stated as follows. First, it must permit satisfactory evaluation of the three-degree-of-freedom electromagnetic suspension as a method for dynamic stability studies. Second, it must permit adequate testing of those design parameters that are critical for extrapolation to a large scale test facility. This establishes priorities among design criteria, such that the working prototype function rather than the true research facility function is emphasized. To meet the first objective, an aerodynamic facility (wind tunnel) and a three-degrees-of-freedom electromagnetic suspension (balance) are needed. The wind tunnel must be capable of producing steady state flow of known description for a length of time sufficient to effect controlled magnetic support of the model and acquisition of minimum dynamic stability data. The balance must be capable of balancing and measuring the aerodynamic forces within reasonable limits of magnet size and power dissipation. Since the coils will operate at very low temperatures, a suitable cryogenic container is an essential part of the system.

The second objective represents a two-way restriction in the choice of actual solutions to individual problems. On the one hand, whenever technically and economically feasible, a more sophisticated approach than strictly necessary for the pilot facility has been adopted if it

represents the most likely solution for a large scale facility. On the other hand, the overall design reflects an attempt to de-emphasize problems that are peculiar to a small balance, but are not likely to arise in connection with a large balance.

Figure 1 shows a complete schematic of the prototype facility. Details of the different components are given in the following sections. Here, a brief discussion of the overall operating procedure is given by way of introduction.

Before the tunnel is started (by actuating the regulating valve R), the model is supported mechanically by a special mechanism contained in the sting B. After the appropriate filling procedure is completed, both liquid nitrogen and liquid helium containers of the dewar C are at optimum levels. At this time the main field coil is energized. Subsequently the drag augumentation coil pair is energized and, at the same time, the flow through the tunnel is started. After the initial transients have subsided the model is ready for transfer from mechanical to magnetic support. When this is done, the gradient coils must be activated, together with the automatic control circuit. The latter is fed information on model position by the set of pick-up coils D. As soon as the model becomes stably supported the sting is retracted as far downstream as necessary to avoid interference with the aerodynamic test. Direct optical access to the model is provided by matching windows in the tunnel wall and the cylinder supporting the pick-up coils. One pair of mirrors V attached to this cylinder is shown in Figure 2. The optical ports will be used for both visual observation and data acquisition.

B. THE AERODYNAMIC FACILITY

In principle, there is a great deal of freedom in the choice of flow simulation parameters for a suitable dynamic stability experiment. Both subsonic and supersonic flow regimes appear interesting from the point of

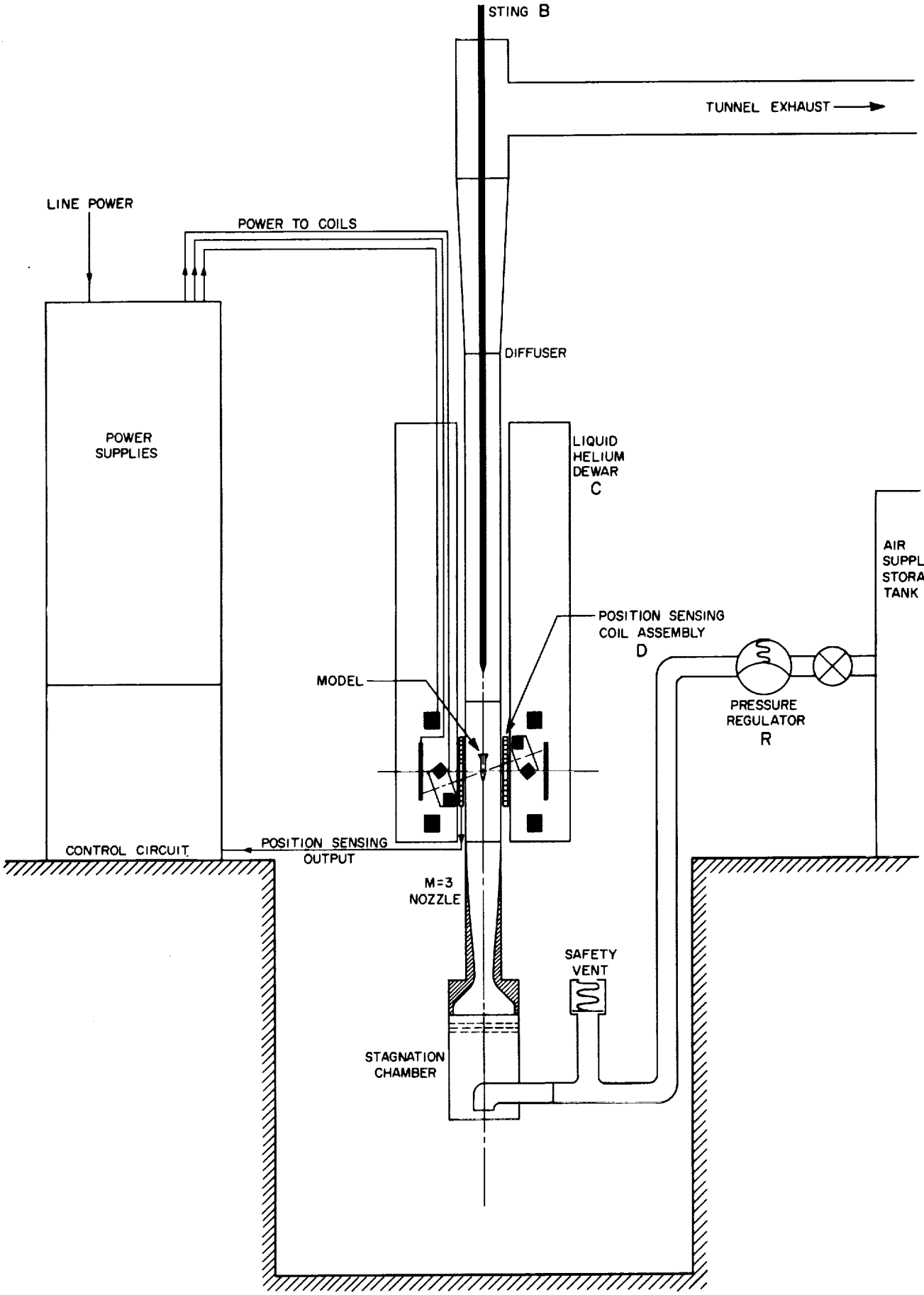

FIGURE 1
COMPLETE SCHEMATIC OF PROTOTYPE FACILITY

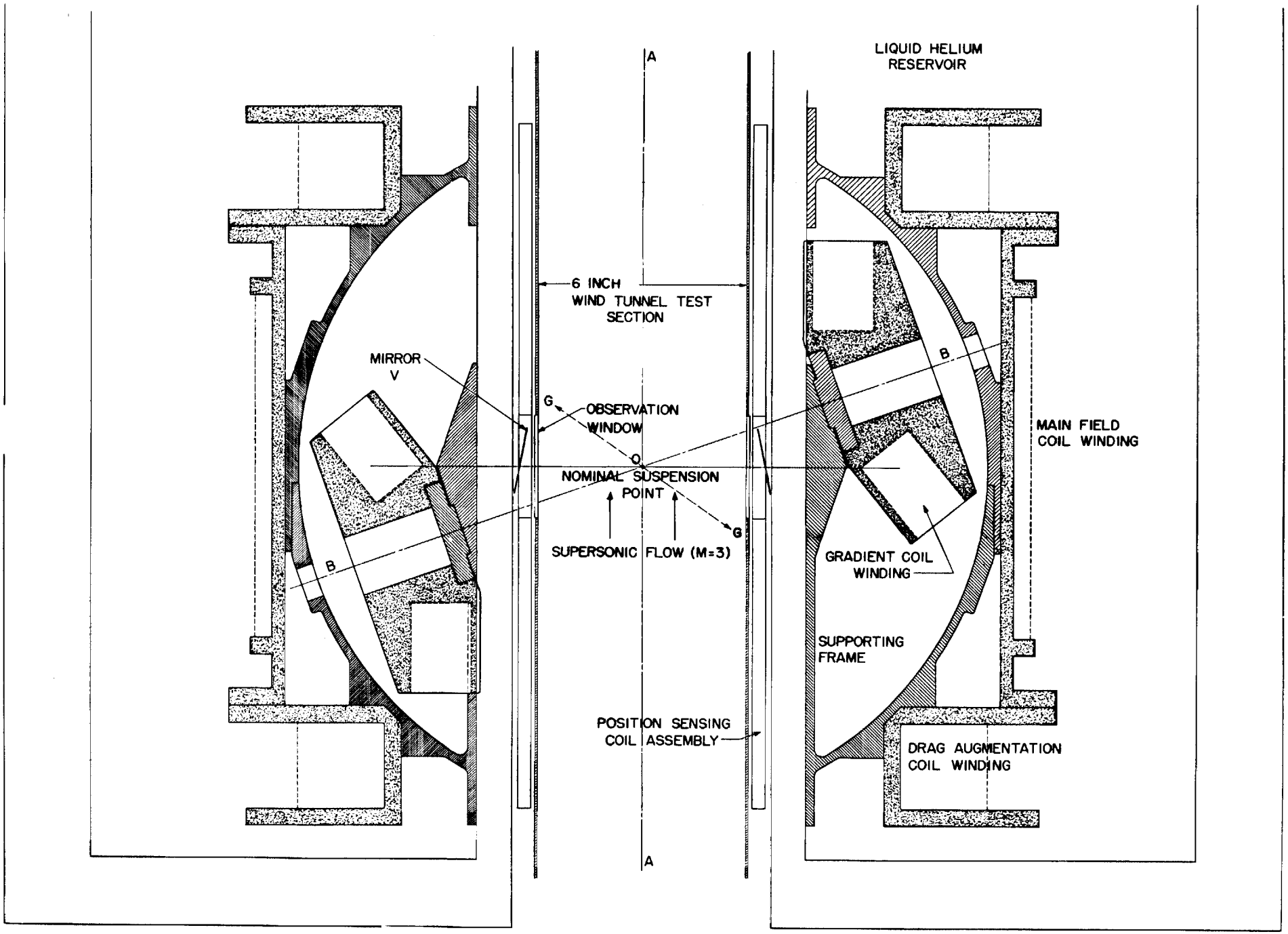

FIGURE 2

COIL SYSTEM AND MOUNTING

view of comparison of results obtained with the electromagnetic balance method to results obtained with more conventional methods. In practice, what is considered an optimum size for the test section of this pilot facility (6 inches diameter) dictates a choice of supersonic flow simulation if reasonably well defined aerodynamic tests are desirable. Reynolds number does not appear at this point as a critical parameter. It will be kept as low as is compatible with the scheme of a blowdown tunnel discharging to atmospheric pressure for two reasons. First, for a given Mach number, a lower stagnation pressure results in lower aerodynamic forces and moments, a desirable feature from the point of view of the electromagnetic balance. Second, a lower Reynolds number represents lower mass flow rate, a most critical feature because of the very limited capacity of the available compressed air supply (1000 ft^3 at 275 psia. storage capacity). It is interesting to compare the variation in the representative design parameters as the Mach number is changed. This is done in Table I, where a test section diameter of 6 inches, a stagnation temperature of 530°R, and normal shock recovery to atmospheric pressure are assumed throughout.

TABLE I

M	A^* in^2	D^* in	PT2/PT1	P_o psia	$\dot{m}$ lb/sec	$(\tau)_{net}$ sec	$(Re_\infty/in) \times 10^{-6}$	q_∞ psia
2	16.75	4.62	.7209	20.4	7.85	136	.46	7.30
3	6.68	2.92	.3283	44.8	6.87	131	.61	7.68
4	2.63	1.83	.1388	106.0	6.37	109	.88	7.82

It is felt that M = 3 represents the best choice. It is commonly agreed among aerodynamicists that low Mach number axisymetric nozzles do not work well. At the same time, at M > 3 water condensation in the expanding air becomes a problem unless a drying procedure more refined than presently available in this laboratory is used. Unquestionably, the most serious limitation that can be anticipated is the short running time. However, this limitation can be automatically removed as soon as a larger storage capacity can be procured for the system. Since the emphasis at present is on showing feasibility of the cold balance concept rather than on extensive research capability, this limitation on run-time appears quite tolerable.

The M = 3 nozzle has been designed using a computer program provided by the gas dynamics group at Langley. A total of 100 points define the supersonic contour between throat and nozzle exit. At this writing detailed drawings of the nozzle and the stagnation chamber are being prepared in order to have these fabricated shortly.

As shown in Figure 1 the whole tunnel test section and part of the diffuser are inside the special dewar containing the coils and cryogenic ~~coolants~~ coolants. This imposes severe constraints in the design of the wind tunnel. Some of the special features required are: 1) Non-metallic construction, in order to avoid eddy currents that might interfere with the operation of the coils; 2) Test section and diffuser must be capable of assembly and disassembly through top and bottom of dewar center opening; 3) There must be sufficient clearance between tunnel and dewar for the detection and data acquisition systems to be accommodated without touching either; 4) Access to the model before and after the tests, including launching and recapturing capabilities, must be effected through the top of the facility, a fair distance away from the model.

The problem of launching and recapturing the model is not a trivial one. This is particularly true in this case because of the rather low

upper limit of tests duration. On the other hand, this problem is not basically different in this facility from that in other facilities where it has been successfully solved. Therefore, though little effort has been directed so far to a detailed design of this important component, it is not anticipated that major difficulties will be encountered when the task is undertaken.

C. THE COIL SYSTEM

As explained in Section II, it was decided to go to an all-superconducting coil system. In the case of the steady state operating coils (main field coil and drag augumentation pair) this choice will result in a definite power and liquid helium saving. As for the gradient coils, the copper of the fully stabilized superconductor compares favorably with the best commercially available aluminum that could be used to wind supercooled magnets. In addition, there is reason to believe that these coils will operate in the superconducting mode at least part of the time, thus effecting a significant saving of liquid helium. Finally, it is felt quite strongly that the large scale system will have to be all-superconducting and, consequently, the operational experience with a similar prototype should prove valuable.

The coils are presently being fabricated by Atomics International according to a final design mutually agreed upon. A scale drawing of the coils and their mounting frame is shown in Figure 2. Fully stabilized superconducting TiNb wire has been specified for all coils in the system. The turns will be wound on reinforced epoxy forms. Connecting posts for lead hook-up will be provided at each coil. A summary of the most important characteristics of the coils is given as Table II. The main field coil is designed to provide a uniform magnetic field at point O, of sufficient magnitude to saturate a ferrite sphere placed there. This coil will operate strictly in a d.c. mode and, consequently, the simplest type of power supply is needed to energize it, the only

requirement being an adequate output impedance so that a constant current can be maintained. Charging time can be of the order of several seconds.

TABLE II

	Gradient	Drag Augmentation	Main Field
Number of turns	192	3000	2500
Maximum current	350 A.	100 A.	100 A.
Maximum voltage	700 V.	---	---
Type of wire	0.135"-7 wire cable	0.030" copper clad TiNb	0.030" copper clad TiNb
Type of operation	unsteady	steady state (d.c.)	steady state (d.c.)
Average current density	2100 A/cm^2	8000 A/cm^2	8000 A/cm^2
Inductance	0.008 henries	3.0 henries	5.1 henries
Central field	---	9×10^3 Gauss	5×10^3 Gauss
Maximum field gradient at 0	45 Gauss/cm	210 Gauss/cm	0

The drag augmentation coil pair is designed to provide a pure gradient of up to 420 Gauss per centimeter at point 0. If a 1-inch diameter ferrite (Magnetic Moment 600 Gauss at saturation) is used as the aerodynamic model magnetic core, the coils are capable of exerting a force of 4.85 pounds on it, along the symmetry or drag axis of the tunnel. This force is sufficient to counter the expected steady state drag force on any model scheduled to be tested in this facility. In terms of drag-over-weight ratio for a spherical core, the figures are 50 for saturated ferrite and

65 for non-saturated iron, independent of diameter. As can be observed in Figure 2, the drag augumentation coils are bolted to the flanges of the main field coil so that, upon assembly, the three form a rigid unit, able to withstand all internal forces. This unit is in turn bolted to the spherical shell that supports the gradient coils.

There are three pairs of gradient coils, one of which is shown in Figure 2. The axes of the other two pairs lie on planes found by rotating the plane of the figure 120° about the symmetry axis of the wind tunnel. Each pair will be connected in series opposition so as to produce a pure gradient along the BB axis at 0. This axis subtends an angle $\tan^{-1}\sqrt{8}$ with symmetry axis AA. If the magnetic moment vector of the spherical core lies on AA, the force exerted by a gradient coil pair acts along GG, at an angle $\tan^{-1}\sqrt{2}$ from AA in the plane determined by the intersection of AA and BB. At maximum current (350 A) each coil pair produces a magnetic field gradient (at 0) of 90 Gauss per centimeter which would result in a force of 0.6 pounds on a 1-inch diameter ferrite sphere magnetized to saturation by the main field coil. This represents a capability of 6.35 force-to-weight ratio for each of the three mutually perpendicular lateral force axes. Under normal operating conditions it is planned to operate the gradient coils at a reference current level of 175 A(mid-range). This d.c. level will contribute a total magnetic field gradient of 78 Gauss/cm at 0 in the same direction as the gradient produced by the drag augumentation coil pair. As a result, the effective lateral force range of each gradient coil pair is designed to be ± 3.2 sphere (ferrite) weights.

D. CRYOGENIC SYSTEM

1. Requirements

The requirements for the cryogenic system are simply stated as follows:

a. It must provide a 4.2°K temperature environment required by the superconducting magnetic balance assembly.

b. There must be sufficient refrigerant capacity to maintain the temperature environment for a time equal to or greater than the blow-down time for the windtunnel under conditions of maximum possible power dissipation in the magnet assembly and power input leads.

c. The physical dimensions of the cryostat must allow convenient accommodation of the magnet assembly, input leads and radiation shields, while providing for complete room temperature access along the axis of the cryostat. Sufficient space along the access must be provided for accommodation of the position sensors and other instrumentation.

d. The cryogenic system must not interfere with the operation of the magnet or position sensing systems.

In addition, the design should be geared toward refrigerant economy and ease of access to the magnet system.

These requirements reflect two decisions made early in the program after review and discussion. First it was decided to include the possibility of more efficient superconducting magnets. Though the present technology with respect to a.c. operation of high field superconducting magnets is not yet advanced enough to project the operating power dissipation, it became apparent that the small additional cost of fabricating the magnets was justified in view of the possibly large savings in terms of power dissipation. This decision required the cryogenic system to provide a 4.2°K environment. Second, it was decided to design for "one-shot" liquid refrigerant operation, rather than operate with a continuous closed cycle refrigerator. This decision was made primarily for economic

reasons,* however, one-shot operation has the additional advantage of simplicity. The refrigerant, thus, would be liquid helium. One-shot operation implies that the cryostat can contain enough liquid to last the duration of one blow-down run on the windtunnel under conditions of maximum power dissipation in all magnets, most likely encountered only under the most violent aerodynamic conditions. Further, to the extent that the superconducting magnets perform with low effective resistance at the frequencies involved, the dissipation will be reduced. Thus, it may be possible to perform many wind-tunnel runs on "one-shot" of liquid helium. These statements can only be speculative at present, since experience with the system is necessary to understand the question of dissipation and hence liquid helium consumption rate.

2. Cryostat Design

The design of the liquid helium dewar is dictated by the above requirements and considerations. All the requirements can be met and the design has been fixed except for requirement d). The problem here pertains to metal dewars only, and the difficulty is that eddy currents induced in the walls of the dewar by the a.c. magnet fields cause attenutation and phase lag of the field at the model location. For this reason, the possibility of building or contracting to have built, a plastic or fiberglass-epoxy dewar system was investigated. Because the technology was not well advanced, though successful fiberglass-epoxy cryostats have been constructed, it was decided to build a simplified model, superinsulated dewar. Hopefully, sufficient construction experience would be gained to decide the feasibility and project the cost of a final plastic dewar system. For reasons which are outlined in paragraph 4) below, this group became somewhat disenchanted with the

*The installation, at the University, of a helium liquifaction and gas recovery system to be operational in April or May 1968 had a major influence on this decision.

plastic dewar and superinsulation system. Therefore, an alternate stainless ~~steel~~ steel dewar design was made which meets the requirements outlined above.

A simplified drawing of the dewar is shown in Figure 3. A detailed drawing of this dewar has been sent to four cryogenic companies for consideration, with the result that two have expressed no interest and two (Gardner Cryogenics and Cryenco) have notified that they would bid.

3. The Eddy Current Problem

As outlined above, the only remaining problem with the stainless steel dewar design is to determine the effect of induced currents in the dewar walls on the magnetic fields at the model position. A preliminary estimate of this effect has been made, based on a very simple physical model, which serves to establish an upper limit on the field attenuation as well as illustrate the physical principles involved.

A plane, conducting sheet of resistivity, ρ, and thickness, t, is placed in a uniform, oscillating magnetic field $B_o \cos\omega t$. The field is assumed confined to a cylindrical shape of radius, R. The geometry is shown in Figure 4. The incident field is assumed to penetrate the conducting sheet unattenuated. The returning lines of force, which penetrate the sheet in the opposite direction at radii greater than R, in order to enclose the source of B_o are neglected. Because of these two assumptions, the result will be an upper limit. The problem is to calculate the induced current density, $J(r)$, on curve C, and the resulting induced field, B_i, at $r = 0$. The electric field due to a time varying magnetic field is given by

$$\oint_C \vec{E} \cdot d\vec{\ell} = - \int \frac{\partial \vec{B}}{\partial \tau} \cdot \vec{n} ds = V_e(r)$$

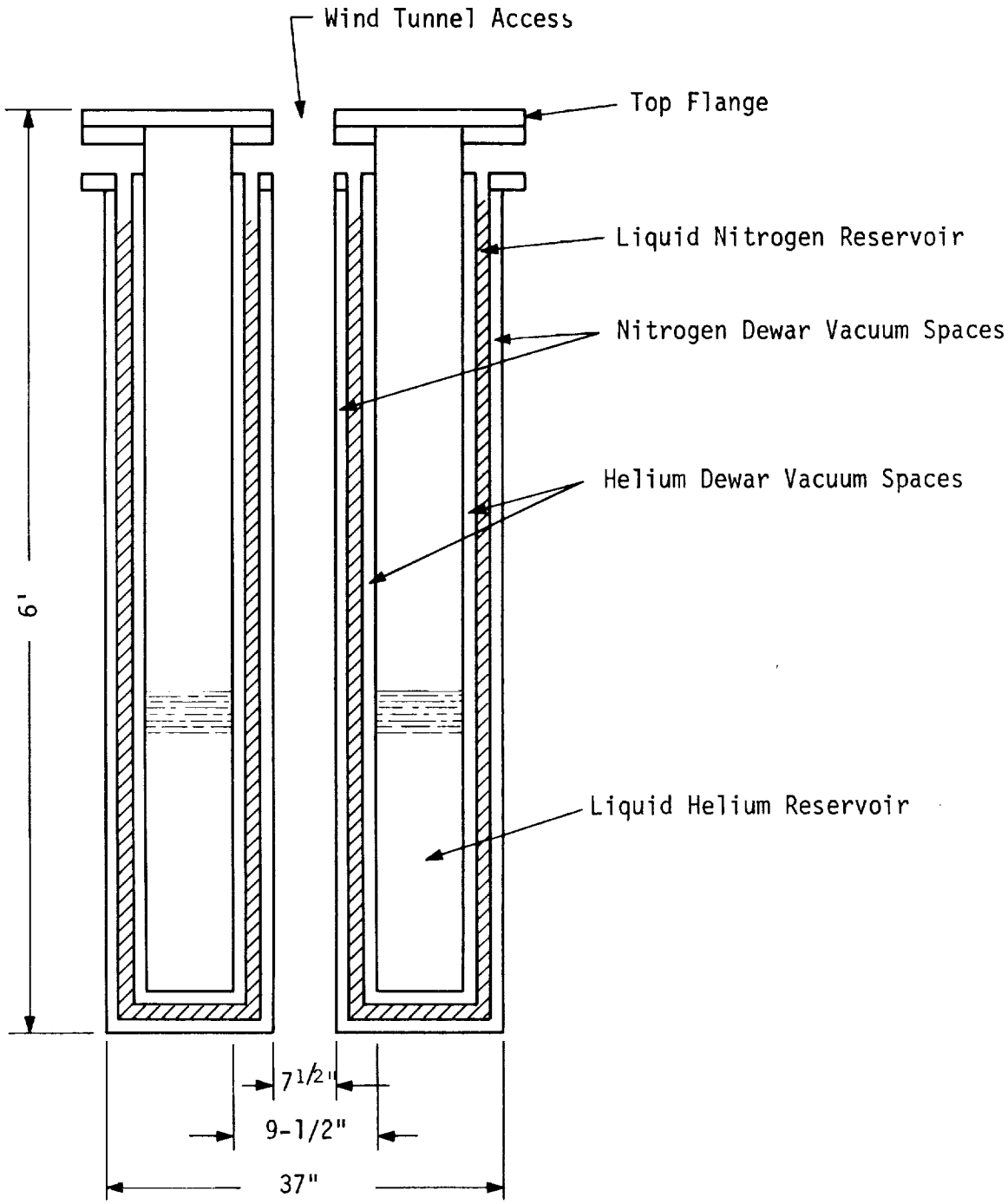

FIGURE 3
LIQUID HELIUM DEWAR

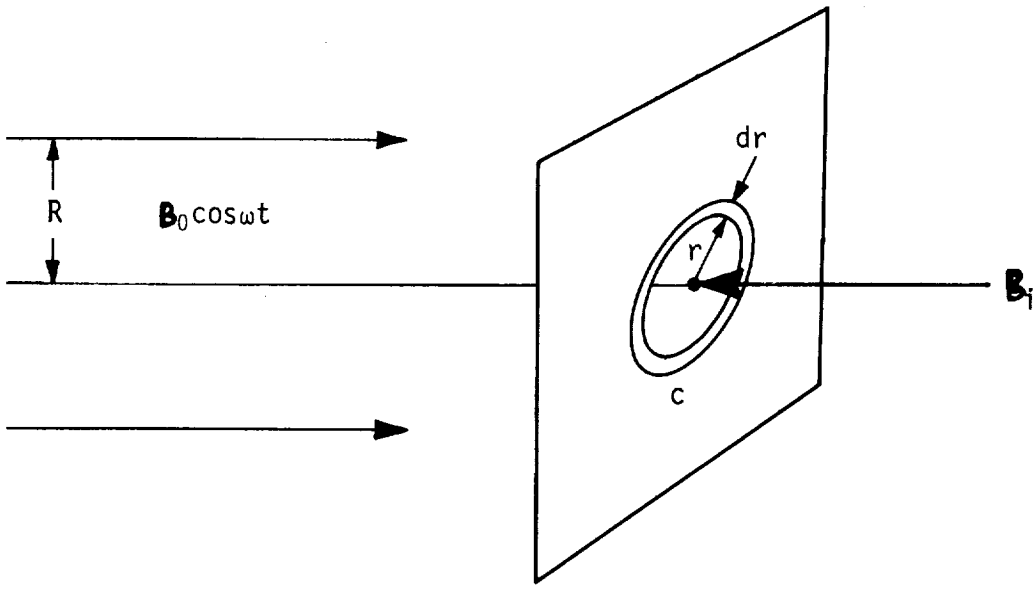

FIGURE 4
GEOMETRY FOR EDDY CURRENT PROBLEM

where $\bar{E}$ is the electric field, $\bar{B}$ is the magnetic flux density, $d\ell$ is an element of length along C, $\hat{n}$ is a unit vector normal to the surface containing C, and ds is a surface element. $V_e(r)$ is the voltage around C. For plane geometry, the induced current density is

$$J(r) = \frac{V_e(r)}{2\pi r\rho} = \frac{\omega B_o r}{2\rho} \cdot \sin\omega t$$

The induced flux density at $r = 0$ due to this current is given by

$$B_i = \frac{\mu}{4\pi} \int \frac{\vec{J}\times\hat{r}}{r^2}\, dv$$

where μ is the permeability, $\hat{r}$ is a unit vector directed from the current element toward the point of observation (in this case the point $r = 0$ on the plane), and dv is a volume element occupied by current.

$$B_i = \frac{\mu t B_o R}{4\rho}\ \omega \sin\omega t$$

The net field at the origin ($r = 0$) is then

$$B_{out} = B_o - B_i = B_o\left[1 + \left(\frac{\pi t R\omega}{4}\right)^2\right]^{1/2} \cos(\omega t - \sigma)$$

where

$$\sigma = \tan^{-1} \frac{\mu t R\omega}{4\rho}$$

Using a radius $R = 25$ cm (approximate radius of a gradient coil), and $\rho = 8 \times 10^{-5}$ Ω-cm as the resistivity for stainless steel

$$\frac{\mu t R\omega}{4\rho} = 0.62 \times 10^{-3}\ ft$$

where f is the frequency and t is the thickness in mm. A commonly used

wall thickness in stainless steel dewar construction is 0.03 inches or 0.762 mm. Thus for four walls of this thickness (t = 3 mm) $\mu t R\omega/4\rho$ = 1($\sigma = 45°$) at a frequency of about 540 cycles/sec. While this is much higher than the frequencies typical of the control system, it does represent an additional pole in the control loop and may have to be compensated.

A more exact treatment of this problem is given by Smythe [6] where a thin circular cylinder of infinite length and radius, a, is placed in a field $B_o \cos\omega t$ normal to its axis. The field inside the cylinder is

$$\frac{3B_o\rho}{t} = \left[9\left(\frac{\rho}{t}\right)^2 + (\mu a\omega)^2\right]^{-1/2} \cos(\omega t - \sigma)$$

where

$$\sigma = \tan^{-1} \frac{\mu t \omega a}{3\rho}$$

Substituting the same numbers as before with a = 3 inches (7.62 cm) we see that $\mu t\omega a/3\rho \cong 1$ for f = 1300 cycles/sec which is somewhat more gratifying than the previous result.

In view of the fact that these frequencies are not comfortably large compared to the control system frequencies, a small experiment to measure the attenuation and phase lag was set up. A diagram is shown in Figure 5. The generating magnet is a model gradient coil which was already built for another purpose, and the power amplifier has already been acquired for use in the position sensing system. The results of this experiment, as shown in Figure 6, indicate that a pole may be conservatively assigned at one kilocycle for the four sheet experiment. Very little interference with the control system will result. On the bases of the above calculations and this experiment, it was decided to

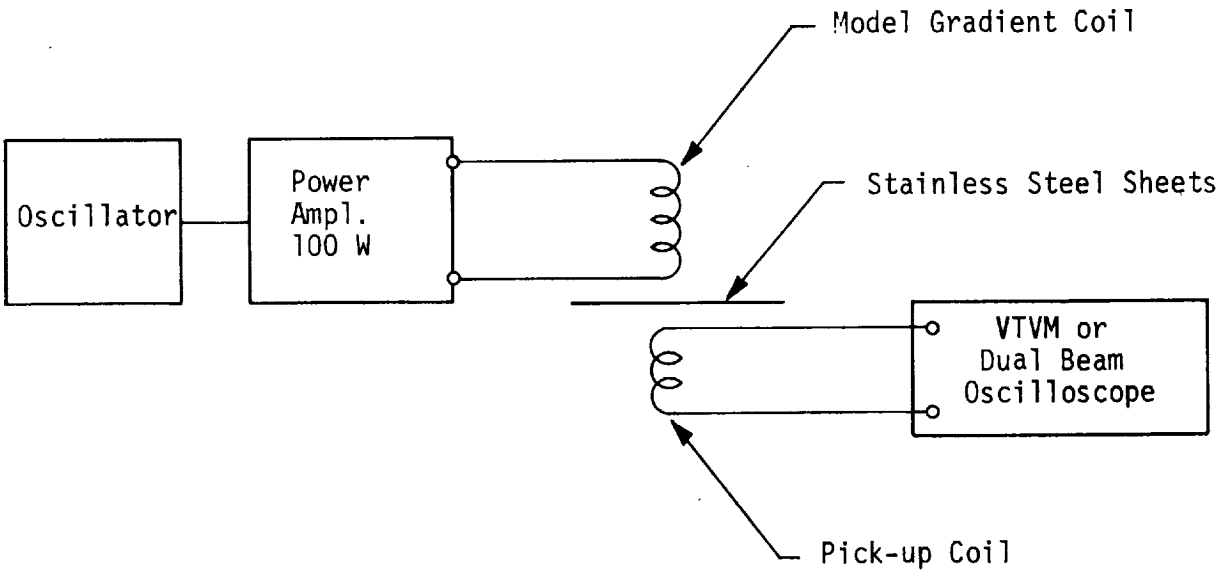

FIGURE 5

APPARATUS TO CHECK THE EDDY CURRENT EFFECT

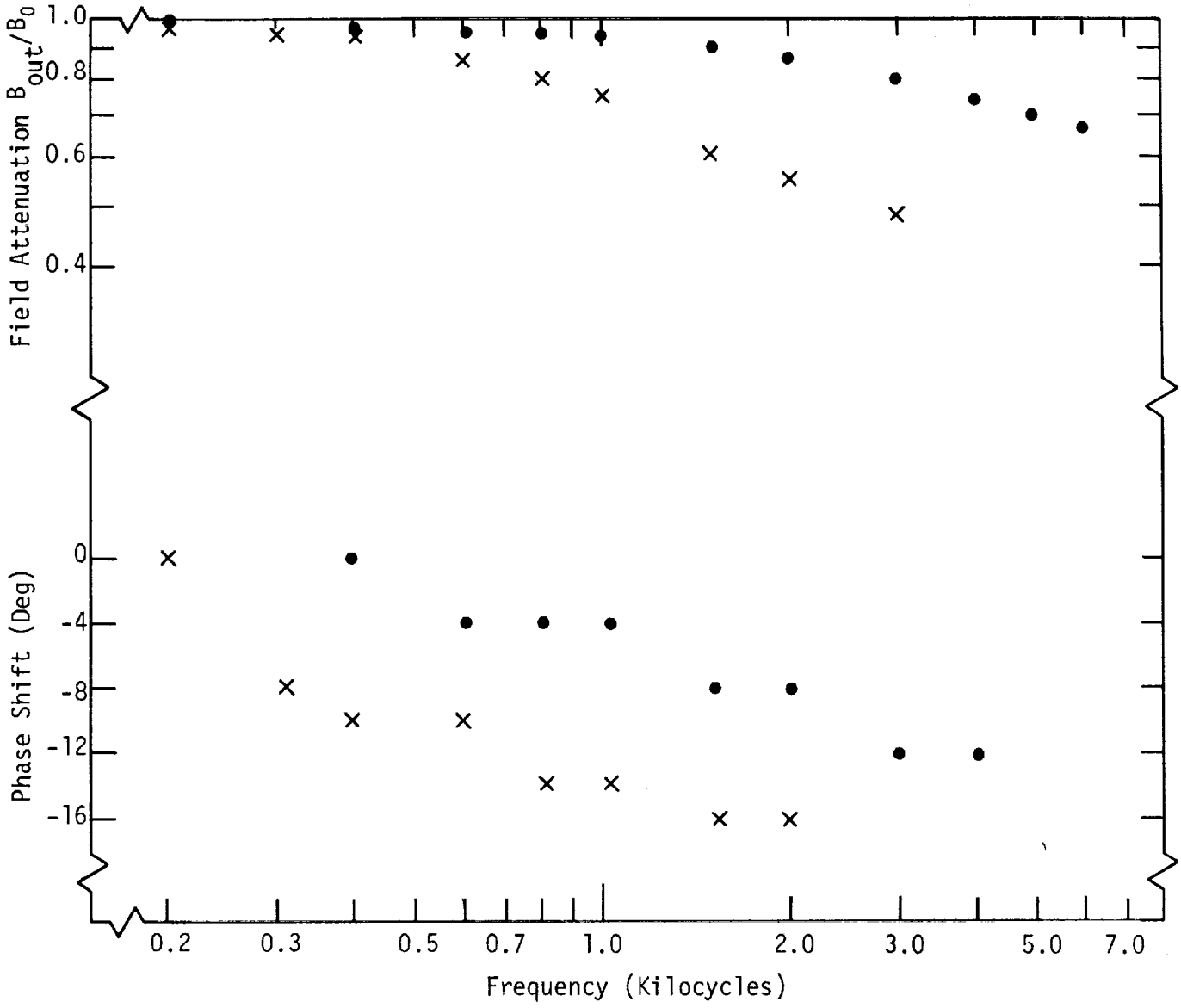

FIGURE 6

FIELD ATTENUATION AND PHASE LAG VERSUS FREQUENCY FOR (·) ONE SHEET 0.03" STAINLESS STEEL AND (x) FOUR SHEETS 0.03" STAINLESS STEEL. RESULTS ARE FOR $B_{o_{rms}}$ = 0.3 GAUSS

proceed with the stainless steel dewar design.

4. Epoxy-Fiberglass Dewar System

In anticipation of the eddy current problem, it had been decided to investigate the possibility of fabricating a plastic or epoxy-fiberglass dewar system. A review of the literature indicated that such a design certainly was feasible, and at least one manufacturer (Hoffman)* had sold several plastic dewars including some in large sizes. It was decided to fabricate a large but simply designed, superinsulated dewar with helium reservoir of epoxy-fiberglass. The experience gained from this construction would: a) indicate the feasibility for the cold balance requirements, b) provide a basis for projecting the cost of a final system should it be decided to fabricate it in this laboratory, and c) indicate any special problems which might arise in such construction. In addition, this dewar would provide a convenient test facility for large superconducting magnets. While the system is not yet functioning, to-date experience indicates that the cost of fabrication, with no special care taken for precise dimensional control, would be less, but perhaps not significantly less, than a comparable stainless steel system obtained commercially. The question of dimensional precision has become quite important for the following reason: It is no longer possible to use superinsulation in lieu of a liquid nitrogen reservoir on the inner dewar walls, since the superinsulation is almost certain to interfere with the electromagnetic position sensing system. Therefore the dewar must have four closely spaced (~ 1/4 inch) walls, rather than two required by a superinsulated system, on the inside surrounding the room temperature access. Experience in winding the present fiberglass-epoxy system indicates that the winding mandrels would have to be especially designed to obtain the required dimensional precision while at the same

*They have since ceased to manufacture dewars of any kind. At the present time there is no manufacturer of plastic or fiberglass-epoxy dewar systems.

time allowing for easy release of the cured wall section. Using liquid nitrogen shielding this would require eight such mandrels (there are eight cylindrical walls as shown in Figure 3). This requirement would elevate the cost well beyond the cost of an equivalent stainless steel system. Thus the construction of this test dewar has shown that a stainless steel system is preferable since the eddy current problem has been resolved. If the test dewar can be made operational, it will provide a useful test facility for superconducting magnets.

Construction Details of the Test Dewar

A diagram of this dewar is shown in Figure 7, where the details of construction are clearly shown except for the technique of fabricating the inner wall. The method is that developed by Brechnu, et. al. [7] for fabrication of a liquid hydrogen bubble chamber at Stanford. The wall is constructed of 22 layers of 10 oz. fiberglass tape 6 in. wide. Interspersed within this winding are five layers of duPont type 100-H Kapton plastic film. The matrix is bounded with low viscosity Union Carbide ERL-2256 epoxy with 18% (by weight) MPDA* hardner. The mandrel, upon which this matrix was wound, was rolled to approximate dimensions from sheet steel. While curing, it was necessary to mount the mandrel horizontally in continuous rotation at about 1 rps. Forty-eight hours is the required curing time at room temperature. Continuous rotation was necessary to prevent the epoxy from becoming unevenly distributed during curing. Considerable difficulty was initially encountered in releasing the curing matrix from the mandrel. This is presumably due to not insignificant shrinkage in the curing process.

Testing of this dewar has progressed to the stage of transferring liquid nitrogen into the reservoir. At this point a low temperature leak, which gradually destroyed the vacuum, was detected in the inner

*Meta-phenylenediamine

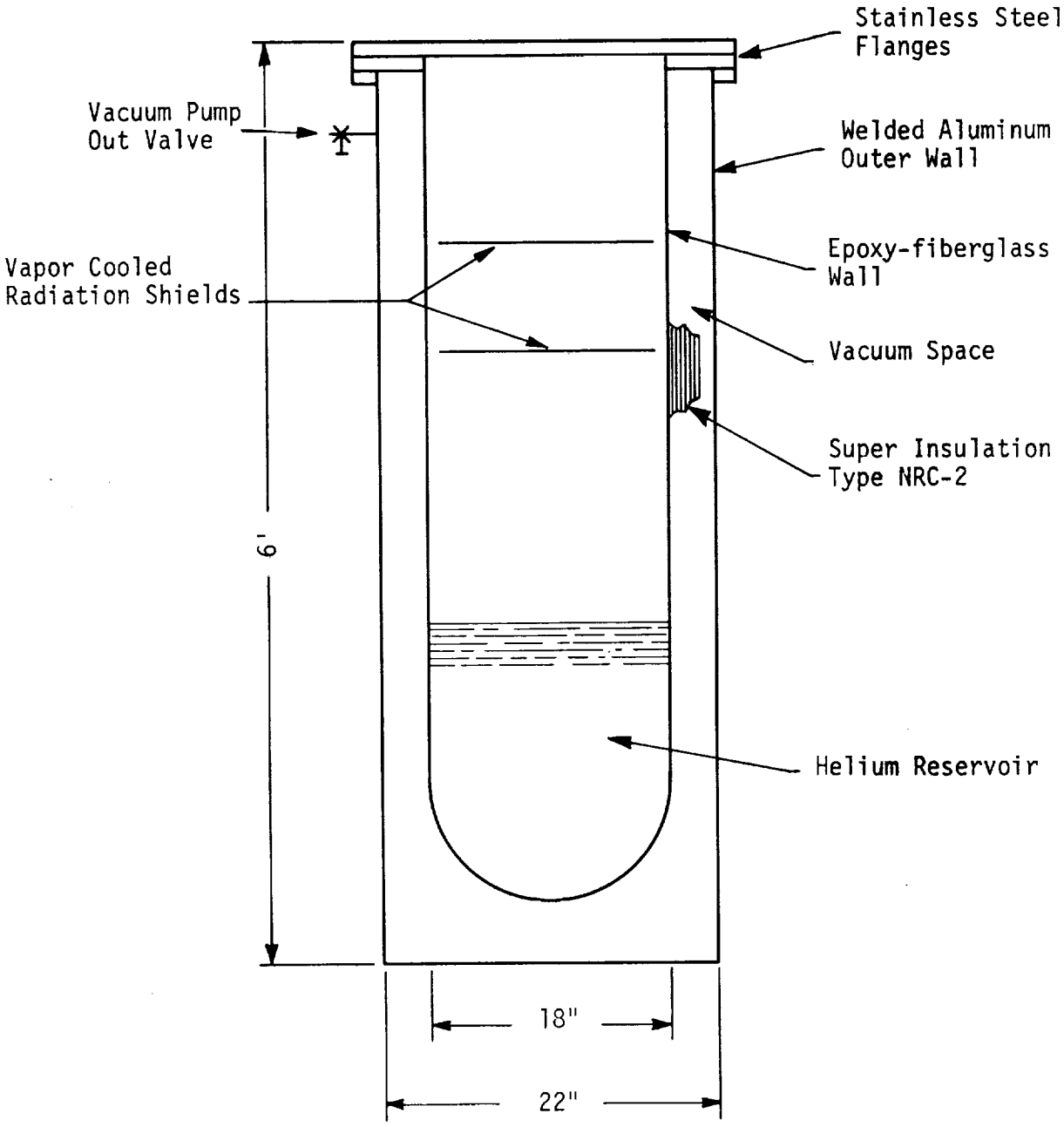

FIGURE 7

EPOXY FIBERGLASS TEST DEWAR

wall near the bottom. At the present time, it is unknown if this leak is actually a flaw in the wall structure (and hence repairable) or is due to nitrogen diffusion through the epoxy-fiberglass matrix. The purpose of the Kapton films embedded in the wall is to prevent this diffusion. It is hoped to answer these questions and attain liquid helium operation within the near future. However, this effort has been assigned a low priority at present.

E. POWER AMPLIFIER

1. Introduction

Three separately controlled power amplifiers are needed to act as current sources to supply the three gradient coil pairs. The proposed control will be a bang-bang system with a small linear mode of current control. Since the coils will have negligible resistance, due to cryogenic cooling, energy supplied to the gradient coils must be retrieved. To do this, the amplifier must have two operating modes: a full rectification mode, supplying maximum power to the coil pair; and, a full inversion mode where energy is removed from the coil pair and returned to the power source.

2. Load Calculations

It is important to know the inductance of each load coil pair. The coil inductance determines the voltage required to change the coil current at a specified rate. The maximum rate determines the maximum coil voltage.

A method to calculate the approximate inductance of an odd-shaped coil is to divide the cross-section into smaller rectangular sections. The self-inductance of each section and the mutual inductance between all of the sections can be calculated using the equations of Figure 8 derived by F. W. Grover [8,9]. The series approximation for the mutual inductance is accurate for the case where the thickness of a rectangular

A. Self Inductance

$$L = L_s - \Delta L$$

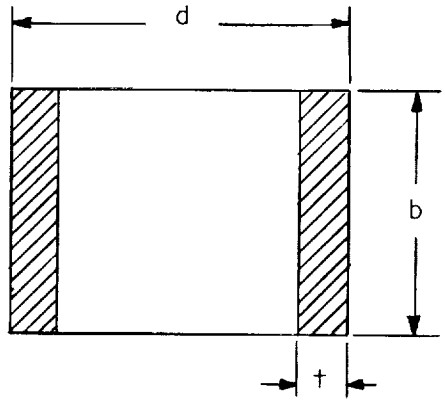

$$L_s = \frac{2\pi dN^2}{10^9}\left[(\log \frac{4d}{b})(1 + \frac{b^2}{8d^2} - \frac{b^4}{64d^4} + \ldots) - \frac{1}{2} + \frac{b^2}{32d^2} + \frac{b^4}{96d^4} - \ldots\right] \text{henries}$$

$$\Delta L = \frac{2\pi dN^2}{10^9}\left[\frac{\pi t}{3b} - \frac{25t^2}{72b^2} - \frac{t^2}{8d^2} + \frac{19b^2t^2}{768d^4} \ldots - (\log \frac{4d}{b})(\frac{t^2}{24d^2} + \frac{7b^2t^2}{384d^4} \ldots)\right.$$

$$\left. - (\log \frac{b}{t})(\frac{t^2}{6b^2} - \frac{t^4}{120b^2d^2} \ldots)\right]$$

B. Mutual Inductance

$q_1 = s-M$

$q_2 = s+M$

$\rho_1^2 = A^2+q_1^2$

$\rho_2^2 = A^2+q_2^2$

$\Delta^2 = a^2+m^2$

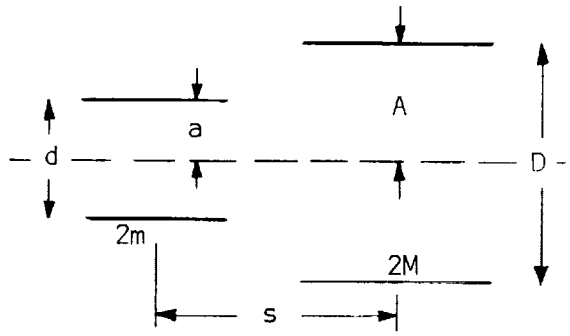

$$M_u = \frac{4\pi^2a^2N_1N_2mq_2}{\rho_2}\left[1 - \frac{A^2\Delta^2}{2\rho_2^4}\left\{\lambda_2 + \left(\frac{\Delta}{\rho_2}\right)^2\lambda_4\left(1 - \frac{7A^2}{4\rho_2^2}\right) + \ldots\right\}\right]$$

$$- \frac{4\pi^2a^2N_1N_2mq_1}{\rho_1}\left[1 - \frac{A^2\Delta^2}{2\rho_1^4}\left\{\lambda_2 + \left(\frac{\Delta}{\rho_1}\right)^2\lambda_4\left(1 - \frac{7A^2}{4\rho_1}\right) + \ldots\right\}\right]$$

$$\lambda_2 = 1 - \frac{7a^2}{4\Delta^2} \qquad \lambda_4 = 1 - \frac{9a^2}{2\Delta^2} + \frac{33a^4}{8\Delta^4}$$

FIGURE 8

section is negligible. The coil shown in Figure 9 was divided into 24 sections. The calculated inductance is

$$L = 1.07 \times 10^{-8} \times N^2 \text{ henries}$$

where N is the number of turns in the coil. Because each coil pair is made of two identical coils in series opposition, the inductance per coil pair is

$$L_{pair} = 2.14 \times 10^{-8} \times N^2 \text{ henries}$$

The mutual inductance between the two coils is negligible.

A value of 192 turns with a current of 350 amperes is needed to produce the desired forces on the model. The inductance per gradient coil pair becomes

$$L_{pair} = 8 \times 10^{-3} \text{ henries}$$

A full scale copper model of a proposed gradient coil has been built and its inductance measured. The measured value was within 1% of its calculated value.

3. Power Amplifier Design

The power amplifiers must supply the coil currents. Only low voltages are necessary to maintain steady-state currents in the coils because they have zero or negligible resistance. However, the voltage necessary to force a change in coil current is given by

$$E = L \frac{di}{dt}$$

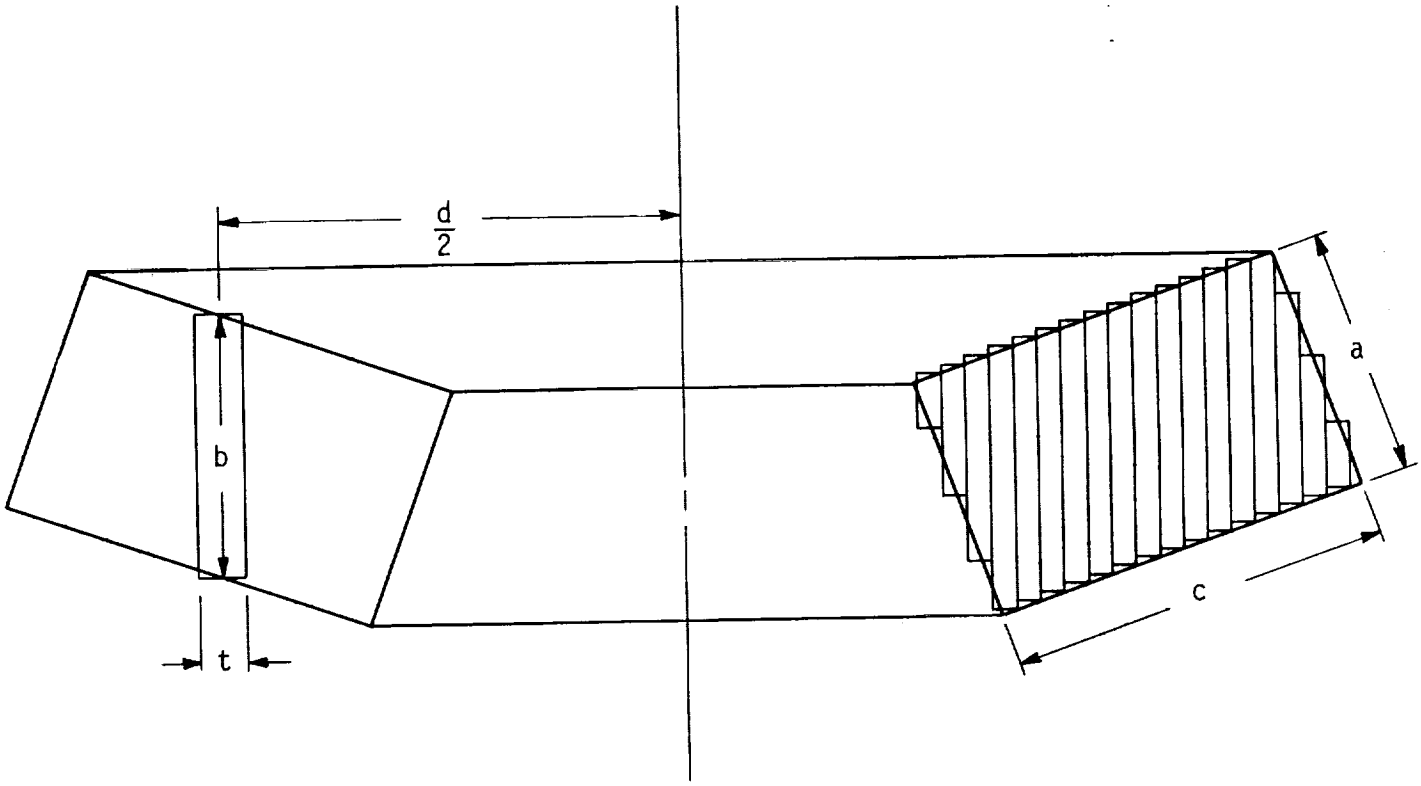

Area = 29.6 cm^2

a = 4.45 cm

c = 6.66 cm

FIGURE 9

COIL CROSS-SECTION

which for a constant forcing voltage, E, becomes upon integrating

$$Et = Li + \text{constant} \quad .$$

To change the coil current from zero to its maximum value in a time, T, gives

$$ET = LI_{max}$$

which for a gradient coil pair gives

$$ET = 2.8 \text{ volt seconds}$$

For the bang-bang control proposed the time T must be minimized; it must be much less than the desired response time of the control. T = 10 milliseconds requires a voltage E = 280 volts.

The combination of large coil voltages and currents eliminates the possibility of a practical power amplifier using power transistors. Furthermore, there is the additional requirement that to effect a reduction of coil current, the energy stored in the coil must be removed, there being no dissipation. Collectively, these requirements lead to the consideration of a power amplifier using controlled rectifiers, essentially a controlled power supply operating from the commercial power line. These have been used previously in similar applications [10,11,12]. Energy is supplied to the coils, i.e., increasing coil current, by the power supply operating in a rectification mode. To reduce the coil current, the energy stored in the coils is transferred back to the power source by the supply operating in an inversion mode. The transfer from rectification to inversion, as well as a linear mode control, is done by appropriate adjustment of the conduction periods of the controlled rectifiers.

Unfortunately, the necessity for commutating of the controlled rectifiers by the alternating current source introduces a time delay in the control action. This delay is between the time that a current reduction is demanded at an amplifier input, and the time that the current actually begins to decrease. For increasing currents there is no delay.

The delay is a function of the conduction angles of the rectifiers at the time that a current change is demanded, the number of rectifier phases and the source frequency. For example, consider the situation illustrated in figure 10a for a six phase rectifier. Prior to the command to reduce the current, the rectifier is operating in a full rectification mode, i.e., the coil current is increasing at the maximum rate. If a control demand to reduce the current at maximum rate occurs at a time coincident with the time that a rectifier is caused to conduct, as shown by an arrow in the figure, the delay time is a maximum. Since the current through the inductor must be continuous, the rectifier in the conducting phase, phase A, continues to conduct until transfer can be made to the next phase in sequence. During this time, while phase A is conducting the <u>average</u> output current remains constant. For the conditions given, this time is $T_D = 4\pi/3\omega$ seconds; ω being the source angular frequency.

Once the change to the inversion mode is effected, the current begins to decrease. During each conduction period of a controlled rectifier, the current decreases by an amount

$$\Delta I = \frac{V_p}{\omega L}$$

where V_p is the peak phase voltage. If the initial current is I_{max} a time

$$\Delta T = \left(\frac{I_{max}}{\Delta I}\right)\left(\frac{\pi}{3\omega}\right)$$

is required to reduce the current to zero, assuming that an integral number of conduction periods is required. Substitution gives

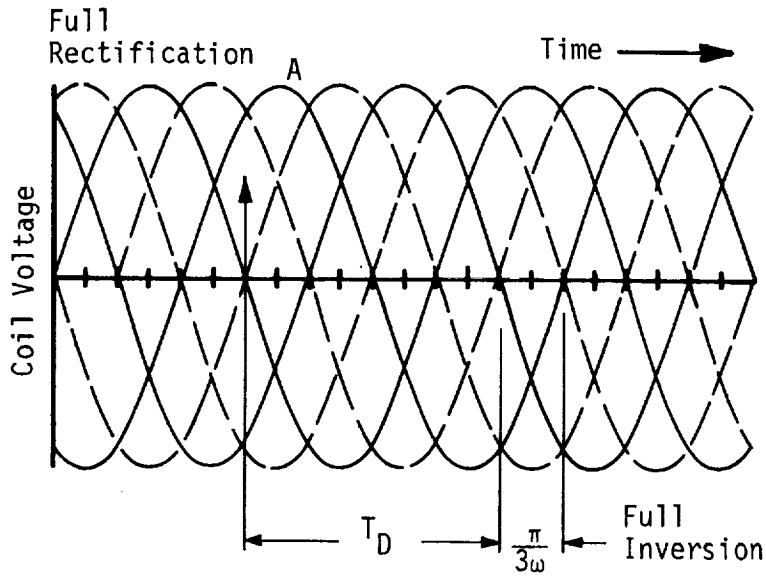

a. Worst Case Delay Time from Full Rectification to Full Inversion

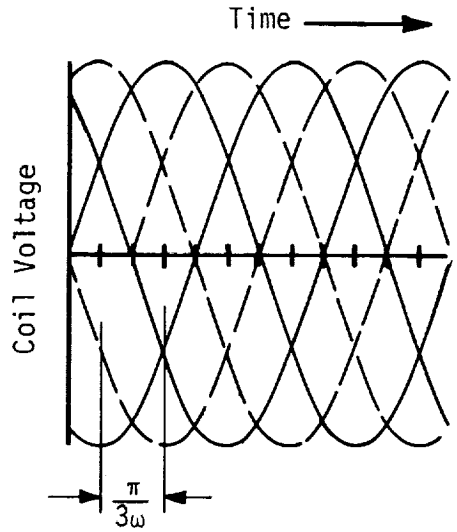

b. Worst Ripple Case

FIGURE 10

SIX-PHASE POWER SOURCE COIL VOLTAGES

$$\Delta T = \frac{\pi L\ I_{max}}{3\ V_p} \quad .$$

The total time to reduce the current to zero is the sum of the dead time and ΔT,

$$T_{max} = \frac{4\pi}{3\omega} + \frac{\pi L\ I_{max}}{3\ V_p} \ ,$$

from which the required peak phase voltage can be determined.

$$V_p = \frac{\pi L\ I_{max}}{3} \left(\frac{1}{T_{max} - \frac{4\pi}{3\omega}}\right)$$

This equation is plotted in Figure 11 as a function of T_{max}, the total switching time. A value of $T_{max} = 16 \times 10^{-3}$ seconds, giving $V_p = 600$ volts was selected as the best compromise between low switching time and reasonable coil voltages.

Because the coil voltage is rectified alternating current, there will be a ripple current in the coil. The largest ripple current occurs when the average coil voltage is zero corresponding to a steady state average coil current. For a six-phase rectifier, the rectifier conduction angle is $\pi/3$, as shown in Figure 10-b. Expanding this coil voltage in a Fourier series gives

$$e = 196.5 \sin 6\omega t + 98.3 \sin 12\omega t + \ldots\ldots$$

where

$V_p = 600$ volts.

Dividing by the appropriate impedances, the rms current is

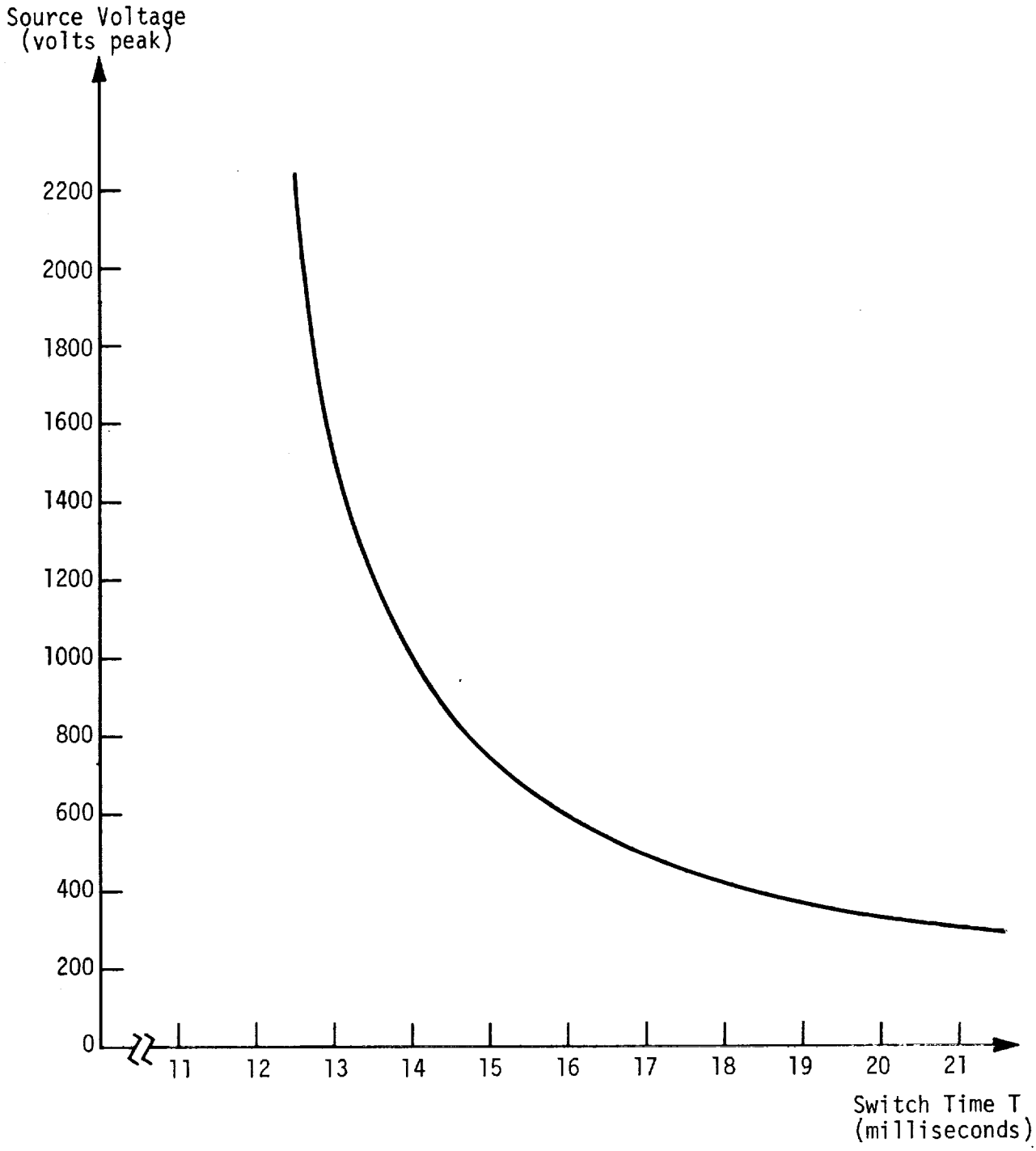

FIGURE 11

MAXIMUM SOURCE VOLTAGE VS. SWITCH TIME T

$$I_{rms} = \frac{1}{\sqrt{2}} \sqrt{\left(\frac{196.5}{6\omega L}\right)^2 + \left(\frac{98.3}{12\omega L}\right)^2 + \ldots\ldots}$$

which on substitution for the inductance, and a 60 hertz angular frequency, gives for the two terms shown I_{rms} = 7.9 amperes. Because the ripple current is considerably less than the design critical current of the coil, it is felt that it will remain superconducting. However, the final effect on the coil performance will be determined experimentally.

4. Power Source Considerations

The energy to drive the power amplifiers will be obtained from the commercial power line. Fluctuations of the power line voltage at a frequency of 30 hertz, must not exceed 0.5%, of the line voltage specified by Virginia Electric and Power Company. The power source presently being considered is a 34.5 KV line with a per unit impedance of

$$R = 0.592 \qquad X = 2.94$$

at a base of 10 MVA. Therefore, the maximum allowable power variation is

$$VA = \frac{(\% \text{ change})}{(Z_p)} \frac{(BASE)}{(1000)}$$

where

$$Zp = \sqrt{R^2 + X^2} \quad .$$

Because the worst case, 630 KVA, is less than the maximum allowable 1666 KVA, the souce voltage fluctuation requirement is met and energy storage is not needed.

5. Status

A list of preliminary amplifier specifications has been given to several vendors. Included was a request for a bid as well as detailed specifications on the systems which the vendors are capable of supplying. It was not specified to the vendors exactly how the amplifier should be synthesized. A copy of the specifications is given in Appendix A.

F. CONTROLS

1. Introduction

The control problem for one channel of a magnetic suspension can be stated as "find a rule for setting magnet current, and thus force, which will give a desired motion to the supported object." One could equivalently try to find the appropriate voltage to apply at the terminals of the magnet to give this current and thus control the motion of the supported object. In either case the control which we must find can either be expressed as a function of time or of the system state for a given set of initial conditions. The present goal is to find a control which is a function of the system state. This is called a feedback control. The control which is a function of time is called an open loop control.

As an example, suppose one wishes to control the motion of a system described by

$$\frac{dx}{dt} = U,$$

in such a way that x tends to zero. Suppose the initial state $x(0) = 1$. Either of the two controls below will produce the response $x(t) = e^{-t}$

$$U_1(s) = -x$$

$$U_2(t) = -e^{-t}$$

Suppose though, that at some time t_1 after the system has started operation, it is subject to a disturbance. The sketch in Figure 12 shows the trajectories yielded by the two controls. The trajectory numbered zero is the undisturbed trajectory.

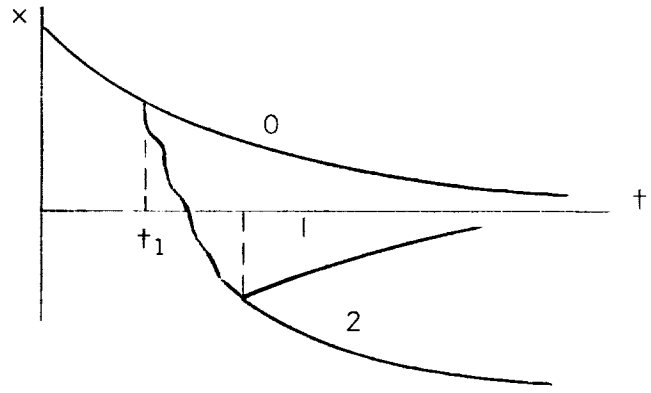

FIGURE 12

x,t TRAJECTORIES

From this, it is apparent that open loop controls are unsatisfactory for use with systems subject to disturbances.

In looking for a control law for the magnetic balance one wants to satisfy several requirements. A feedback control law is needed, not an open loop control law. It must be a control law which can be constructed physically, i.e. a physically realizable control. Last, one wants to look for a control law which is best (or at least better) in some sense. Mathematically, one is looking for a physically realizable, feedback control law which is optimal or at least near optimal.

In general terms, for a magnetic support fast, smooth operation is desirable. If the magnet coils have a finite resistance, i.e., do not

stay in the superconductor mode all the time, the Joule-heating in the coils should be minimized. Possible optimal control problems to consider are then, minimum time, minimum energy (heating), minimum time integral of squared error, or some combination of these. The optimal control law for a particular criterion may be a non-linear function. In general it will be a function of all the state variables. The differential equations for one channel of the 3-D magnetic support are:

$$m \frac{d^2x}{dt^2} = ki$$

$$L \frac{di}{dt} = E \ .$$

In these equations x is the position, i is the current in the coil, E the applied voltage, m is the mass of the model, L the coil inductance, and k is a force to current constant of proportionality. Here, E is the variable we must control. This system of equations is third order. One expects then that if an optimal control for this system can be found, it will be a nonlinear function of $x, \frac{dx}{dt}$, and i. Unfortunately, the physical implementation of a nonlinear function of three variables, although not impossible, would be technically quite difficult. In a particular problem, matters can probably be simplified by expressing the control as a function of two variables where one of these variables is a second function of two variables. For example, write $G(x, y, z) = H(x, f(y, z))$. This still requires generating functions of two variables. Construction of the control will be reasonably straight forward if the control law can be expressed in such a way as to require only the generation of nonlinear functions of a single variable. It will be possible to do this if i is regarded as the control variable in the problem and then ask what control E yields the i which is wanted.

Let us examine several optimal control problems for

$$\frac{d^2x}{dt^2} = U$$

where there may or may not be bounds on U. The eventual goal will be a feedback control but it will be necessary to examine open loop controls as well.

First we examine the minimum energy control problem. The optimal control U* minimizes

$$J = \int_0^T U^2 dt.$$

Since force and current are proportional in this problem, this integral is proportional to the time integral of i^2R. The problem is stated with a limit on terminal time because there is no solution to the unbounded time problem. Gottlieb [13] circumvented this problem by considering.

$$J = \int_0^\infty (u^2 + k^2)dt \quad \text{where}$$

k is a constant. His results are quite similar to those obtained here although not as easy to work with. The problem is discussed by Athans and Falb [14]. Application of the Pontryagin maximum principle yields an optimal open loop control of

$$U^*(t) = -\frac{2}{T^2}(3\xi_1 + 2\xi_2 T) + \frac{6}{T^3}(2\xi_1 + \xi_2 T)t$$

where $\xi_1 = x(0)$ and $\xi_2 = \dot{x}(0)$.

It is simple to show then that $x(T) = \dot{x}(T) = 0$.

J can be evaluated using the optimal control U^*. Then

$$J(U^*) = \frac{2}{T^3}(\xi_1, \xi_1)\begin{pmatrix} 6 & 3T \\ 3T & 2T^2 \end{pmatrix}\begin{pmatrix} \xi_1 \\ \xi_2 \end{pmatrix} \quad .$$

The value of J is a function of the terminal time and the initial conditions. The optimal control unfortunately is an open loop control and since it is a function of both terminal time and initial conditions, it appears that one will be unsuccessful at trying to find a feedback control U(x) which is also optimal. One may however, find a feedback control U(x) which gives a value of J which is not too much larger than J[U*]. Since J[U*] is the optimum, it can be used as a standard for judging other control schemes.

In finding U*(t), magnitude constraints on U were not included. If this is done, one finds that U*(t) can still be evaluated if T is not too small. It is obvious that introducing a constraint on the value of U will increase J[U*] if the unconstrained U does not already satisfy the constraints.

As more and more severe constraints on U are introduced, the behaviour of U* for a particular (T, ξ_1, ξ_2) is as shown in Figure 13 in the sequence of curves below in order of increasing severity.

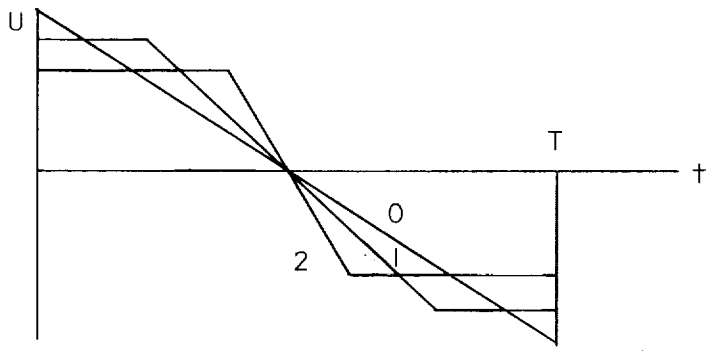

FIGURE 13

CONSTRAINTS ON CONTROL LAW

The limiting case is the one for which T corresponds to the minimum time optimal control with a particular constraint.

The minimum time problem is discussed in many works, [14] or [15] for example. It is stated, find a control U(t) subject to $|U| \leq$ UMAX which carries on initial state $x(0) = \xi_1$, $\dot{x}(0) = \xi_2$ to $x = \dot{x} = 0$ in minimum time. In other words, minimize $J = \int_0^t dt$

For this problem a feedback control law can be found:

$$U^*(x) = -UMAX\left(sgn\left[x + \frac{\dot{x}|\dot{x}|}{2UMAX}\right]\right)$$

For initial conditions having $\dot{x}(0) = 0$, $T = 2\sqrt{\frac{\xi_1}{UMAX}}$.

The terminal time for general initial states is more complicated. The following expression holds, for initial states that start with U(0) = - UMAX.

$$T = 2\sqrt{\frac{1}{UMAX}\left(\xi_1 + \frac{\xi_2^2}{2UMAX} + \frac{\xi_2}{UMAX}\right)} .$$

The joule heating for a minimum time controller is just

$$J = \int_0^T U^2(t)dt = T(UMAX)^2 .$$

Suppose one selects a terminal time T and calculates the corresponding UMAX on the assumption that the initial velocity is zero (i.e. $\xi_2 = 0$). It is found that the heating is

$$J = \frac{16\xi_1^2}{T^3} .$$

For $\xi_2 \equiv 0$ and no constraints on U, the minimum energy control yields

$$J[U^*] = \frac{12\xi_1^2}{T^3} .$$

Further, it is known that the introduction of constraints on U for the minimum energy problem will increase $J[U^*]$. It is seen that the time optimal control does not appear to be much more expensive in terms of heating than the minimum energy control. Since the minimum time control is a feedback control it appears to meet most of the criteria for a good control. One must check to insure that a linear control will not do almost as well though since it would be easier to construct.

Minimization problems of the form

$$\min J = \int_0^\infty (x^2 + rU^2)\, dt \quad r > 0$$

lead to linear feedback controls. Without solving this particular problem, suppose a linear second order system is constructed.

If the system differential equation is

$$x'' + 2\zeta\omega x^1 + \omega^2 x = 0 \text{ and } j = \sqrt{-1},\ 0 < \zeta < 1,$$

$$U = x_0\omega^2 \left[1 - 2\zeta^2 + 2\zeta\sqrt{1 - \zeta^2}\ j\right] e^{-(\zeta + \sqrt{1 - \zeta^2}\, j)\,\omega t},$$

where
~~The~~ initial value X_o may be a complex number.

The joule heating is now

$$J = \int_0^\infty U\,\overline{U}\, dt = x_o\overline{x}_0\omega^4 \int_0^\infty e^{-2\zeta\omega t}\, dt.$$

$$J = \frac{|x_o|^2\,\omega^3}{2\zeta}$$

To make a satisfactory comparison with the other problem setting $\zeta = \frac{1}{\sqrt{2}}$ will give a qualitatively good response. The main question is

how should ω be chosen? If one chooses it so that the maximum control effort is equal to UMAX, it is found that the system is much too slow.

Using the same problem as before:

$$\omega^2 \zeta_1 = \text{UMAX} = \frac{4\zeta_1}{T^2}$$

or $\omega = \frac{2}{T}$. The joule heating

$$J = \frac{4\sqrt{2}\ \zeta^2}{T^3}$$

which looks good until one asks what the actual response time of the system is?

It is difficult to make a comparison since the settling time for a linear system is infinite. If the time for the response to decay to ten percent of its initial value is chosen ω can be estimated in terms of T. This yields $\omega \sim \frac{2\pi}{T}$ and

$$J = \frac{\sqrt{2}\ \zeta_1^2}{2} (2\pi/T)^3 = \frac{4\pi^3\sqrt{2}\ \zeta_1^2}{T^3}$$

If the results are normalized for the three control laws against the bounded time minimum energy and hold T and ξ_1 constant, then the ratio is

1:1.33:14.5

with the linear system worst. This result is very sensitive to the manner in which the time is defined for the linear system but in any case the linear system is definitely inferior. It could be excluded simply because it calls for very high control values (values of magnet current).

The minimum time or bang-bang control appears to be the most satisfactory choice. It will be necessary to overcome several difficulties with it. One of these is the problem of finding the voltage control law for the magnets. Another problem is that the energy dissipation of the minimum time system is continuous if there are disturbances. A way must be found to "turn it off" for small values of position error.

These difficulties will be circumvented in the physical construction of the control law. If the switch in the bang-bang control is replaced with a saturable element fed by a multiple of the minimum time control law, then

$$U(x) = \mathrm{Sat}(K[x + \frac{\dot{x}|\dot{x}|}{2UMAX}]) \ .$$

For large K this will behave very much like a switch. Physically this is reasonable since the system will require some sort of current limiting to protect the magnets anyway.

It can be proven mathematically that this control law will produce a stable system. Unfortunately, for small amplitudes it has less damping than any stable linear system. Lags in the power supply will make the system unstable. This does not present a serious problem though. In implementing the non-linear function $\dot{x}|\dot{x}|$ an analog computer function generator will be used. This uses straight lines to approximate the non-linear function. It is only the slope of $\dot{x}|\dot{x}|$ near zero which presents problems. If one approximates this with a function having ~~a nonzero~~ an appropriate slope the system will be stable.

For small disturbances, the system will behave like a linear system. It will have the desirable characteristic that the energy dissipation will go to zero in the absence of disturbances. If there are disturbances, the energy dissipation will be proportional to the square of the magnitude

of the response in the linear mode. The size of this linear mode is determined by varying the constant K. Its other properties are controlled by the character of the control law for small x, $\dot{x}$.

The rest of the design consists of making suitable modifications to the control law to compensate for effects which have been neglected heretofore. These effects are the time lags in the power supply. If these time lags can be calculated it is possible to calculate corrections to the control law for them provided they are small compared to T.

These calculations have been made and the entire system simulated on a digital computer assuming that the current control systems are linear with a voltage limit. A graph of one such simulation is given in Figure 14.

It remains to obtain a better model for the power supplies and their behaviour and then make another simulation with the improved model to see what further modifications should be made to the minimum time control law. This should be straight forward since all that is needed is accurate information about the time lags in the power supply-coil systems.

One object of this analysis is to produce a control law which can be constructed from off the shelf components. The control law described above can be set up on an analog computer. Any of the minor modifications can be introduced at any time simply by following this philosophy in the physical implementation. Appropriate components to do this are available from several manufacturers so no difficulties are expected.

Delet

The drag augmentation coils will have a separate control system. In this system the current in the drag coils will be controlled using only the time integral of the system error along the tunnel axis. In this way, for any steady state drag force (within the system capability),

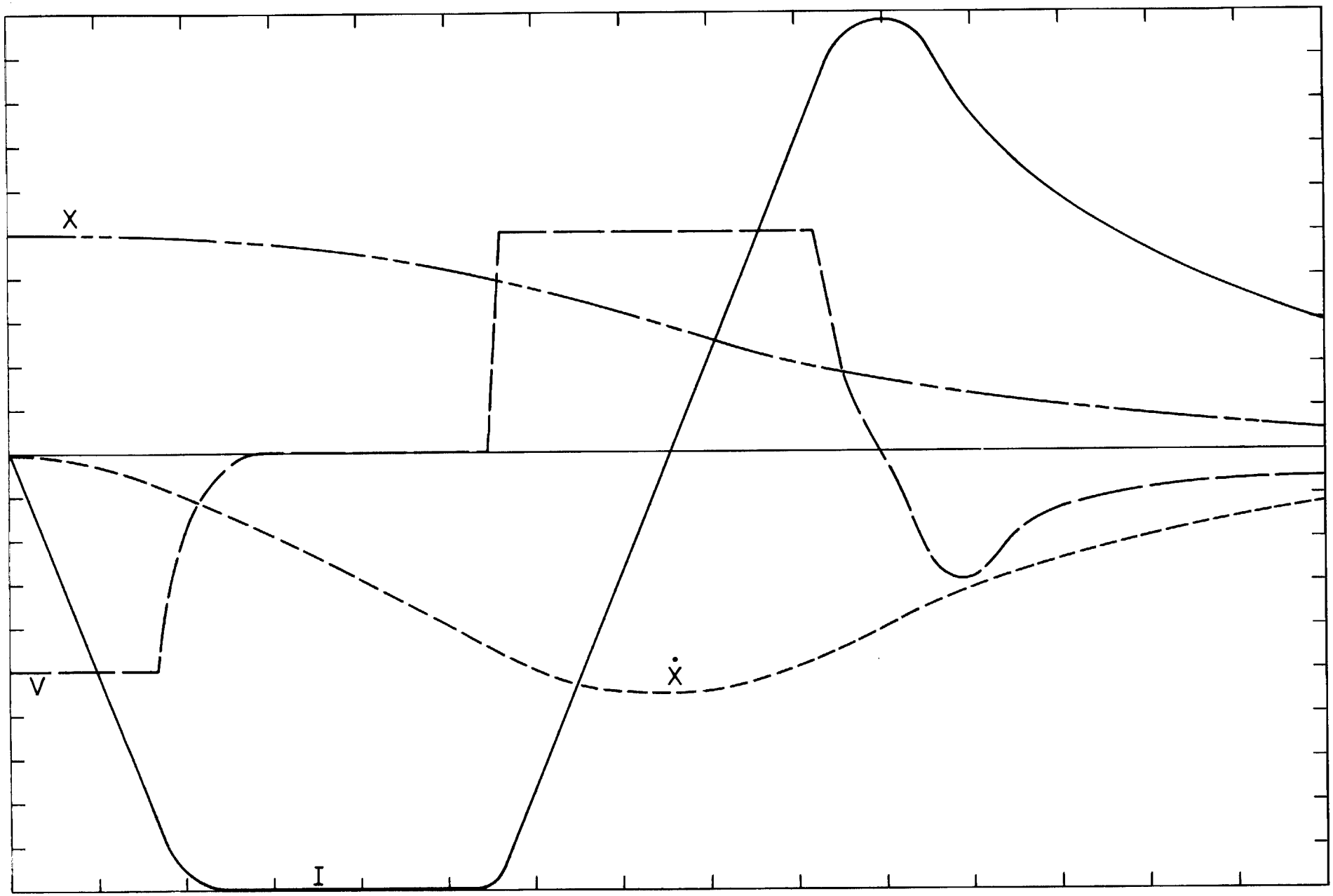

FIGURE 14
CONTROL SYSTEM SIMULATION

the position error will go to zero as $t \to \infty$. This system will be kept quite slow so that it will not interact with the other system. The drag augmentation system will be an accurate system for measuring the steady state component of drag. The other force components will be controlled in the 3-D system.

2. Control System Position Sensor

In the course of choosing a position sensor for the proposed wind tunnel balance system, several possibilities have been reviewed, and will be briefly discussed here. The system which has been judged most suitable is an electromagnetic system very similar to that developed by the group at MIT [16]. Before discussing it more thoroughly, the general position sensing requirements will be outlined and each system considered will be briefly reviewed.

a. Requirements

Any position sensor suitable for use on the wind tunnel balance system herein described must perform two functions: 1) read three linear coordinates, for example x, y and z, and 2) read again the three linear coordinates, possibly in a different coordinate system, along with at least two angle variables, e.g. pitch and yaw.* The first function is necessary to provide the information input to the automatic control system for a three dimensional balance. The second function is necessary for the recording of aerodynamic data which is the ultimate output of the machine. These functions, may be combined in a single system, or performed separately by two or more coordinate sensing systems.

*Complete kinematic information may be obtained by adding roll rate to these variables. The roll rate sensing function is, however, likely to be provided by a separate, possibly optical, system.

The requirements are the following:

1)Read the linear variables over a range of ± 3 cm to a precision of ± 0.1 mm.

2)Read the angular variables over a range of ± 10° to a precision of ± 0.1°.

3)Be drift free in the sense that reliable readings may be taken over a period of several hours without recalibration.

4)Provide this information over a band width of from zero to 1 kc.

5)Be adaptable to models of different shapes.

6)Have sensors small enough to fit within the 1/2 inch cylindrical annulus of 6 in. diameter between the wind tunnel and the cryostat.

7)Have zero (to first order) coupling between the coordinate read-outs.

b. Systems Reviewed

The two position sensing systems with which the various groups at the University of Virginia have had the most experience are optical and "Q-coil" sensing systems. The former has been developed in more-or-less sophisticated versions for use on three-dimensional balance systems, while the latter, a rudimentary electromagnetic sensor, has been used only on one-dimensional systems. Several possible optical systems have been reviewed. They all suffer from the following disadvantages: 1) they are complex, for example, 4 light beams are necessary to read one linear and one angle variable; 2) except for highly symmetrical model shapes (spheres or cylinders) the outputs are coupled and the degree and functional dependence of the coupling depends on model shapes; and 3) the optical systems are not easily adaptable to read large values of the variables being limited to about $\pm \frac{1}{2}$ cm linear motion. While these problems can be overcome, a simpler and more convenient system would be desirable.

A radioactive coordinate sensing system which would functionally supply the three linear coordinates only has also been analyzed. Since the radiation field (from a point source) is spherically symmetric, this system would be completely uncoupled in addition to being simply constructed and independent (to first order) of model shape. The disadvantages are that the output is a nonlinear function of position $f(1/r^2)$, and in order to attain the required precision (± 0.1 mm), a rather strong radioactive source is required (e.g. 1.64 millicuries of 60 kev x-radiation). This source strength is sufficient to require special handling.

Finally, the electromagnetic coordinate sensing system in use by the MIT group was reviewed. This system appears to have a minimum of disadvantages while adequately meeting the requirements outlined above, and therefore has been adopted with slight modifications.

c. The MIT Electromagnetic System

1) Principle of Operation

This system is based on the differential transformer principle. The coil lay-out and coordinate system are shown in Figure 15. In operation, a Helmholtz pair of coils, E_1 and E_2, oriented symmetrically around the origin and perpendicular to the x (tunnel) axis are driven by a power amplifier at a constant frequency ω_0. An oscillating field, $H_o \sin\omega_o t$ is generated at the origin of the coordinate system. A similar Helmholtz pair, x_1, x_2, is connected in series opposition and located symmetrically and co-axially with E_1 E_2. Ideally, the voltage induced in this pair is zero in the absence of field perturbations. An axisymmetric object, either conducting or magnetic, may be located at the origin, and a dipole moment is induced in this object by the excitation field from E_1 and E_2. If the object is at the origin, the field perturbations seen by x_1 and x_2 are identical and the induced voltage is still zero. A voltage

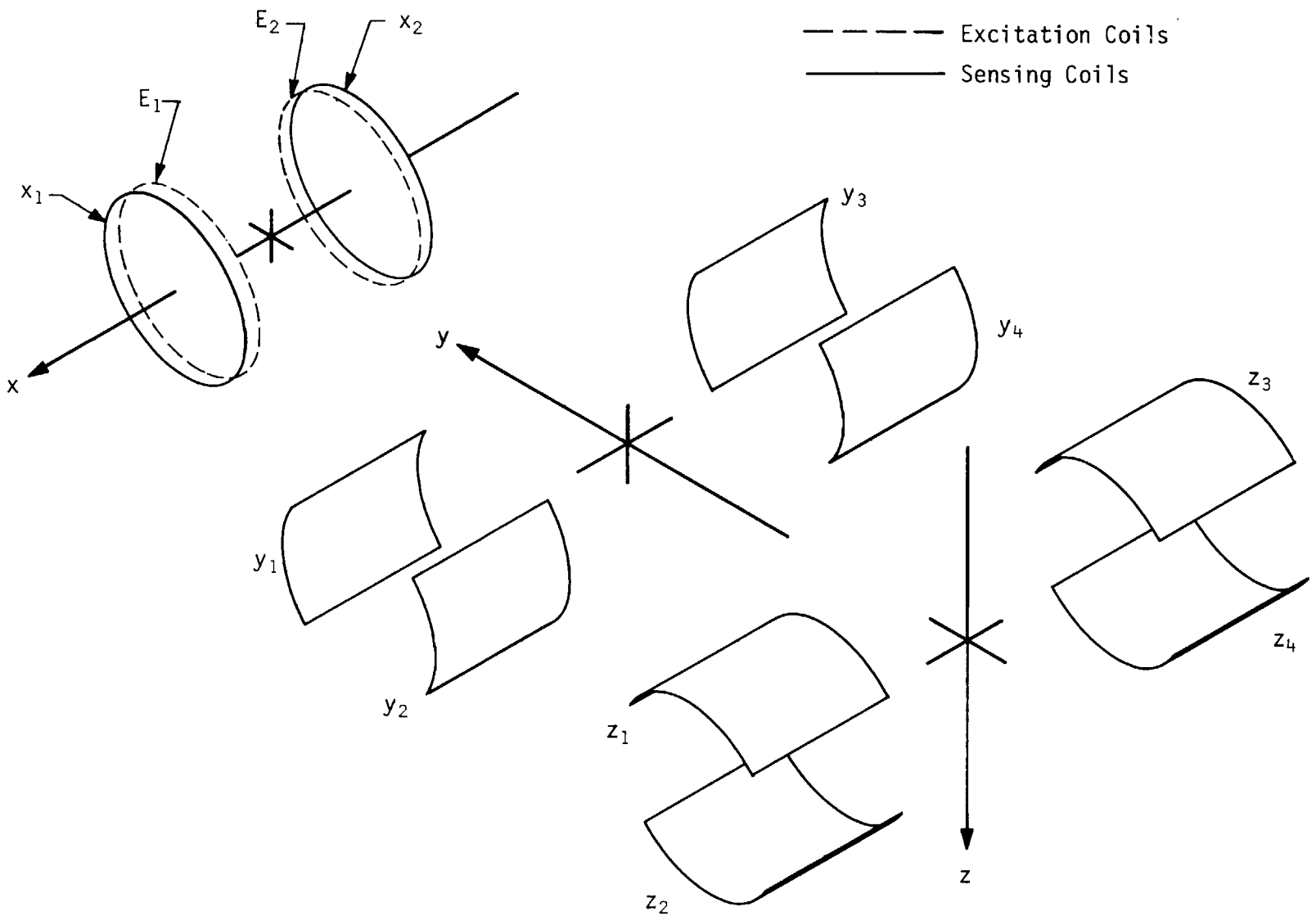

FIGURE 15
SENSOR COIL SYSTEM LAYOUT

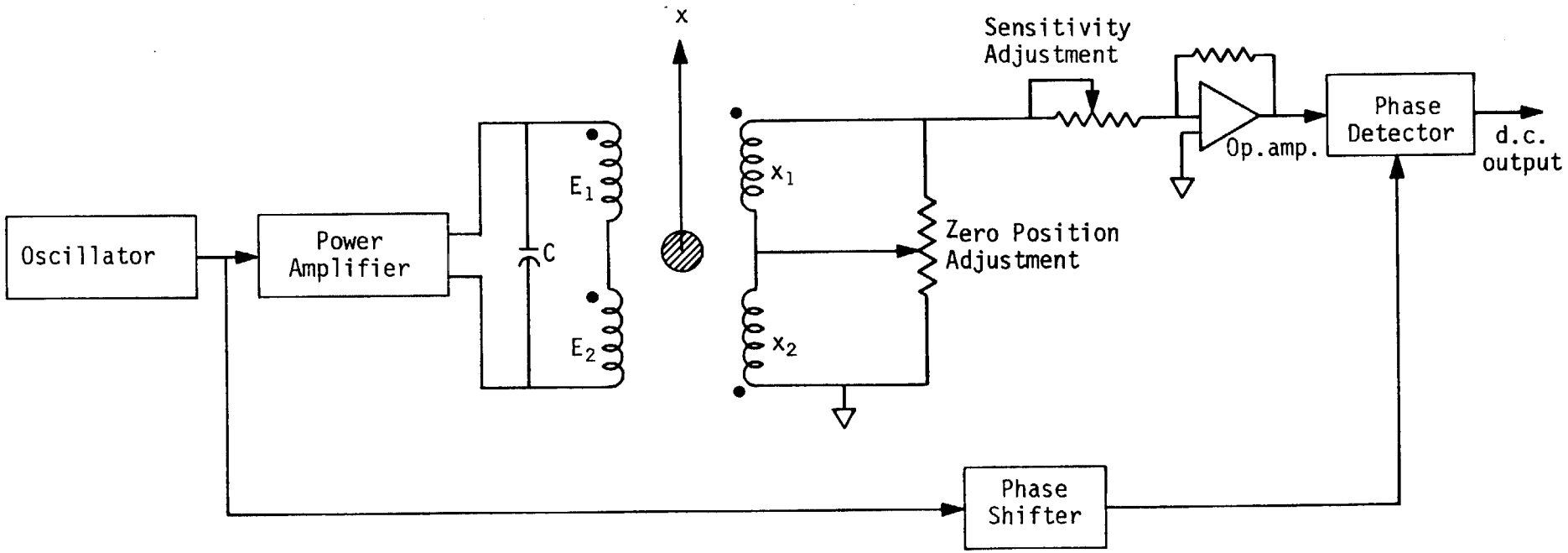

FIGURE 16

x AXIS POSITION SENSING SYSTEM

will be induced for positive or negative displacements of the object along x, and the phase relation for these displacements is π. Thus an x axis coordinate sensing system could be constructed as shown in Figure 16.

The remaining coils, z_1 through z_4 and y_1 through y_4 serve to sense coordinates y and z. In addition pitch and yaw angles can be measured as described below.

2) Calculation of Sensitivity

The sensitivity of this system is not difficult to calculate. The geometry is shown in Figure 17. A spherically symmetric,perfectly diamagnetic (superconducting) object located at the origin has been assumed. The excitation field Ho, provided by E_1 and E_2 is assumed uniform in the

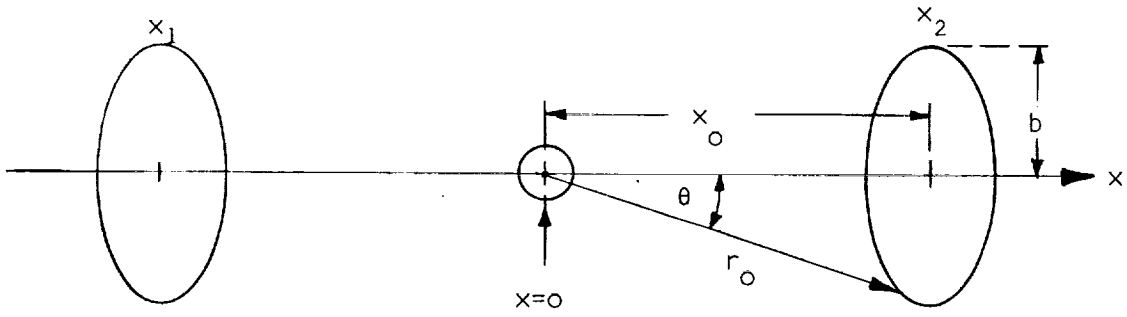

FIGURE 17

GEOMETRY FOR CALCULATING x AXIS SENSITIVITY

space between x_1 and x_2. An appropriate field solution in the presence of the spherical perturbation at the origin is

$$\vec{H}(\vec{r}) = \vec{H}_o\left[1 + \frac{a^3}{2}\nabla\left(\frac{\cos\theta}{r^2}\right)\right]$$

where a is the radius of the sphere. The total perturbed flux threading the coil x_2 may be calculated from the second term in brackets according to

$$\phi_{xz} = \int \vec{B}\cdot\hat{n}ds = \mu H_o \frac{a^3}{2}\int \nabla\left(\frac{\cos\theta}{r^2}\right)\cdot\hat{n}ds$$

where μ is the permeability, $\vec{n}$ is a unit vector normal to the plane containing x_2 and ds is an elemental area on the plane surface subtended by x_2. From the above

$$\phi_{xz} = -\frac{\mu H_o \pi a^3 b^2}{(b^2 + x_o^2)^{3/2}}$$

A similar expression obtains for the coil x_1, and since the pair are connected in series opposition, the appropriate quantity for calculating the induced voltage is $\phi_{x_1} - \phi_{x_2} = \Delta\phi(x)$. Introducing a displacement $x \ll x_o$ in the positive x direction, the result is

$$\Delta\phi_x = -\mu H_o \pi a^3 b^2\left[\frac{1}{\{b^2 + (x_o - x)^2\}^{3/2}} - \frac{1}{\{b^2 + (x_o + x)^2\}^{3/2}}\right]$$

which upon expanding and neglecting terms of order x^3 and higher becomes

$$\Delta\phi_x \cong -\mu H_o \pi a^3 b^2\left(\frac{6x_o}{r_o^5}\right)x \quad ,$$

where $r_o^2 = b^2 + x_o^2$.

Finally, the induced voltage may be calculated, including the fact that H_o is an a.c. field, say $H_o \sin\omega t$, from

$$\frac{V(x)}{x} = \frac{1}{x}\frac{d\phi(x)}{dt} = -\frac{6\pi\omega\mu H_0 a^3 b^2 x_0}{r_o^5}\cos\omega t$$

with units of volts per unit length per turn.

Since the geometrical factors have been more-or-less fixed by the tunnel geometry, the sensitivity may be estimated using the following values:

$\omega = 15.7 \times 10^4$ rad/sec (25 kc)

$\mu = 1.23 \times 10^{-6}$ henry/meter

$H_o = 2040$ amp. turns/meter

$a = 1$cm

$b = 8.25$ cm

$x_o = 5.5$ cm.

$r_o = (b^2 + x_o^2)^{1/2} = 9.8$ cm

whence

$$\frac{V(x)}{x} = 3 \text{ millivolts/millimeter turn (peak)}$$

The values for ω and H_o will be shown below to be near optimum for the power amplifier chosen.

A similar calculation can be performed for the y and z coils though the geometry, as shown on Figure 13, is more difficult. The result is

that the y and z sensitivity per turn is about 1/2 as large as the x sensitivity. Therefore these coils will be wound with twice as many turns. The present design calls for 100 turns each for the x coils and 200 turns each for the y and z coils. The sensing coil sensitivity should then be about 300 mv/mm.

3) Optimization of the Excitation Coils E_1 and E_2

The excitation coils, as shown in Figure 14, form a parallel resonant circuit with the capacitor, C, which is driven by a power amplifier. Optimization proceeds from seeking the conditions under which NI (ampere turns) for the resonant circuit is maximized. As shown below, the optimum design is one which maximizes NI and Q while matching the resonant impedance to the impedance of the power source. For $Q \geq 10$ optimization is independent of series or parallel resonance. Parallel resonance has been chosen since it avoids the difficulties arising from the very high voltages which occur in a series resonant circuit.

The design of the excitation coils has been predicated on the choice of a suitable power source. A Bogen MO 100A, 100 watt public address amplifier with a maximum voltage output of 115 volts at an impedance R_o, of 240 Ω has been chosen. The coil geometry was also assumed fixed in the Helmholtz pair configuration shown in Figure 13, where the winding thickness, h, is 1/8 inch; the winding width, g, is 3/4 inch; the inside diameter, 2b, is 6.5 inches; and the pair separation, $2x_o$, is 4.33 inches. The circuit diagram is shown in Figure 18, where the inductance and capacitance are ideal and the series resistors represent the dissipation of these elements. R_t is the resistive impedance of the circuit at resonance, I_s is the power source current, and I_t is the resonant circulating current.

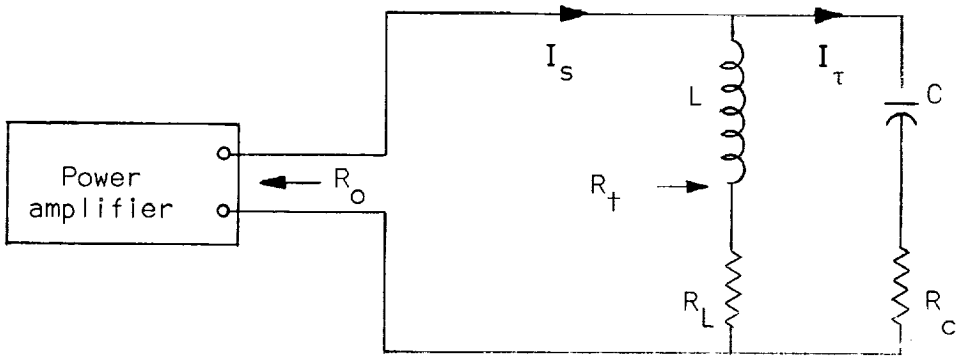

FIGURE 18

RESONANT EXCITATION COIL CIRCUIT DRIVEN BY POWER AMPLIFIER

Since $I_t = QI_s$, the coil NI may be maximized by maximizing Q, which in turn is inversely proportional to $R_L + R_C$. Clearly, R_L may be reduced nearly to zero by using fewer turns of larger wire in the coil, thus reducing L, while increasing C to maintain resonance. The dissipation in the capacitor will thus determine the maximum Q. Therefore, at resonance $R_t \simeq Q^2R_C$; and, for maximum power transfer $R_t = R_o$. Thus, Q^2R_C is fixed by the power source impedance. Assuming that there exists some relation between R_C and C, the capacitor could now be chosen. Since the coil geometry is fixed, the only remaining variables are the inductance, L; which can be varied by adjusting the wire diameter, d_c; and the number of turns, N, and the resonant frequency, ω. With the geometry fixed, however, there is a constraint on N since it is required that $R_L << R_C$. Thus the only variable left is ω.

The appropriate equations are:

$\omega L = 1/(\omega C)$ resonance

$$R_L = \frac{8\rho bN}{d_o^2}$$

where ρ is the resistivity, b the radius of the coil, and d_o the diameter of the copper in the wire. Further,

$$\frac{N}{2} = \frac{gh}{\pi d_o (t + \frac{d_o}{4})}$$

where gh is the cross sectional area of the winding slot and the denominator is the total cross sectional area of an individual wire with insulation thickness, t. The inductance of such a coil is given by

$$L = 2FN^2b - \frac{0.032N^2bh}{g}(0.693 + B_s)$$

in microhenries with the dimensions in inches. F and B_s are tabulated functions [17]. Using these equations, along with the constraints outlined above, N, L and hence ω can be calculated. The following values have been obtained:

$C = 1.0\mu f$

$L = 43\mu h$

$R_L = 0.03\ \Omega$

$R_c = 0.13\Omega$

$Q = 40$

$N = 14$ turns

$R_T = Q\ (R_L + R_c) = 268\Omega$

$f = \omega/2\pi = 25$ kc

$I_S = 0.61$ amps.

From this last figure, one can calculate H_o in amp. turns per meter for the Helmholtz pair separated by a distance of twice their radius:

H_o = 2040 amp. turns/meter which is the number used above in the sensitivity calculation.

The excitation coils are actually to be wound of stranded, insulated wire. The strand diameter is chosen as the maximum diameter for which skin-effect resistance is negligible for the frequency of interest. In this case there are 140 strands of No. 32 gage formvar insulated wire in the cable.

4) Generalization to a Five-Dimensional Position Sensing System

In section 1) the principle of operation of the position sensing system in the x dimension was discussed in detail. Here the purpose is to explain how the coil configuration shown in Figure 15 can be used to sense the linear coordinates y and z as well as the pitch and yaw angles θ_p and θ_y. Consider the coil configuration shown in Figure 19. (The exploded perspective is Figure 15)

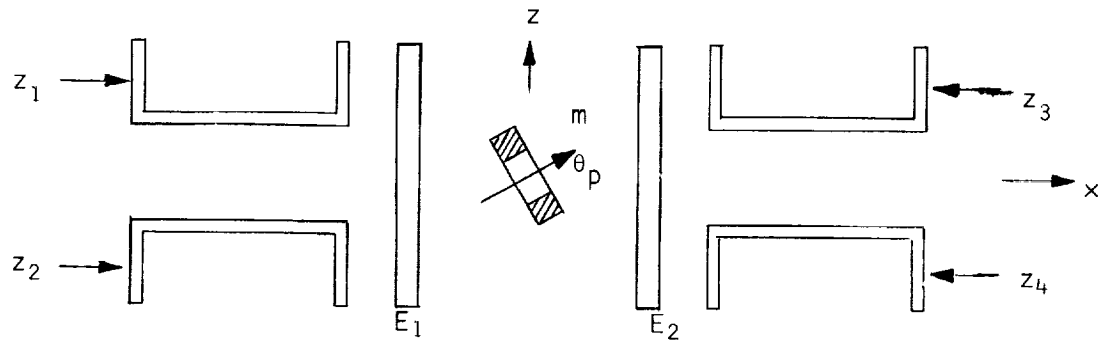

FIGURE 19

x-z PLANE VIEW OF EXCITATION AND z COORDINATE SENSING COILS

The object at the origin represents a conducting ring which is fixed in the body of the model. The presence of the ring will induce a perturbation in the excitation field which can be expanded in multipoles about the origin. The leading, and largest, term is a dipole moment, $\vec{m}$, oriented along the axis of the ring at angle θ_p with the x axis projected in the x-z plane.

Consider first the case of $\theta_p = 0$ and the coordinate z is to be sensed. The pair z_1 and z_2 are connected in series opposition. The induced voltage, say $(z_1 - z_2)$, is then added to the voltage induced in the pair z_3 and z_4, also connected in series opposition; thus,

$$V(z) = (z_1 - z_2) + (z_4 - z_3)$$

where the algebraic signs are defined by requiring a positive voltage to be induced when a north pole is moved through the coil from inside the tunnel. For this system, the following statements may be understood:

a) $V(z) = 0$ to first order for motions of the ring by the x, y, θ_p and θ_y directions.

b) Since $\vec{m}$ is an oscillating moment, (at frequency ω) there is a unique phase relation between V(z) and the excitation field, i.e. the voltages induced for positive and negative z are 180° out of phase.

Statement a) implies that there is no coupling between the coordinate outputs to the extent that voltages induced by higher multipoles may be neglected compared to those due to the dipole moment.* Statement b) signifies that phase sensitive (synchronous) demodulation of V(z) will

*No complete analysis of this problem has been made, however, it can be seen, for example, that an octopole moment will yield a response (i.e. $V(z) \neq 0$) for displacements in y and θ_y but not for x and θ_p.

provide the algebraic sign of the z displacement.

5) Five-dimensional Coordinate Sensing System

An identical analysis applies for the y, θ_p, θ_y voltages. A schematic for the five dimensional coordinate sensing system is shown in Figure 20. This is not a complete schematic, since the variable phase nulling circuits which are necessary to balance each coil pair in the phase plane have been omitted, however, it serves to illustrate the principle of operation.

The coordinate transformation operation which would be accomplished after the demodulator outputs have also beem omitted. This transformation is necessary since the position sensor and magnetic balance coil systems operate in different frames of reference. An appropriate transformation is the following:

$$x' = a_{11}x + a_{12}y + a_{13}z$$

$$y' = a_{21}x + a_{11}y + a_{23}z$$

$$z' = a_{3_\omega}x + a_{32}y + a_{33}z$$

where the primes indicate the balance coordinate system. This operation can be performed quite simply with three summing amplifiers as shown in Figure 21, where $a_{11} = R/R_{11}$, $a_{12} = R/R_{12}$, etc.

6) Status of the Coordinate Sensing System

The design of the system, with the exception of the phase plane nulling circuits, is complete; and estimates of the performance have been made as shown in the preceeding paragraphs. All of the blocks as shown on Figure 20 are items which may be purchased as units. Three companies are being considered for the operational amplifiers: Burr-Brown, Nexus, and Analogue Designs. Each company offers a suitable, general purpose

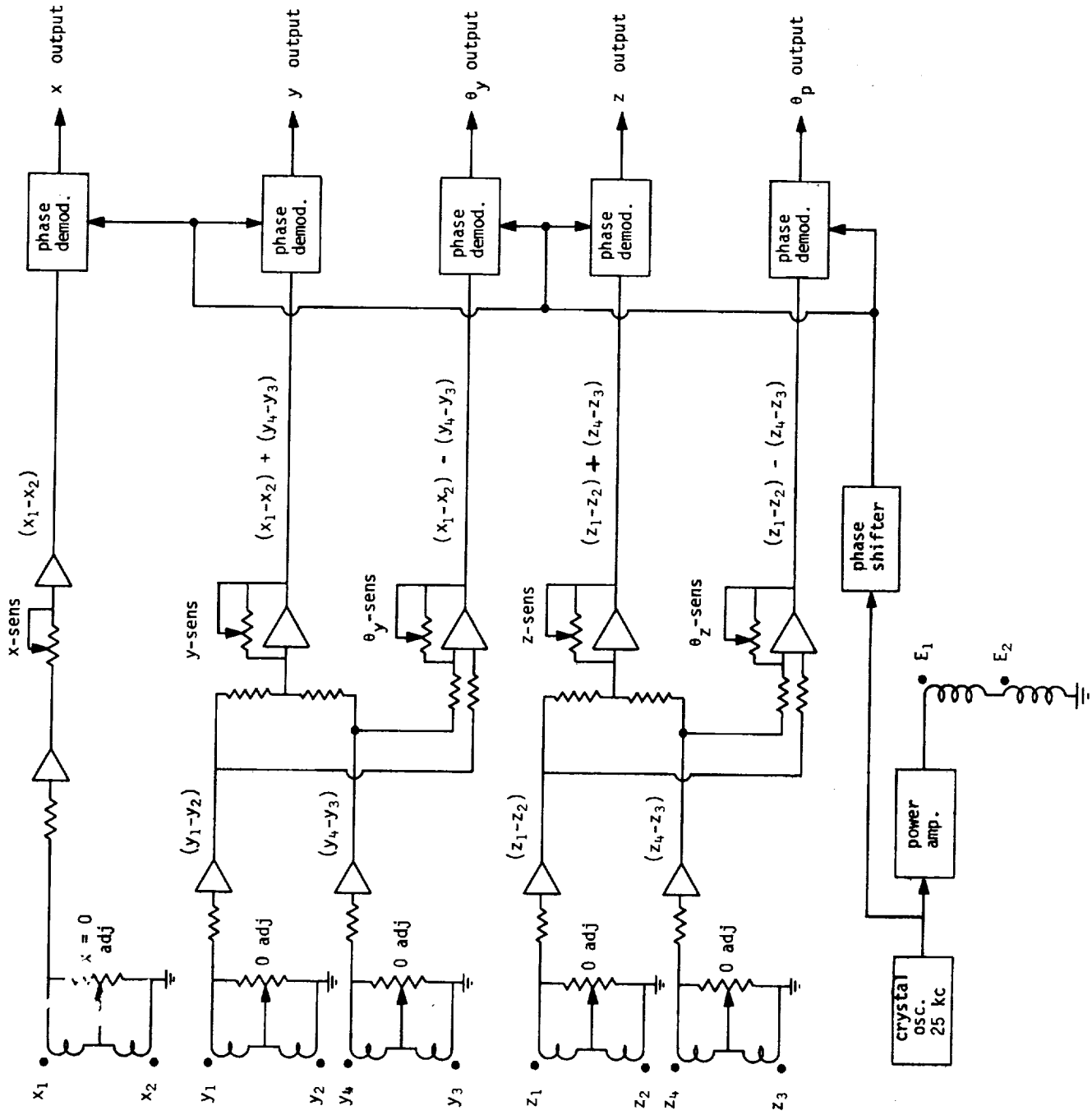

FIGURE 20

FIVE-DIMENSIONAL POSITION SENSING SYSTEM

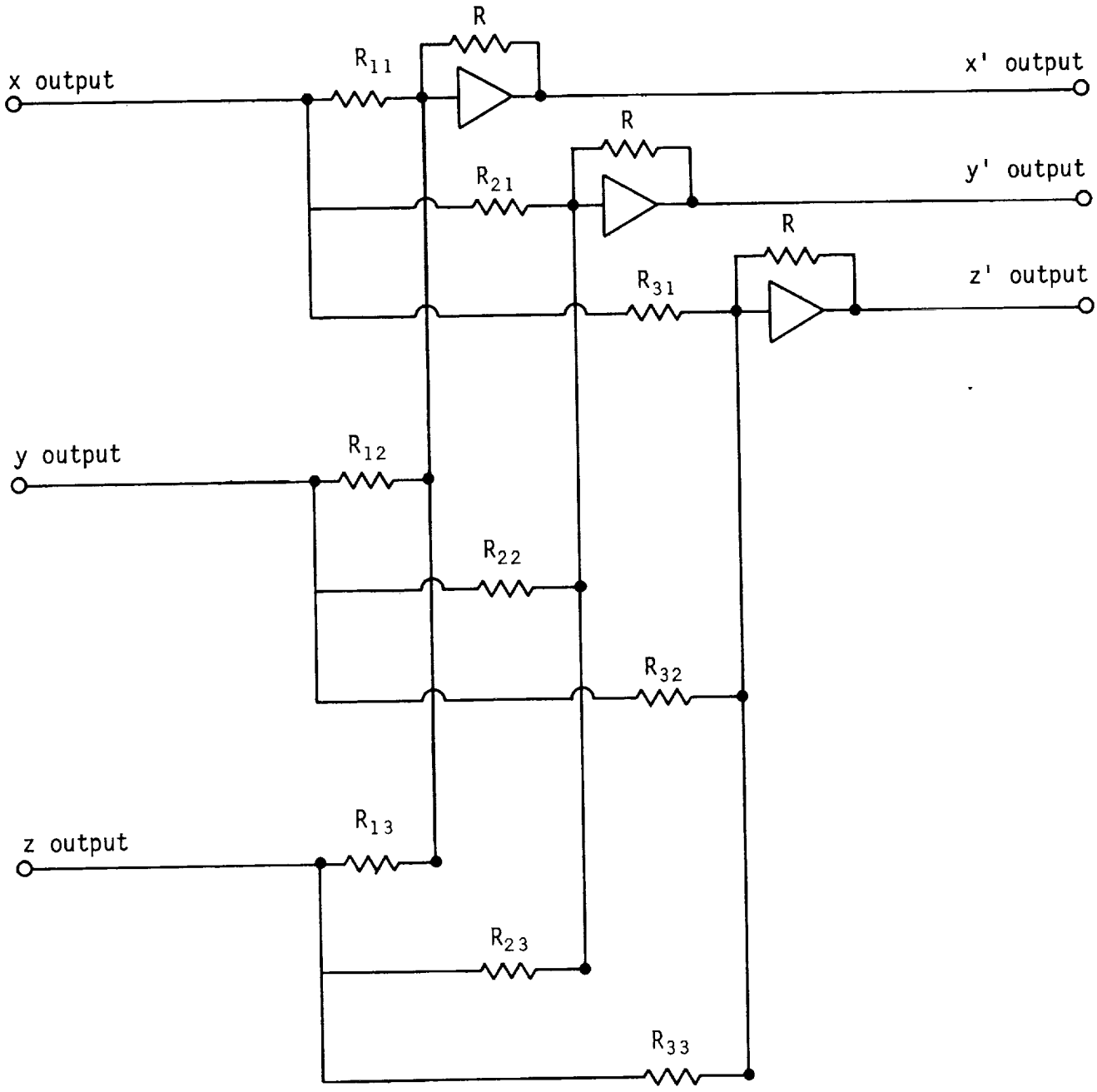

FIGURE 21
COORDINATE TRANSFORMATION SYSTEM

unit in the price range from $13 to $20 each.

The coil system is nearing completion with the lateral (y and z) sensing coils completed, and the excitation and x sensing coils in the process of being wound. It is expected that a working breadboard model of the complete system will be completed within the next three months. A reasonable estimate for completion of the final system would be the end of the summer.

G. AERODYNAMICS AND MODELS

A quantitative analysis of various body shapes typical of those to be tested resulted in the following observations:

1. To restrain the center of a magnetic sphere embedded in a simple shape (e.g. a sphere or cone) a drag force capability of approximately 25 to 50 times the weight of the magnetic sphere (g's) is necessary.

2. To restrain the center of the magnetic sphere embedded in a typical missile or reentry shape, a lateral force capability on the order of 5 to 10 "g's" per degree total angle of attack is necessary. It should be noted that steady state angles of about three degrees are desirable for data resolution (both steady and transient data).

3. Frequencies of model oscillation will be and/or can be made high (above 10 cps); and due to uncertainties in model aerodynamics (e.g. the location of center of the aerodynamic pressure) frequencies below 10 cps will be difficult to achieve reliably.

It appears that the required balance force - frequency combination necessary to hold a magnetic sphere embedded in the model fixed in the tunnel will require extremely large and fast force capacity and will be

extremely costly. An alternative approach would be to allow the model to oscillate at a frequency which is large compared with the balance response frequency (i.e. design the balance to have a low frequency response, say, 10 cps). This will have the effect of eliminating the balance response to rapid lateral oscillatory motions, hence the above mentioned large lateral forces can exist without the balance compensating for them. There are two requirements in order to achieve satisfactory operation under these conditions. These are:

1. That the lateral displacement associated with a free-free oscillating model are sufficiently small - about one centimeter or less. The balance will not compensate for the lateral forces in this ~~move~~ mode and the magnetic sphere will be free to ~~mode~~ move in the lateral plane. It will be necessary to keep the model within a reasonable distance from the centerline for data resolution.
2. That the lateral forces at frequencies within the range of the balance are sufficiently small. That is, the forces associated with frequencies below 10 cps be within the capability of the balance restoring force.

A later subsection gives the details for satisfying condition one, and it is clear that for a large class of models the motion can be contained to a sphere of one centimeter or less. Another subsection gives an analysis of the mechanisms for low frequency lateral forces, and it can be concluded that a lateral force capability of two "g's", with a frequency response of about 10 cps is sufficient to compensate for low frequency disturbances.

Summarizing these results we can say that if the balance is designed so that it is capable of responding to low frequency disturbances (up to 10 cps) with a 2 "g" or higher capability; and if the model oscillates freely, within limits - at a frequency greater than 10 cps - then the magnetic sphere will remain within a suitable distance (less than 1 cm.)

of the release point. This will enable investigation of model aerodynamics at relatively large angle of attack, since the balance will not have to compensate for the high frequency, large lateral forces. The phrase Quasi-6 degree of motion mode is used to describe this mode of motion, where the word Quasi is used to indicate that the model is free in translation at frequencies higher than some given (balance response) frequency. For data at small angles of attack, sufficient care can be taken in model design to enable the balance to "hold" the magnetic sphere fixed, if desired, although the data can be gotten equally well operating the balance in the Quasi-6 mode.

The model should be designed so that shock waves reflecting off the walls of the tunnel do not interact with the model, a requirement which limits the length (or size) of the model. This can be accomplished by designing the leading edge of the model to have an appropriate angle. The variables determining the largest allowable leading edge angle, β, are:

1. body radius at trailing edge of model, r_o, inches
2. body length, ℓ_t, inches
3. maximum angle of attack, α
4. maximum displacement, X, inches

Figure 22 can be used to obtain the maximum leading shock angle allowed as a function of the appropriate variables (where the prototype tunnel size, 6", and operating conditions, M = 3, have been assumed). With the maximum acceptable angle gotten from this figure one can obtain the necessary leading edge geometry. As an example, figure 23 gives the cone half angle which produces the desired shock angle. Any cone half angle less than that obtained from Figure 23 can be used to obtain a flow pattern in which the model will be free from shock reflections. A similar figure can be generated for nose shapes other than a cone.

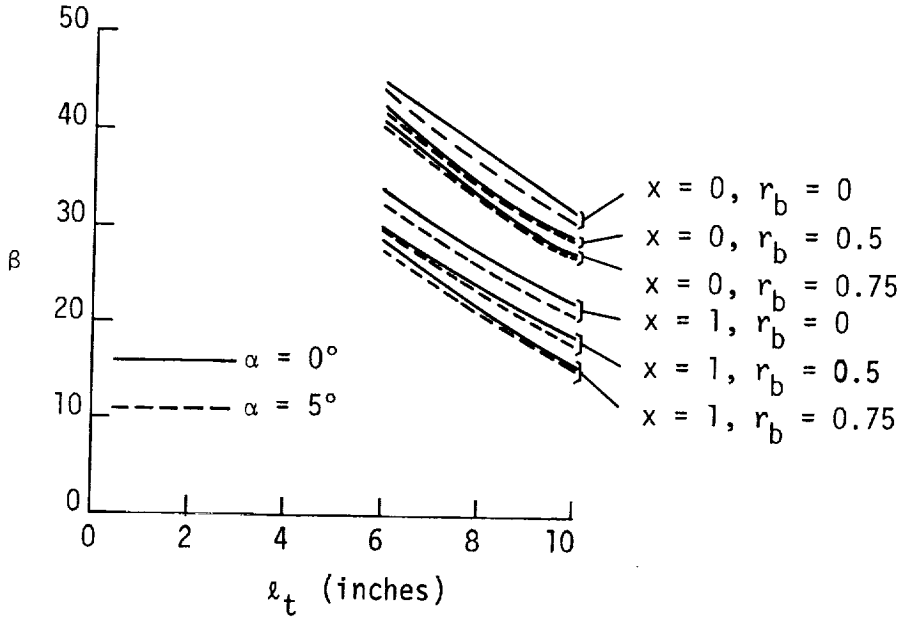

FIGURE 22

MAXIMUM SHOCK ANGLE TO OBTAIN NO INTERFERENCE

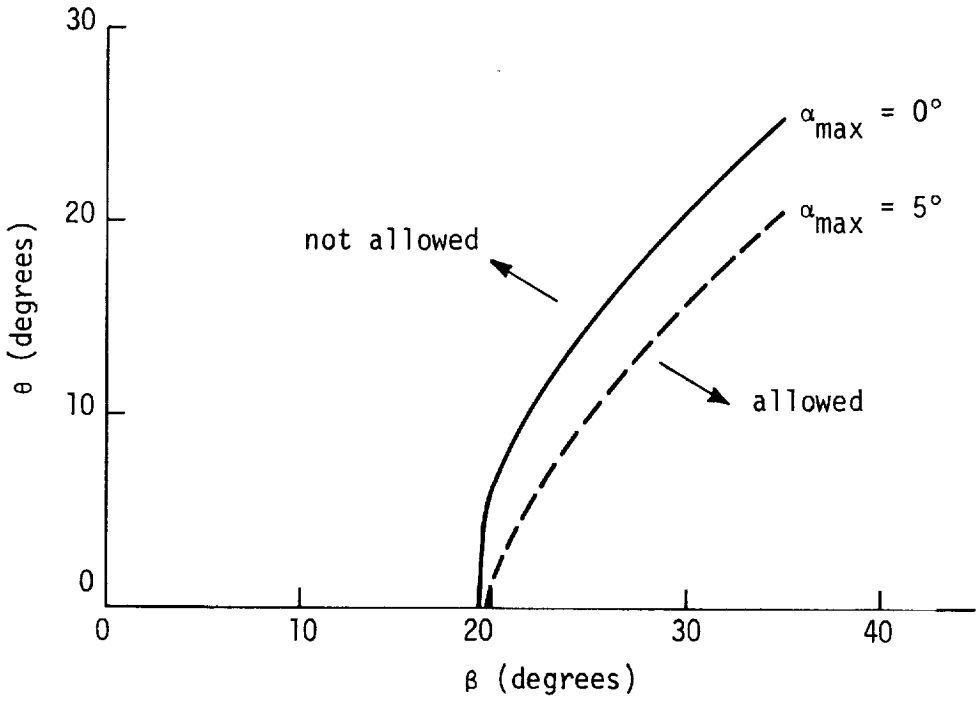

FIGURE 23
MAXIMUM ALLOWABLE CONE HALF ANGLE

1. Models

The following is a proposed model sequence with pertinent data for each model. Conditions corresponding to the prototype design (M = 3, P_o = 3 atmos.) are assumed.

a. Model No. 1 (Homogeneous Sphere)

Although in general the use of a magnetic sphere made of ferrite is anticipated it should be noted that the measurable quantities for a sphere are limited to position and drag and for this reason an iron sphere appears more desirable. The iron sphere is capable of producing a larger force and hence gives a more favorable maximum allowable drag force to sphere weight ratio.

The following calculations indicate the range of sphere sizes allowable.

Sphere weight = $\frac{4}{3}\pi r^3 \rho_{sph}$ where ρ_{sph} is the sphere weight density, gm wt/cm^3

r is the sphere radius, cm.

Drag = $C_D\, q\pi r^2$ where C_D is the drag coefficient

q is the dynamic pressure, gm wt/cm^2

πr^2 is the reference area, in^2

For a Mach number of 3.0 and stagnation pressure of 3 atmospheres.

Drag = $1600r^2$ gm wts.

and the sphere weight is given by

Wt = $4.18\, \rho_{sph} r^3$.

The ratio of the drag to the sphere weight is

$$\frac{\text{Drag}}{\text{Wt}} = \frac{383}{\rho_{sph} r}$$

Figure 24 gives this ratio versus sphere diameter for ferrite and iron spheres. As noted above the iron sphere gives a larger allowable range of sphere sizes.

Summarizing, a ferrite sphere with a diameter of 3 centimeters or larger can be successfully supported; and an iron sphere with a diameter of 1.5 centimeters or larger can be successfully supported.

b. Model No. 2 (Cone)

A fifteen degree total included angle cone is proposed for the second model. A scale model sketch is shown in Figure 25 showing the major components of the cone. The nose is made of bismuth in order to keep the total center of gravity ahead of the center of pressure of the model. The materials to be used are indicated on Figure 25. The following is the pertinent data for this model.

Total Included Angle	15°
Total Weight	0.3 lbs.
Sphere Weight	0.048 lbs.
Center of Gravity	3.15 inches from the nose tip.
Lateral Moment of Inertia	.40 lb-in^2
Center of Pressure	4.0 inches from nose tip
Lateral Force	10 "g"/degree angle of attack
Natural Aerodynamic Frequency	26 cps
Zero-Lift Drag	2.2 lbs

With these numbers a zero angle of attack drag to sphere weight ratio of 46 is obtained. Since the model is suspended in the tunnel so as to have its weight acting in a direction opposing the drag the balance must be capable of compensating for a drag to weight ratio of 39.6. At a maximum angle of attack of 3 degrees this increases to approximately 41.5, well within the balance capability.

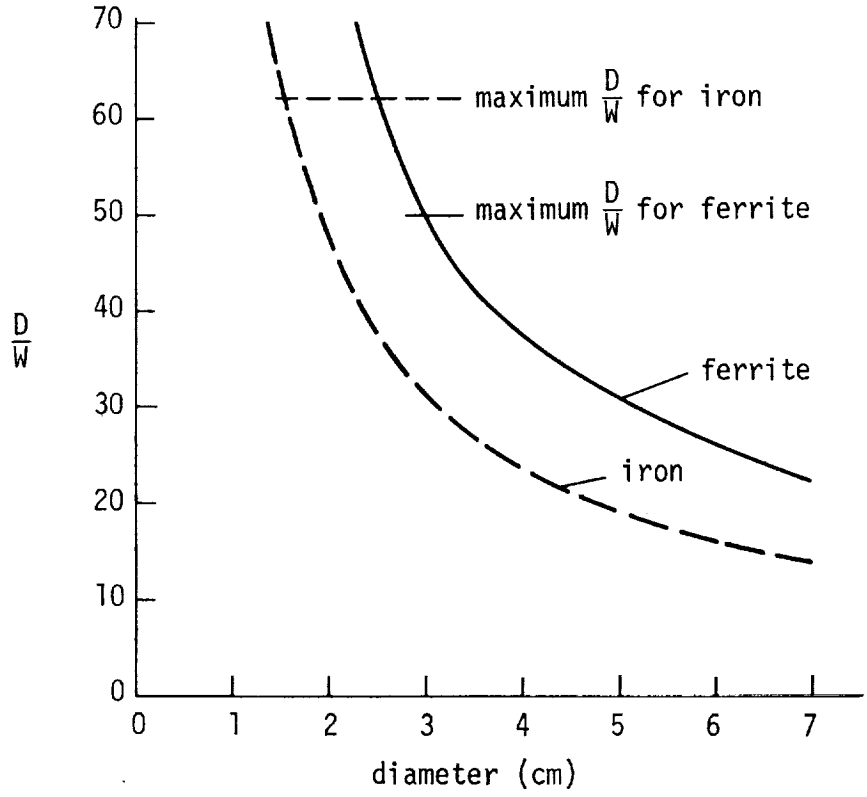

FIGURE 24
DRAG TO WEIGHT RATIO VS. DIAMETER

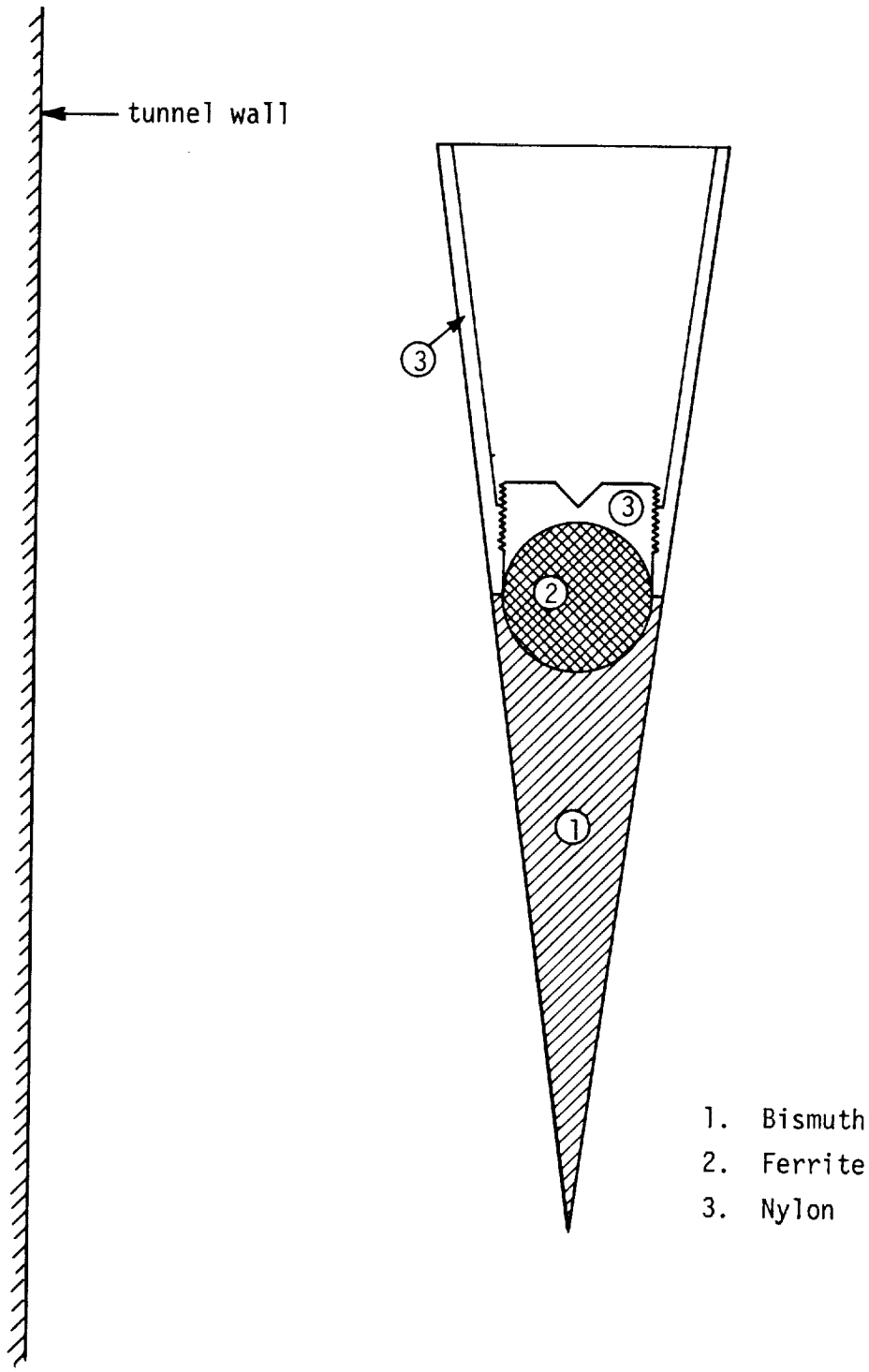

FIGURE 25
15-DEGREE CONE MODEL, FULL SCALE

Since the oscillatory frequency is large compared with the balance frequency the cone will be in the Quasi-6 mode. The maximum displacement from the tunnel centerline is .055 inches/degree. For a three degree maximum angle of attack this results in a displacement of .165 inches or .42 centimeters.

2. Lateral Displacement in the Quasi-6 Mode

Consider the model to be oscillating at a steady state oscillatory frequency and to be free of any tunnel start up or release impulse effects. Also consider the model to be held rigid in the longitudinal direction (drag). Assume the motion to be in a plane (two dimensional) thus reducing the problem to two degrees of freedom - one translational and one rotational. A schematic diagram of the system is shown in Figure 26. In the absence of balance forces (gradient coils) the body is free to oscillate about the center of mass of the sphere and translate in the plane of the paper at the acrodynamic frequency. Since the rotational motion is sinusoidal in the steady state one can concentrate on the translational equation. For a constant mass system, which the model is, Newton's law gives

$$ma = m\ddot{y} = \Sigma F_y$$

where:

m is the mass of the model

$\ddot{y}$ is the acceleration of the center of mass

F_y are the forces in the y direction.

The sum of the forces in the y direction is given by

$$F_y = F_{y_\alpha}\alpha + F_{y_q} q + F_{y_{\dot{\alpha}}}\dot{\alpha}$$

where:

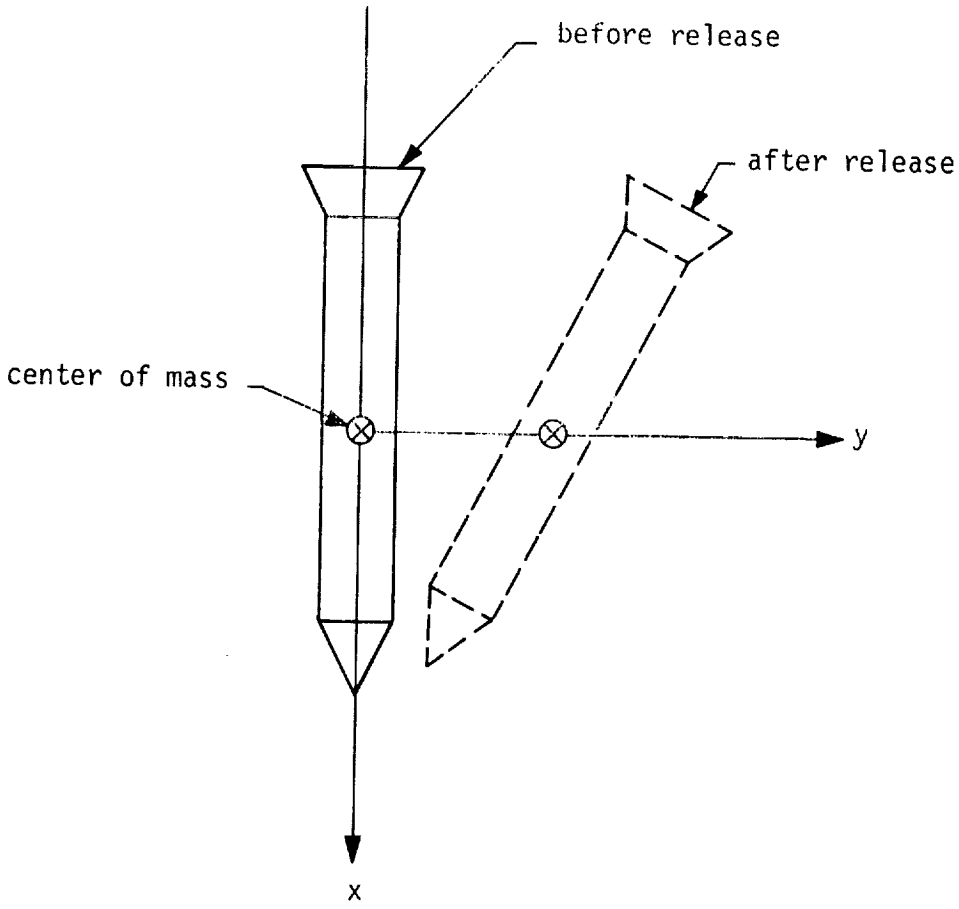

FIGURE 26
CONFIGURATION FOR LATERAL DISPLACEMENT

α is the angle of attack

$F_{y_{\dot{\alpha}}}$ is the force derivative due to flow lag

$F_{y_{\dot{q}}}$ is the force derivative due to pitching velocity q.

We can then write

$$m\ddot{y} = F_{y_\alpha}\,\alpha + F_{y_q}\,q + F_{y_{\dot{\alpha}}}\,\dot{\alpha}.$$

To simplify the problem further a conservative approach can be taken; that is, damping may be neglected. Setting $F_{y_q} = F_{y_{\dot{\alpha}}} = 0$ gives

$$m\ddot{y} = F_{y_\alpha}\,\alpha.$$

The angle of attack oscillates at a frequency ω_n (aerodynamic natural frequency) which is approximated by

$$\omega_n^2 = -\frac{M_{z_\alpha}}{I_z}$$

where:

M_{z_α} is the aerodynamic pitching moment derivative

I_z is the moment of inertia of the model about the z axis.

The sinusoidal oscillation can be written as

$$\alpha = \alpha_{max}\cos(\omega_n t)$$

where α_{max} is the maximum angle of attack and is given by (as shown in a three-dimensional analysis):

$$\alpha_{max} = \frac{M_o}{M_{z_\alpha}}$$

M_o being the net overturning moment about the center of moments.

This gives

$$\ddot{y} = K_1 \cos(\omega_n t)$$

where

$$K_1 = \frac{F_{y_\alpha}{}_{\alpha\ max}}{M_{z_\alpha}{}_{m}}$$

Over small angles of attack ($\alpha < 10°$) we can assume F_{y_α} and M_{z_α} to be essentially constants and the quotient equal to the distance between the center of pressure and the center of mass of the model, $(x_{cp} - x_{cm})$.

Integrating we get

$$v(t) = \dot{y} = \int \ddot{y} dt = \frac{K_1}{\omega_n} \sin(\omega_n t) + K_2$$

and

$$d(t) = \iint \ddot{y} dt dt = \frac{-K_1}{\omega_n^2} \cos(\omega_n t) + \frac{K_1}{\omega_n^2} .$$

The maximum high frequency displacement is

$$d_{max} = \frac{K_1}{\omega_n^2} .$$

Recalling that

$$\omega_n^2 = \frac{-M_{z_\alpha}}{I_z}$$

we can write

$$d_{max} = \frac{{}_{\alpha}{}_{max} I_z}{m(x_{cp} - x_{cm})} .$$

For the class of models to be tested some nominal values for the quantities appearing in the above equation are:

α_{max} = .052 radians = 3 degrees

I_z = .7 gm wt-cm-sec^2

m = .1 gm wt-sec^2/cm

$(x_{cp} - x_{cm})$ = 1 cm.

With these numbers we get a d_{max} = .36 cm. It can be concluded from this that the maximum displacement can be kept within 1 cm of the centerline.

3. Mechanisms for Lateral Forces

There are many mechanisms which result in lateral forces and hence, lateral displacements. The purpose here is to outline the causes of lateral forces and investigate their effect on the lateral displacement of the model; keeping in mind that the operation of the balance can be made to disregard oscillations at frequencies higher than some predetermined value - in this case about 10 cps. The mechanisms to be considered are:

a. Aerodynamics (both symmetric and assymmetric)
b. Model geometry (principal axis shift)
c. Magnetic forces
d. Flow angularity
e. Flow unsteadiness
f. Disturbances upstream of the model.

1) Aerodynamics, Model Geometry and Magnetic Forces

A linearized, three dimensional analysis of a (nearly) axially symmetrical, aerodynamically and inertially, body leads to an equation of the form [18]

$$\ddot{\vec{\alpha}} + \vec{N}_1 \dot{\vec{\alpha}} + \vec{N}_2 \vec{\alpha} = N_3 e^{ipt} + \vec{N}_4$$

where

$\vec{\alpha} = \beta + i\alpha$, the complex angle of attack

p is the roll rate

$N_1 \ldots N_4$ are complex functions of the parameters of the problem.

The general solution is

$$\vec{\alpha} = \vec{k}_1 e^{s_1 t} + \vec{k}_2 e^{s_2 t} + \vec{k}_3 e^{ipt} + \vec{k}_4$$

where

$\vec{k}_1$, $\vec{k}_2$ are the nutation and precession arms of the complex angle of attack, $\vec{\alpha}$, and rotate at approximately the aerodynamic natural frequency of the model

$\vec{k}_3$ represents the portion of the angle of attack due to body fixed forces and moments and rotates at the roll rate of the model

$\vec{k}_4$ represents a constant contribution to the complex angle of attack due to constant external forces and moments.

For the Quasi-6 mode the arms of the total angle of attack due to nutation and precession are rotating at a rate which is fast compared with the balance response and can be neglected. The other two arms however, do contribute to the lateral force. The spin arm, $\vec{k}_3$, rotates at the roll rate of the model; which may or may not be large compared with the balance response frequency. The trim arm, $\vec{k}_4$, does not rotate and is therefore a fixed quantity. Simplifying the expressions obtained in the solution for

the complex angle of attack, it can be shown that the spin arm is approximately

$$|\vec{k}_3| = \left| \frac{p^2}{p^2 - \omega_n^2} \Delta \right|$$

where:

p is the model roll rate

ω_n is the aerodynamic natural frequency, and

Δ is the angle between the (aerodynamic) symmetry axis and the (inertial) principal axis.

For $p = \omega_n$ we get the familiar pitch-roll resonance phenomenon; that is, the angle of attack becomes infinite (no damping has been assumed). For the case where $p \neq \omega_n$ the magnitude of the spin arm is a function of the magnitude of the principal axis shift. A conservative estimate for Δ is approximately one-tenth of a degree. For this value we obtain the following values of $|\vec{k}_3|$ (Figure 27) as a function of the ratio of model roll rate to the aerodynamic natural frequency.

The lateral force will be given by:

$$F = C_{N_\alpha} qS |\vec{k}_3|$$

where:

C_{N_α} is the slope of the normal force coefficient

q is the dynamic pressure

S is the reference area on which C_{N_α} is based.

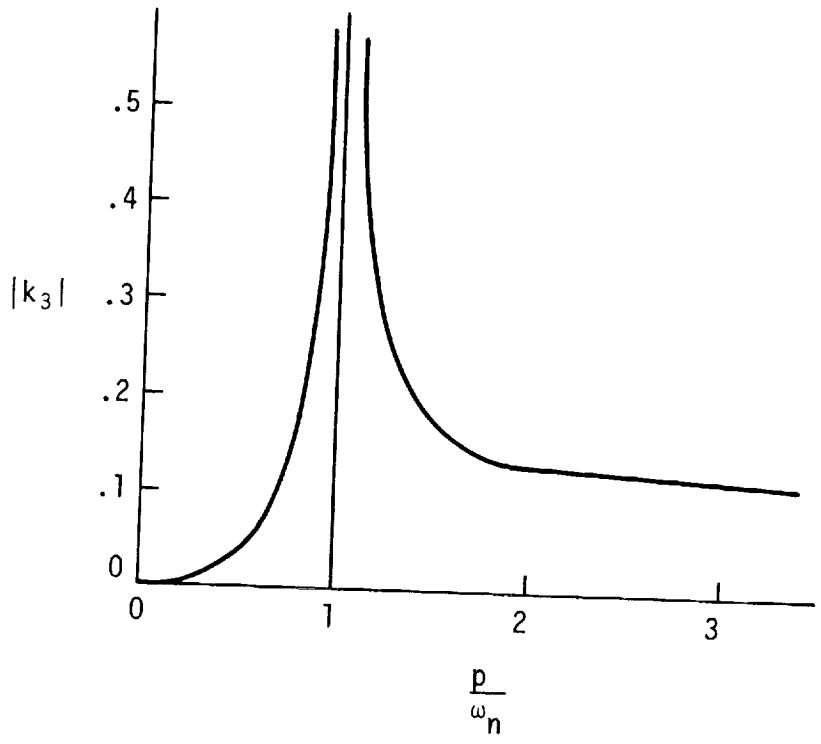

FIGURE 27
ROLLING TRIM ANGLE

Substituting values into this equation for a typical model results in a lateral force to sphere weight ratio of

$$\frac{F}{W_{sph}} = 10|\vec{k}_3| \text{"g's"}$$

where $|\vec{k}_3|$ is in degrees. From the figure above it is seen that for a 1.5 "g's" maximum lateral force the model roll rate to aerodynamic natural frequency ratio is given by:

$$\frac{p}{\omega_n} \leq 0.8 \quad \text{or} \quad \frac{p}{\omega_n} \geq 1.65$$

This means that if the roll rate of the model is kept outside the above limits the lateral force generated will be less than 1.5 "g's". In particular for the case in which the roll rate is less than the balance response time the limits on the ratio given above will ensure a lateral force of less than 1.5 "g's". For the case where the roll rate is large compared with the balance response frequency this condition may be neglected. The neglect of damping makes these estimates conservative.

The trim arm, $\vec{k}_4$, can be approximated by

$$|\vec{k}_4| = \frac{M_B}{M_{z_\alpha}}$$

where:

M_B is the net constant external moment acting on the body, and
M_{z_α} is the aerodynamic restoring moment.

For typical models M_{z_α} is approximately 3 foot-pounds per radian. Without some special and probably difficult to contrive arrangement, one cannot conceive an appreciable constant external moment (neither proportional to

α nor rotating with the body) acting on the model. Thus there should be little or no constant lateral force due to this term.

2) Flow Angularity

Flow angularity gives rise to a lateral force due to the fact that the flow is not necessarily parallel to the geometric tunnel axis. This results in a force due to a component of drag in the lateral direction as shown in Figure 28.

This lateral force is given by

$F = D\sin\alpha$.

A conservative estimate of flow angularity is about one degree and for typical models the drag is on the order of 25 "g's". This results in a lateral force of approximately 0.45 "g".

3) Flow Unsteadiness and Disturbances Upstream of the Model

It is felt that the contributions to lateral force due to disturbances upstream of the model and flow unsteadiness are negligibly small and can be controlled by judicious tunnel design.

4) Summary

When one sums all of the pertinent lateral forces (those occurring at a frequency lower than the balance response) one finds that the lateral force can be kept less than or equal to 2.0 "g's". This is the force that the balance must be capable of compensating for since it is only this part of the total lateral force that is within the balance response frequency.

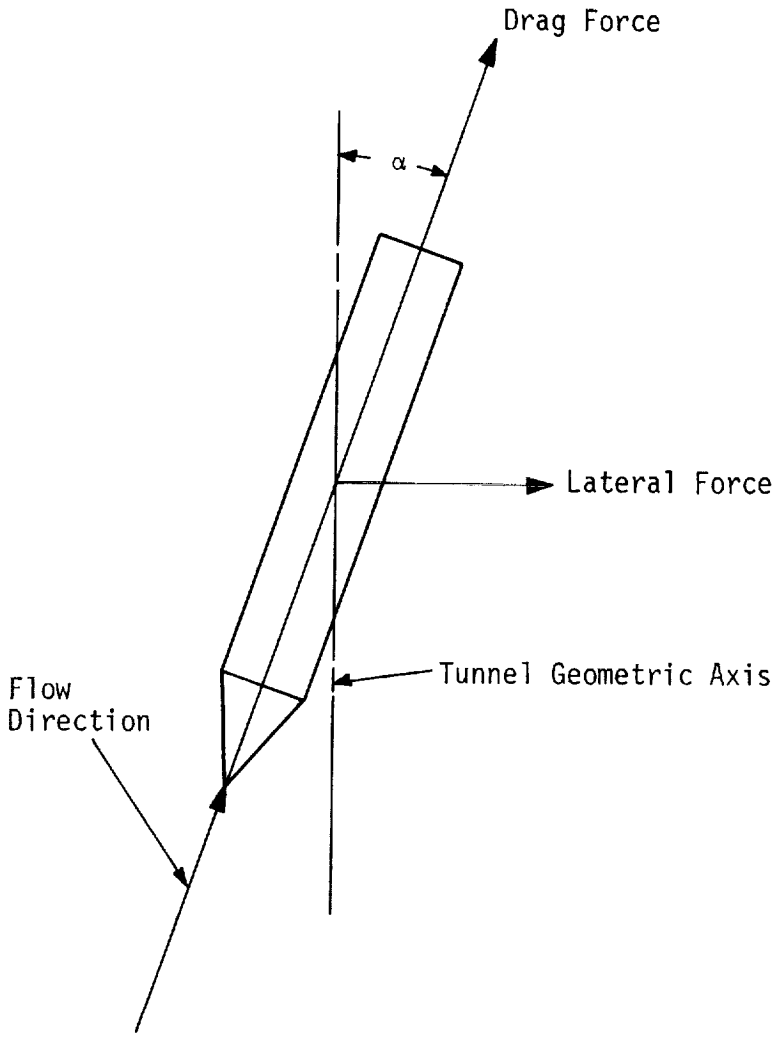

FIGURE 28
FLOW ANGULARITY

H. AERODYNAMIC DATA ACQUISITION

As indicated earlier, the decision has been made to de-emphasize the effort to achieve precision in the aerodynamic data acquisition system for the prototype phase. The primary reason for this decision was that a near optimum precision method for the prototype is likely to be different from that for a large tunnel and thus the objective of scalableness is little served. Among the other factors involved in the decision were: simple spread of effort, information and experience on which to base a precision system design, a better appreciation of precision needed, and the thought that something quite less than ultimate precision is required to demonstrate the feasibility of this approach to dynamic stability. It is still expected that aerodynamic data of sufficient accuracy will be obtained so that, for example, one can successfully study the data reduction problem. Moreover, as summarized in a later section, precision data systems have been studied theoretically, and a relatively low level effort in this area will continue.

The aerodynamic data required in the general case, corresponding to inverting the equations of motion for the aerodynamic forces and moments, are three translational positions, three angular positions, the first and second time derivatives of these six variables, and the balance forces and moments acting on the model. In principle, and in practice with at most some relatively simple calibration procedures, the balance forces and moments acting on the model may be derived from the currents in the coils of the balance system. These quantities are easily outputted and recorded. This section will summarize the present thoughts and plans concerning model motion data acquisition.

1. Aero Data from Balance Sensor.

A modified MIT position sensor system to provide error signals for the balance has been chosen, is currently under construction, and tests on it will begin shortly. The translational position of the model (and

derivatives) is required for the balance control system, also is part of the aerodynamic data, and will be appropriately outputted for this purpose. A to-be-tested modification corresponds to choosing an appropriate passive detector element in the model, e.g. a properly oriented shorted current loop, such that a suitable combination of the basic signals is proportional to the model pitch and yaw angles. If the bench tests give the expected results it will most probably be included in the system especially since this modification is more a matter of arrangement detail than hardware change. Such a shorted loop, with its axes parallel to the model symmetry axis will give rise to an eddy current damping moment as the angle between the loop axis and the main magnetic field changes. Since both the damping moment and the sensor signal vary inversely as the electrical resistance of the loop, the question of how massive the loop must practically be is important and will be tested. Theoretical estimates are encouraging. Anticipating the use of a (saturated) ferrite sphere, the basic sensor requires some modification to allow eddy current induction and thus is confronted with the damping moment aspect. For example, a thin conducting film on the ferrite sphere surface would produce the translation position signals and damping yet due to spherical symmetry give no angle data. Thus it seems reasonable to use a configuration which supplies the most information for the same penalty.

2. Separate Pitch and Yaw Angle Sensor

Should it appear that the technique described in the above paragraph is significantly inferior to some simple scheme at measuring pitch and yaw angles, then such a simple scheme will most probably be implemented. "Simple" here might mean intercepted light beam systems, the geometry of which is tailored to the particular model, using differential intensity measurement to produce angle data. Such a simple system suffers considerable sensitivity and/or accuracy degradation due to (especially

lateral) translation of the model, though it is probably possible to choose beam geometries so that this penalty is reduced to a reasonable level. In any event, a simple light beam system is currently a likely prospect for a possible separate pitch and yaw angle sensing system, and probably will be used unless the MIT sensor proves outstandingly effective.

3. Roll Rate Data

Several schemes have been considered to measure the model roll rate, corresponding to the third orientation angle. Among these are 1) an rf method similar to the MIT sensor but with the exciting field perpendicular to the tunnel axis, 2) simple pulse counting from illuminated longitudinal lines on the model, and 3) high speed photography laterally or from downstream. It is anticipated that the roll rate will be moderate in value and reasonably constant for many of the early models and is not likely to be an especially crucial part of the aerodynamic data. Thus it will be quite likely that simplicity will be the dominant criterion in the choice, not yet actually made, of the initial roll rate sensor.

I. SCALING CONSIDERATIONS

It is of considerable interest, in view of the philosophy of the cold balance prototype project, to review the current state of the art with respect to scaling the system to larger tunnel and balance sizes. Some of these considerations are quite firm and have been reported earlier. Other important aspects cannot be confidently scaled at the present time. The following list of items or aspects generally proceeds from those more certain to those less certain in scalableness.

1. Balance Coil Configuration

For non-ferromagnetic cored coils of given normal conductors at constant temperature and constant current density, one can show quite

exactly that on scaling by the factor ℓ (all linear dimensions multiplied by the factor ℓ):

$$\left.\begin{array}{l} B \sim \ell \\ \nabla B \text{ is invariant} \end{array}\right\} \text{at any point in space}$$

Coil mass, I^2R, coil volume $\sim \ell^3$

Heat leakage thru dewar $\sim \ell^2$

Note: When the required ∇B changes with ℓ, the scaling laws are more complicated since a gradient coil geometrical efficiency factor becomes involved due to changes in the relative coil geometry for a near optimum design. Since the geometrical efficiency factors for superconductor coils are usually nearly maximum, this (favorable) effect will be neglected.

2. Forces on the Model

For a sphere of given magnetic material with B large enough to saturate it, the balance forces go as*

$$F_{bal} \sim (\text{Vol.})\,(\nabla B)_{g.c.} \sim \ell^3 \nabla B_{g.c.} \quad \text{(g.c. gradient coil)}$$

Neglecting the variations in aerodynamic force coefficients (with M and Re), scaling results in

$$F_{aero} \sim C_f q S \sim \ell^2 q; \; q = \frac{1}{2}\rho V^2$$

and the ratio of the balance forces to aerodynamic forces goes as

$$\frac{F_{bal}}{F_{aero}} \sim \frac{\ell^3 \nabla B}{\ell^2 q} \sim \frac{\ell \nabla B}{q} .$$

*Here and in what follows the subscript g.c. refers to gradient coil, thus $B_{g.c.}$ refers to B due to a gradient coil pair.

Postulating that the ratio of balance forces to aerodynamic forces remains constant on scaling, and making a choice of how q should scale, shows how the required ∇B scales. Two rather extreme cases are considered; corresponding to assuming that the Reynolds number based on the model dimension (at constant tunnel velocity) remain constant or is directly proportional to ℓ:

A) $Re_{mod} \sim$ Constant $\rightarrow \rho \sim \frac{1}{\ell}$; $q \sim \frac{1}{\ell}$

$$\frac{F_{bal}}{F_{aero}} \sim \ell^2 \nabla B; \quad \nabla B \sim \frac{1}{\ell^2}$$

B) $Re_{mod} \sim \ell$: $\rho \sim$ constant; $q \sim$ constant

$$\frac{F_{bal}}{F_{aero}} \sim \ell \nabla B \quad ; \quad \nabla B \sim \frac{1}{\ell}$$

3. Gradient Coil Magnetic Field Energy

This quantity is, of course, very pertinent to power supply consideration. Since

$$B_{g.c.} \sim \ell \nabla B_{g.c.}$$

one has

$$(F.E.)_{g.c.} \sim \int_{Space} B^2 d(vol) \sim \int \ell^2 (\nabla B)^2 d(vol)$$

and

A) $Re_{mod} \sim$ Constant: $(F.E.)_{g.c.} \sim \int \ell^2 (\frac{1}{\ell^4}) d(vol) \sim \ell$

B) $Re_{mod} \sim \ell$: $(F.E.)_{g.c.} \sim \int \ell^2 (\frac{1}{\ell^2}) d(vol) \sim \ell^3$

4. Aerodynamic Oscillation Frequency

For the simple 2D model of a rotational ~~oscillator~~ oscillator, a fairly good approximation is, neglecting M and Re dependence of aerodynamic moment coefficient:

$$f^2 \sim \frac{\text{Moment of force}}{\text{Moment of inertia}} \sim \frac{qs\ell}{\rho_{mod.} \ell^5} \sim \frac{q}{\ell^2}$$

then

A) $Re_{mod} \sim$ Constant: $q \sim \frac{1}{\ell} \rightarrow f \sim \frac{1}{\ell^{1.5}}$

B) $Re_{mod} \sim \ell$: $q \sim$ Constant $\rightarrow f \sim \frac{1}{\ell}$.

5. Model Translation Characteristic Time.

It is difficult to be precise about the model translation problem. The basic requirement is easily stated: The model must be retained in the tunnel. From that point on, the consideration quickly became immersed in details such as position sensor range, nature of the disturbances producing translation, dead time and rise time of the closed control loop, etc., many of which are uncertain (the probable disturbances on the model are quite uncertain.) Here a very simplified, overall view is taken in order to arrive at some reasonably definite conclusion. The reader might be well advised to refrain from taking the result too literally.

Consider a step input lateral aerodynamic force on a model initially at rest, and ask how far the model moves in time τ. (Whether or not such a case would occur, its magnitude, how it might scale, etc. are quite uncertain.)

Assuming:

$z \sim \ell$ for an allowable translation

$F_{aero} \sim \ell^2$ for the step input force

one gets:

$$z = 1/2 \left(\frac{F_{aero}}{m}\right)\tau^2$$

$$\tau = \sqrt{\frac{2mz}{F_{aero}}} \sim \left(\frac{\ell^3 \ell}{\ell^2}\right)^{1/2} \sim \ell$$

If one associates a frequency $\frac{1}{\tau}$ with the time τ, the result is that the frequency scales $\frac{1}{\ell}$.

Such simple consideration leads one to expect that, to perhaps a zeroth approximation an overall characteristic balance response time, τ, required to retain the model in the tunnel, scales as ℓ.

As an illustration of a somewhat more realistic model of the translation problem, the following case is considered. Suppose that at $t = 0$, a model initially at rest is subjected to a step input lateral acceleration a, that at $t = \tau_d$ (the dead time) the acceleration decreases linearly to -a at $t = \tau_d + \Delta t$ ($\Delta\tau$ is a rise time for the closed loop balance), and that the acceleration remains at -a until $t = 2\tau_d + \Delta\tau$. The acceleration, velocity, and displacement profiles are shown schemetically in Figure 29.

Straightforward integration yields

$$d_{max} = a(\Delta\tau)^2\left\{\frac{1}{6} + \frac{\tau_d}{\Delta\tau} + \left(\frac{\tau_d}{\Delta\tau}\right)^2\right\} .$$

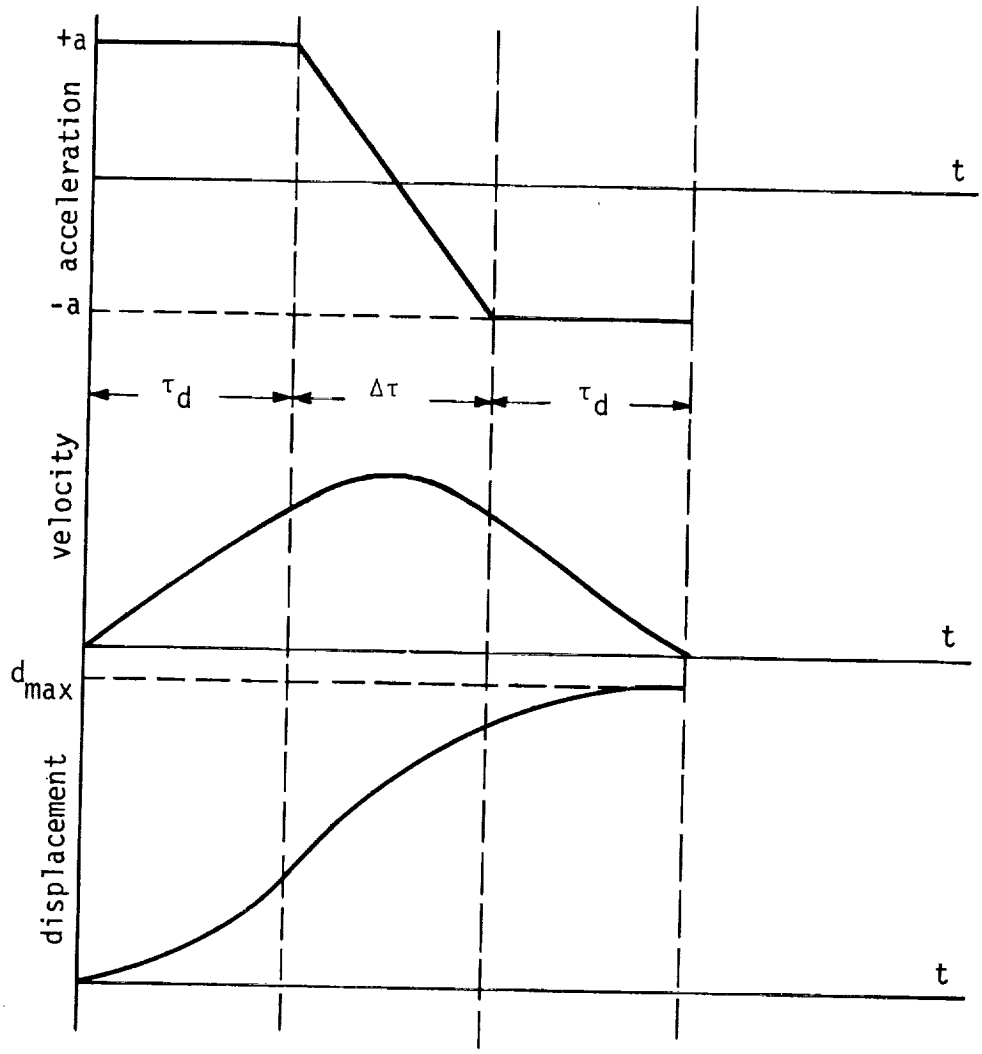

FIGURE 29
ASSUMED ACCELERATION, VELOCITY AND DISPLACEMENT PROFILES

Thus we have a model of a balance with a dead time of τ_d, a rise time of $\Delta\tau$, and a step lateral disturbance (presumably aerodynamic in origin) acceleration of the model. To see how the scaling goes, it seems reasonable to assume that d_{max} scales as ℓ, and that a scales as $1/\ell$. Then one may ask how $\Delta\tau$ must go with ℓ if, given a $\sim 1/\ell$, d_{max} does go as ℓ. Using subscripts 0 and ℓ to indicate the original and scaled cases, one has

$$(d_{max})_\ell = a_\ell (\Delta\tau_\ell)^2 \{\frac{1}{6} + \frac{\tau_d}{\Delta\tau_\ell} + (\frac{\tau_d}{\Delta\tau_\ell})^2\}$$

$$(d_{max})_o = a_o (\Delta\tau_o)^2 \{\frac{1}{6} + \frac{\tau_d}{\Delta\tau_o} + (\frac{\tau_d}{\Delta\tau_o})^2\}$$

Taking the ratio

$$\ell = \frac{1}{\ell} \frac{(\Delta\tau_\ell)^2}{(\Delta\tau_o)^2} \frac{\{\frac{1}{6} + \frac{\tau_d}{\Delta\tau_\ell} + (\frac{\tau_d}{\Delta\tau_\ell})^2\}}{\{\frac{1}{6} + \frac{\tau_d}{\Delta\tau_o} + (\frac{\tau_d}{\Delta\tau_o})^2\}}$$

and rearranging

$$x^2 + 6yx - \ell^2\{1 + 6y\} - (\ell^2 - 1)6y^2 = 0$$

where

$$X = \frac{\Delta\tau_\ell}{\Delta\tau_o} \quad \text{and} \quad y = \frac{\tau_d}{\Delta\tau_o}$$

and it has been assumed that the dead time (dependent on the AC power frequency) does not change on scaling. The appropriate solution for $(\ell - 1) \geq 0$, since $x = 1$ when $\ell = 1$, is

$$X = \{3y^2 + \ell^2(1 + 6y + 6y^2)\}^{1/2} - 3y$$

If $y = 0$ (i.e. $\tau_d = 0$) then $x = \ell$ or $\Delta\tau_\ell = \ell\Delta\tau_o$. For y very small one has

$$X = \ell + 3y(\ell - 1) \quad , \quad y << 1$$

and at large y, no simple approximation has been found. Table III lists some typical values

TABLE III

$Y = \frac{\tau_d}{\tau_o}$	ℓ	$x = \frac{\Delta\tau_\ell}{\Delta\tau_o}$
.5	4	$7.92 = (4)^{1.49}$
1	4	$11.5 = (4)^{1.76}$
2	4	$18.6 = (4)^{2.11}$
4	4	$32.5 = (4)^{2.51}$
.5	8	$17.3 = (8)^{1.37}$
1	8	$25.9 = (8)^{1.56}$
2	8	$41.8 = (8)^{1.79}$
4	8	$76.3 = (8)^{2.08}$

It is apparent that $\Delta\tau_\ell$ depends on τ_d, $\Delta\tau_o$, and ℓ in a reasonably complicated way. Nevertheless, it is clear that rise time or frequency response is an important and expensive parameter for the high power inductive systems of concern here.

6. Gradient Coil Power

Considering a characteristic time $\tau = \frac{1}{f}$, a measure of the gradient coil power is

$$P_{g.c.} \sim \frac{(F.E.)_{g.c.}}{\tau} \sim f(F.E.)_{g.c.}$$

A) $Re_{mod} \sim$ constant: $P_{g.c.} \sim \frac{\ell}{\ell^{1.5}} \sim \frac{1}{\sqrt{\ell}}$

B) $Re_{mod} \sim \ell$: $P_{g.c.} \sim \frac{\ell^3}{\ell} \sim \ell^2$

Since the required gradient coil power is an important consideration in the total system it is interesting and important that this parameter depends so sensitively on the manner in which the Reynolds number scales. A repeat of the above manipulations leaving Re_{mod} as a variable, results in

$$P_{g.c.} \sim \frac{(Re_{mod})^{2.5}}{\ell^{0.5}}$$

which shows the strong dependence of the gradient coil power on Re_{mod}.

A comparison of the operating conditions in the wind tunnel to be used with the cold balance prototype with some other installations [19] is shown in Table IV. The comparison shows that the Reynolds Number per foot typical for the prototype system is approximately at the upper end of the range for these typical four foot supersonic tunnels. Thus one may conclude that the above case B), i.e. $Re_{mod} \sim \ell$ (or constant Reynolds number per foot) is a probable worst case.

The scaling considerations outlined above are felt to be quite reliable first order relationship. Of course, should the extropolation to a larger size not be a simple scaling (multiplication of all linear dimensions by ℓ) additional considerations are involved.

TABLE IV

Facility	Mach No.	Po(psia)	q(psf)	$Re/_{ft}$
Langley Unitary Test Sec. 1	1.47 2.86	4 to 30 4 to 50.9	250 - 1860 110 - 1400	$(1.0 - 7.8) \times 10^6$ $(1.56-7.1) \times 10^6$
Langley Unitary Test Sec. 2	2.29 4.63	4 - 29.4 15 - 142	170 - 1260 95 - 905	$(.76 - 5.6) \times 10^6$ $(.82 - 7.8) \times 10^6$
Langley 4' x 4'	1.25-2.6	4 to 30	250 - 1368	$(1.4 - 6.6) \times 10^6$
UVA prototype to Langley Unitary	1.5 -2.85	15 - 65	~1120 - 4000	2×10^7
UVA Cold Balance Tunnel	3	45	1100	7×10^6

7. The Prototype from the Scaling Point of View

An inherent characteristic of the magnetic balance is that the conditions to be established by the balance to effect support of the model are, over a very wide range, independent of the model size. Specifically, a given balance will support (balance the weight) of a 1 cm magnetic sphere with the same currents in the balance coils as required to support a 1 mm magnetic sphere, provided only that both diameters are small with respect to a characteristic balance dimension. This fact is embodied in the statement that the balance force on the sphere is proportional to the product of the sphere volume, its magnetization (magnetic moment per unit volume), and the magnetic field gradient produced by the balance. This fact is the justification for taking the ratio of the balance force to the sphere weight as a performance parameter for the balance. Since the aerodynamic forces, in first approximation, are proportional to a projected area of the model and model weight on simple scaling goes as the volume, it is

obvious that the balance forces required to balance the aerodynamic forces varies with model size.

For example, consider the simple cases of the 1 cm and a 0.1 cm sphere in a given tunnel-balance system (same q, sphere magnetization). Then to a first approximation (same C_D) the gradient coils must have currents to balance the 0.1 cm sphere drag 10 times as large as those required to balance the 1.0 sphere drag. The effect is to try for maximum model size, for a given tunnel size, in order to minimize the balance gradient requirement. To put it in another way, in view of the fact that gradient coil current densities are limited, smaller model sizes in a given tunnel require relatively larger (filling more space) gradient coils which produce gradient at the support position less and less efficiently.

The same sort of considerations hold on scaling the tunnel and balance to larger size. Since the aerodynamic forces scale approximately as the square of the scale (fixed relative model size now), the balance forces need only go as ℓ^2, and the gradients need only go as $\frac{1}{\ell}$, then the relative gradient coil size decreases and become more efficient. Thus, the basic balance design problem for a given performance becomes easier and simpler. Of course, the coil weight, power, etc. increase with an increase in size but at a rate less than that one might guess on first thought.

Such considerations as these, together with other considerations such as aerodynamic frequency range, easily available A.C. power frequency, etc., result in the definite conclusion that a near optimum balance system design is a more difficult problem at the prototype size (6") than it is at, say, a 4' or 8' size.

8. Cost and Complexity of Gradient Coil Power Supplies

The gradient coil power supplies represent, especially in the larger sizes, a significant fraction of the total investment for a cold magnetic balance system. Unfortunately, the scaling problem for this item is

complicated - so much so that it appears impossible to make a reliable and significant statement concerning it. As indicated in the above items, one could for a given extrapolation arrive rather reliably at a peak power rating. From there on, the problem becomes quite involved. In particular one gets involved in:

a. Whether or not energy storage is necessary, and if so, methods.
b. Basic power frequency and possible changes
c. Dead or waiting time interactions (apparently it is clear that the SCR method is most suitable in the larger sizes, so that triggering time delays are indicated). Appreciable triggering delays effectively make the scaling problem nonlinear.
d. Peripheral problems, such as the desirability of maintaining balance high frequency response in the small amplitude, linear mode.

About the only thing which becomes clear is that after an accumulation of experience with the cold balance it will be most appropriate to do a detailed study of the gradient coil power supply scaling problem.

SECTION IV
SHORT RANGE PLANS

From the material presented in the previous sections it should be apparent that the concept of a prototype cold balance developed by the University of Virginia group represents advanced technology along several fronts. Therefore it should not be surprising that a recent thorough reassessment of objectives and accomplishments clearly pointed to the need of additional time and financial support for the successful completion of the intended task. To that effect, a formal request for extension of the present grant has been made [20]. The plans outlined below have been drawn under the assumption that this request will be granted.

After considerable analysis and discussion of the prototype balance desirable properties and capabilities in relation to the overall objectives of this project, the design of nearly all major components is frozen at this point and most of the effort from now until the end of the grant period will be directed towards the physical realization of this design. In this sense, short range plans are definitely hardware oriented for the most part. This doesn't mean that a longer range perspective will be abandoned or that interesting fine points will be overlooked for the sake of expedience. It rather means that it is recognized that the task of assembling and testing a complex and novel apparatus should be expected to be an absorbing and time consuming undertaking. The timetable that follows should be considered a guideline to expected progress rather than a rigid work schedule. Only those items that represent a major responsibility of one of the senior members of the research group have been included.

Beginning of Summer 1968: - Aerodynamic facility assembled and ready for calibration
- Liquid helium dewar finished and ready for shipment to Atomics International

Position sensing device at the breadboard stage

- Current leads finished
- Overall facility under construction
- Detailed design of control circuit underway.

End of Summer 1968:

- Aerodynamic facility fully calibrated
- Position sensing device fully checked and calibrated
- Overall facility ready for assembly of balance components
- Dewar and coils installed. Fitting of cryogenic components underway
- Start assembly of control circuit.

Beginning of 1969:

- Power supplies for d.c. coils have been installed and tested
- Power supplies for a.c. (gradient) coils are in and are installed and checked
- Control circuit essentially finished
- First generation aerodynamic models.

Beginning of Summer 1969:

- Complete system ready to be tested, first the electromagnetic balance alone; then the balance and the wind tunnel together.

End of Summer 1969:

- Complete system tested as a unit. Enough data should be available to show feasibility of concept and ability of extrapolation to larger systems.

SECTION V
LONG RANGE PLANS AND PROSPECTS

This section is concerned with longer range plans and possibilities ranging from items which undoubtedly will receive attention in the prototype phase to those which lie in the quite distant future. The latter category is, of course, contingent upon certain conditions and requirements and in some instances must remain for the present speculative. Generally, however, the contingencies correspond to an adequate success in the prototype phase and a continuation of magnetic balance related efforts.

1. Specifically Superconductor Problems

The reader is aware that the detailed operating characteristics of a superconducting coil magnetic balance system are not known; and cannot be confidently extrapolated from currently existing information. Many of these, certainly those amenable to study and of importance to the balance operation, are certain to be investigated (essentially) as soon as the balance becomes operable. For example, the following areas certainly are pertinent:

a. Losses (heat production) due to unsteady (AC) current operation and how they depend on the important parameters. A limitation is that the coil configuration and detailed properties will be fixed. Nevertheless, it may be possible to predict with greater confidence how the losses would go with relatively minor coil modification. In any event, it will be important to establish a firm base of loss characteristics.

b. It will be important to determine the extent of mutual interaction loss effects. For example, the main field coil operating by itself with a steady current should exhibit no losses, but

the unsteady current mode of the nearby gradient coils may induce losses in the main field coil. If significant, this interaction must be evaluated. Several such interactions may be present. It is easy to design tests for these effects.

c. It is possible that shielding effects can cause significant changes in the magnitude of and/or phase delays in the gradients produced at the support point by currents in a gradient coil pair. Thought such effects would be unimportant if sufficiently small, they ought to be evaluated (especially since such an evaluation appears to be easy.)

No other specific superconductor problem areas have been anticipated. It is worthwhile to note that the system design is reasonably conservative. For example, the system should operate even if the gradient coils never have a superconductive current contribution. This statement cannot be made about the drag augmentation and main field coils, since these coils have less copper stabilization.

2. Power Supply Scaling Study

The gradient coil power supply system is an important component in the overall system, both from the point of view of operating characteristics and system cost. As indicated in an earlier section, the problem of scaling the gradient power supply to a larger system size is quite involved. Not only are there many balance parameters, some of them currently uncertain, but the problem also depends on the manufacturing or industrial state of the art. For example, minimum specifications for force magnitude and frequency response are reasonably uncertain.

When the prototype phase will have provided some operating experience, hopefully eliminating some of the uncertainties in the power supply specifications, it certainly seems appropriate to make a thorough investigation of the power supply scaling problem. The only questions would seem to be precisely when it should begin and what the magnitude of the job will be.

3. Magnetic Support Element - Materials and Shape Possibilities

A considerable total amount of thought, dispersed over the entire grant period, has been devoted to ideas, schemes, facts about, etc., related to the shape of the magnetic element embedded in the model and the magnetic material of which it is made. The important effects may be listed as follows:

a. To a good first approximation the force on the model due to a given gradient produced by a gradient coil pair is directly proportional to the product of the volume of the magnetic element and its magnetization i.e. its total magnetic dipole moment. This is true as long as the linear dimension of the element is small compared to, say the tunnel diameter and its shape does not depart drastically from spherical. Only moderate changes can be made in the volume of the element, assuming that one always uses models as large as feasible for the given tunnel. The magnetization of the element is proportional to the main magnetic field at low fields and saturates to a constant value at sufficiently large main fields. The saturated magnetization, M_s, of a material depends on the material, ranging from about 20 kilogauss for iron to essentially zero for non-magnetic materials. The prototype design is based on the use of a ferrite which an M_s of about 600 gauss. A large M_s is obviously desirable. It is also interesting that saturation is approached as the main field increases at a rate which depends on the shape of the element - a prolate ellipsoid saturates, parallel to the long axis, faster than a sphere.

b. A general shape magnetic element at a fixed general orientation experiences a moment or torque about on axis perpendicular to the (uniform) main field. Consider an ellipsoid of revolution (a shape sufficiently general for the present discussion). If the symmetry axis is at an angle $\theta < 90°$ with the main field direction, a torque which tends to reduce θ acts on the ellipsoid. This shape anisotropy exists for an ideal magnetic material which has no dissipation, i.e. the shape anisotropy

torque is conservative. At small angles the torque is proportional to the angle and to the eccentricity of the ellipsoid and is independent of any angular velocity.

c. If the magnetic element, of any shape, is rotating about an axis which is not parallel to the main field, two kinds of torques act due to the motion. First, if the element is electrically conducting, eddy currents are induced in it and give rise to a torque on the element. One component of the eddy current torque tends to reduce the angular velocity (dissipative component) and one component tends to precess the spin axis to be parallel to the main field (a non-dissipative component.) The eddy current torque is proportional to the angular velocity, the square of the main field, the angle (at small angles) between the spin axis and the main field, and the electrical conductivity of the magnetic element.

Second, for real magnetic materials, the rotational hysteresis is non-zero, and has a wide ~~large~~ range of values for different materials. Rotational hysteresis results from a dissipation of energy in the material due to a change in the direction (without change in magnitude) of the magnetization, and the rotational hysteresis torque tends to reduce the angular velocity and has no conservative (non-dissipative) component. The rotational hysteresis usually is fairly sensitive to magnetization, passing through a maximum below saturation and decreases to a constant, residual value at large fields.

From these "magnetic facts" it is possible to proceed to a consideration of the advantages and penalties to be derived in departures from the initial simple concept of a perfect sphere of perfect magnetic material in the two areas of real material choices and non-spherical shapes. In the area of materials, two rather extreme cases have been given considerable thought. First, the ferrite materials appear to be a realistic approximation to the perfect case. They, as a class, have very high electrical resistance, so that eddy current torques are virtually non-existant.

Further, as a class, they exhibit relatively low values, in the saturated state, of rotational hysteresis. The penalty for this performance is that their saturated magnetization is not large. One of the oldest commercially available ferrites, Feroxcube, has an $M_s \sim 600$ gauss, close to the largest ferrite M_s. This is the material on which the prototype design was based.

The Second, often considered material, iron, probably is near the other extreme in the material choice. The saturated magnetization is the largest of any material. In the (nearly) pure state it is an electrical conductor, though as a conductor not a very good one. The rotational hysteresis of iron is probably larger than that for any other material. From the point of view of support alone, iron is the most efficient choice. It is of interest to note that the prototype, with a main field of ~ 5000 gauss, would not fully exploit the support efficiency of iron, giving only a factor of 2 in magnetization over the saturated (M_s = 600 gauss) ferrite. If the tunnel balance system were large enough, and iron would serve the total purpose, an optimum balance design would likely have a main field in the 40-60 k gauss range and the iron magnetization in the 10-15 k gauss range, requiring gradients in the range of 1/16 to 1/24 of that required for a ferrite sphere. However in that case, while the rotational hysteresis might be close to its residual saturated value, and perhaps not intolerably large, the eddy current torques for pure homogeneous iron might well be intolerable.

All of this points to the significant aspects of the magnetic element material problem. It is obviously desirable to obtain large magnetization and small torques. Three statements may be made:

1) The tolerable level of dissipative (damping) torques must be established, so that appropriate trading off of support advantage and damping torque penalty may be made. Estimates have been made which indicate that iron may be acceptable with respect to damping, but actual operation, data reduction, etc. is needed to qualify the effect on information extraction.

2) A thorough investigation of special physical form or iron and/or iron composites is needed. For example, sintered iron or powdered iron in a non-conducting matrix suggests itself.

3) A thorough investigation of other ferromagnetic materials, e.g. the garnets, together with actual tests ought to be made.

The general effect of other-than-spherical shapes for the magnetic element is quite straightforward, and basically corresponds to arranging a balance induced torque on the element (model) for some special purpose. As indicated above a prolate ellipsoid of revolution will experience a conservative (spring-like) torque tending to keep its symmetry axis parallel to the main field. A general ellipsoid would tend to line up with its long axis parallel to the main field and experience different rotational springs in perpendicular directions. In the limit, a circular disc would rotate freely about one lateral axis (the symmetry axis of the disc) and experience a large restoring torque about an axis in the plane of the disc and perpendicular to the main field.

Such conservative, shape anisotropy torques induced by the balance have no especially significant disadvantages. They add to the usually well known (or easily measured) static aerodynamic moment to produce the total or effective model static moment and would make no direct contribution to the total dynamic moments. Examples of how shape anisotropy torques could be utilized are as follows:

1) For a given model configuration it may be difficult to arrange that it is aerodynamically stable, or sufficiently aerodynamically stable, about its center of mass without a severe penalty in support capacity (relative size of magnetic sphere). A prolate ellipsoid of revolution, instead of the sphere, could provide the additional stability with no penalty in support capacity. One can

imagine that a configuration quite unstable aerodynamically could be made stable in this fashion.

2) Very analogous to 1) the use of prolate ellipsoids of various excentricities allows considerable adjustment of the basic (aerodynamic) oscillation frequency.

3) The use of a prolate ellipsoid combined with an adjustable main field might allow the examination of a portion of a roll-pitch resonance response curve in a simple fashion in a single run.

4) A prolate ellipsoid, with its symmetry axis inclined to the model symmetry axis would induce an angle of attack of the model.

5) It is conceivable that the use of a general ellipsoid, giving different oscillation frequencies, in perpendicular lateral planes could contribute significantly to extracting certain kinds of information. Indeed, the question of how well some certain degrees of freedom may be suppressed is an interesting one.

This list most probably does not exhaust the possibilities. It certainly is to be expected that efforts in the area of materials and shapes will begin as soon as feasible after the prototype is operational. Further, it does not seem overly optimistic to expect significant results from these efforts.

4. Precision Aerodynamics Data Acquisition

It has been indicated that the prototype program will not include a near optimum precision aerodynamic ~~Aerodynamic~~ data acquisition subsystem. The present thought is that a serious effort in this area is simply deferred to a post prototype phase when, hopefully, the prototype will remain at University of

Virginia as a research (and perhaps further development) tool. Nevertheless, considerable theoretical thought and effort have been devoted to the problem, one of the results being that one basic method of data extraction has been analyzed reasonably thoroughly. Since the present report is already rather lengthy and since a precision system is not to be included in the prototype phase, the decision has been made to include here only a brief summary of this analysis and to submit a detailed separate report on it at a later time.

a. Lined Model Data Extraction

The basic principles of the method is as follows. Assume that the model in the tunnel is rolling at a moderate (nonzero) rate, has a section near its center which is cylindrical or near cylindrical, is executing periodic three dimensional translation, and is executing periodic rotational oscillations about two other lateral axis. This is the general kind of (Quasi-6 degree of freedom) motion typical models are expected to experience. Imagine that an appropriate number of fine longitudinal lines, capable of being sensed by optical systems looking laterally at the model, are scribed on the center section. If the lines were generally equally spaced but with a small fraction of them displaced somewhat in the same direction around the model, the direction of rolling of the model about its symmetry axis could be deduced by the method described.

Analytically, coordinate systems are defined as follows. $O'x'y'z'$ is a tunnel fixed reference frame with $O'x'$ parallel and opposite to the tunnel wind direction. $Oxyz$ is a body fixed reference frame with Ox parallel to the model symmetry axis. (The analysis may utilize an aero ballistic or non-rolling frame instead of the body fixed frame if desired.) Convenient motion variables are three components of the position of O with respect to O' (the translation variables may be referred to $O'x'y'z'$ or $Oxyz$) and three ordered orientation angles of $Oxyz$ with respect to $O'x'y'z'$. The standard

transformations from the moving to fixed frames or vice versa are available, and straightforward even if tedious.

The crux of the method involves mathematical statements corresponding to the intersection of a "looking line" fixed in the tunnel frame and a line scribed on the model. Physically a looking line corresponds to an optical system looking along that line and producing a train of pulses upon seeing successive lines on the model. An appropriate number of well chosen looking lines, and the associated trains of pulses, permits the evaluation of the three orientation angles and their time derivatives from appropriate time intervals in single pulse trains and between pulse trains, given model parameters and the model translational position and velocity. The expressions are so complicated that computer reduction should be used. For the same reason a quantitative error analysis is quite involved and actually has not yet been done.

Nevertheless, some qualitative conclusions may be reached by inspection of the results. First, it is apparent that the presence of model translation velocities tends to reduce the accuracy obtainable for the orientation variables and their derivatives. The translation effect may be reducible by suitable axial location of the (lateral) looking lines, but the translation accuracy degradation likely will remain a significant effect. Second, some of the required time interval data, corresponding to pulse intervals from the same model line from lateral, parallel but axially displaced looking lines, can be quite small. Thus the pulse resolution and synchronization between trains must be quite good, with the result that the entire system would likely be not inexpensive. Perhaps the most pleasing feature of the method is that angular velocity information is directly calculated from the data, thus requiring only one differentation to furnish the motion input to the equations of motion. However, only an adequate error analysis can demonstrate that the apparent advantage is real.

Casual thought has been given to other precision data acquisition methods. Doppler laser methods have been suggested, seem to offer

possibilities (also with the direct angular velocity feature), and seem to be better suited to larger installations. Surely in a possible larger facility methods based on systems internal to the model (e.g. inertial systems) would be seriously considered. In any event, operational experience with the prototype will improve the base from which a precision system can be designed for the prototype complex.

5. The Post Prototype Era at University of Virginia

It is the current hope and expectation that the cold balance prototype program will demonstrate the basic feasibility of the system and its associated approach to aerodynamics, and will show with considerable confidence that scaling to larger tunnels is practical and even efficient in terms of benefits to be obtained. Specifically, the University of Virginia group is optimistic to the point of expecting NASA to embark, within a reasonable time after the end of the prototype program, on the design and construction of a significantly larger balance-tunnel complex. The University of Virginia group hopes and expects that NASA, pursuant to its policy of cooperation with and aid to the academic community, will leave the prototype system with University of Virginia as a stimulant to research and student training in an area vital to NASA's interest.

Already considerable thought, ranging from generalities to specific problems, has been given to what can be done with a balance-tunnel system of the kind the prototype is expected to be. The really unique features of the University of Virginia magnetic balance approach to aerodynamics are:

a. No physical model support ~~(no string)~~ (no sting)

b. Free ~~translateral~~ translational motion above a certain frequency—the Quasi-6 degree of freedom mode.

c. Free rotational motion, subject only to balance induced conservative and non-conservative moments related to the shape and material of the magnetic support element embedded in model.

d. Basic idea of observed or measured model motion and balance forces and moments giving, via. the equations of motion, information on the aerodynamic forces and moments (analogous in principle to the gun range and free flight techniques.)

Item a. is common to any magnetic balance system for a tunnel (e.g. the MIT system). The other three items are specific to the University of Virginia system; indeed, the most undesirable aspect of the University of Virginia approach is that it is difficult, if not impossible, to suppress particular degrees of freedom. It has been remarked that the University of Virginia approach provides the closest thing to free flight ever attainable in a wind tunnel.

It is easy to name the general areas in which the prototype should prove to be a useful tool: dynamic to virtually static wake studies (both near and far, due to non-physical support) and unsteady aerodynamics (ranging from measurement of specific dynamic stability derivatives to fundamental studies of unsteady flow phenomena). The tool is so new and unexploited that undoubtedly many potential uses have not yet surfaced. The remainder of this subsection will be devoted to the listing with brief comments a few particular problems which seem to be especially appropriate.

1) With a missile configuration model in a Quasi-6 mode - with both roll and aerodynamic frequencies larger than the balance response frequency - a quite good simulation of a rolling, pitching, translating missile is given. If the roll rate to aerodynamic frequency ratio can be varied, it would be possible to investigate the phenomenon of roll-pitch resonance. At the very least, model modification (e.g. center of mass location) could be made to change this ratio, probably requiring separate runs, to obtain successive points on the response curve. Even more interesting is the possibility of changing the roll pitch ratio during a single run so that a part, at least, of the response curve could

be measured. One possibility to effect this is to use a prolate ellipsoid instead of a sphere and adjust the magnitude (slowly) of the main magnetic field, which ~~charges~~ changes the total restoring moment and thus the model pitching frequency. A realistic, laboratory investigation of the roll-pitch resonance phenomenon would be quite unique, very probably giving considerabel quantitative insight into the nonlinearities involved.

2) Undisturbed wakes of models would be available for study in a magnetic balance-tunnel system. To the extent that the model can be arranged to be in a non-lifting, non-oscillatory steady state (in principle, a good prospect) zero lift wake can be studied. It is easier to arrange an oscillatory (in rotation and translation) steady state, so that dynamic (model not in a static orientation) wakes are available. Since for a given system, it is difficult to reduce the model size due to the larger force capacity required, the near wakes are more readily available rather than the far wakes. Wake investigations seem to be an important avenue for studying configuration aerodynamics, and therefore the magnetic balance approach appears potent in this area.

3) A classic problem in aerodynamics, but perhaps one of more academic than practical interest, is that of the separation of C_{m_q} and $C_{m_{\dot{\alpha}}}$. The Quasi-6 mode of motion offers at least a chance of separating the two. Since the fundamental aerodynamic mechanisms are different for the two, it would appear that the ability to separate them quantitatively would enable a more fundamental study of the separate phenomena. From a more pedestrian point of view, it is believed that a demonstration that C_{m_q} and $C_{m_{\dot{\alpha}}}$ can be separately measured would constitute an undeniable validation of the University of Virginia approach to dynamic stability.

4) One of the important problems in the aerodynamics of the slender sounding-rocket type configuration is that of the importance of the

magnus (force and especially moment) coefficients and how quickly they go nonlinear with pitch angle. Since the parameters (roll rate, pitch angle, etc.) can be easily adjusted and since information extraction does not depend on linear performance, it appears that a study of magnus effects in this type of configuration is interesting from a fundamental point of view, valuable from a practical point of view, and straightforward to accomplish.

5) One of the current, interesting thoughts is that it is perhaps possible to design experimental situations so that valuable (dynamic stability related) information can be extracted simply and easily, e.g. by means of one or two easily measured parameters such as some frequency. (Indeed, the extreme of this point of view is that for some situations even qualitative observations correspond to valuable information.) It seems likely that a linear regime is a requirement for such simple experiments, which of itself is not drastic since linear aerodynamics is quite traditional even if the offspring of mathematical expediency. Though specific cases cannot be cited, the exploitation of the "simple" experiment idea is likely to receive considerable attention.

The above list is certainly not exhaustive. The University of Virginia group believes that the existence of the prototype system, with operating characteristics approximately as presently envisioned and being a new and unexploited research tool, will enable an important fundamental and applied research program for a long time. Use and experience would undoubtedly give birth to new problems and new approaches to old problems. The prospect is exciting!

REFERENCES

1. H. M. Parker, G. B. Matthews, and A. R. Kuhlthau, "A Prototype Cold Magnetic Wind Tunnel Balance," Research Laboratories for the Engineering Sciences, University of Virginia, Proposal No. AEEP-NASA-235-66U, June 1966.

2. H. M. Parker, "Semi-annual Status Report, NASA Grant NGR-47-005-029, December 1, 1964 to May 31, 1965," Research Laboratories for the Engineering Sciences, University of Virginia, Report No. AST-4030-101-65U, July 1965.

3. H. M. Parker, "Theoretical and Experimental Investigation of a Three-dimensional Magnetic-suspension Balance for Dynamic-stability Research in Wind Tunnels," Research Laboratories for the Engineering Sciences, University of Virginia, Semiannual Status Report No. AST-4030-102-66U, March 1966.

4. H. M. Parker, "Theoretical and Experimental Investigation of a Three-dimensional Magnetic-suspension Balance for Dynamic-stability Research in Wind Tunnels," Research Laboratories for the Engineering Sciences, University of Virginia, Semiannual Status Report No. AST-4030-103-67U, April 1967.

5. H. M. Parker, "Theoretical and Experimental Investigation of a Three-dimensional Magnetic-suspension Balance for Dynamic Stability Research in Wind Tunnels," Research Laboratories for the Engineering Sciences, University of Virginia, Semiannual Status Report No. AST-4030-104-67U, December 1967.

6. W. R. Smythe, Static and Dynamic Electricity, McGraw-Hill, New York (1950), p. 417.

7. H. Brechnu, et. al. in Advances in Cryogenic Engineering, Vol. 11; K. D. Timmerhaus, ed.; Plenum Press, New York (1966), p. 300.

8. R. W. Grover, "Inductance Calculations" (book); D. Van Nostrand Inc., New YOrk, 1946.

9. H. B. Dwight, "Electrical Coils and Conductors: (book); P. 232-271. McGraw-Hill Book Company, New York, 1945.

10. P. Bowles, Hadley, H., Marchbanks, M. J., and Wilking, J. J. "Magnet power supply for the 7GeV proton synchrotron Nimrod: Part I General" Proceedings I.E.E., Vol. 3; p. 561-572, 1963.

11. J. A. Fox, P. Taylor, "Magnet power supply for the 7GeV proton synchrotron Nimrod: Part II. Rotating machines" Proceedings I.E.E., Vol. 3, No. 3; p. 573-590. 1963.

12. _____, "The supply system for the magnet of the proton synchrotron of the Cern on Geneva," The Brown Boveri Review, Vol. 46, No. 6: p. 327-349, 1959.

13. G. L. Gottlieb, An Energy Optimal Control Low for a System With Bounded Time and Control. ASME Paper, 65-WAI-AUT-14.

14. M. Athens, P. L. Falk, Optimal Control, McGraw-Hill Book Co., 1966.

15. L. S. Pontryagin, V. G. Boltyansbii, R. V. Gambre Lidze, E. F. Mischenko, The Mathematical Theory of Optimal Processes, Inter Science Publishers, 1962.

16. Interim Technical Report No. 128, Massachusetts Institute of Technology, Cambridge, Massachusetts.

17. F. E. Terman, Radio Engineers' Handbook, McGraw-Hill Book Co., Inc., New York (1943), p. 60.

18. I. D. Jacobson, "Dynamic Stability of Sounding Rockets," Master's Thesis, University of Virginia, 1967.

19. W. T. Schaefer, Jr., Characteristics of Major Active Wind Tunnels at the Langley Research Center. NASA TMX-1130, July 1965.

20. H. M. Parker, "Letter to NASA on Grant NGR-47-005-029 Requesting a) Time Extension, b) Additional Funds, and c) Change in Principal Investigators," Research Laboratories for the Engineering Sciences, University of Virginia, Proposal No. AEEP-NASA-341-68U, March 1968.

APPENDIX A

GENERAL DESIGN REQUIREMENTS FOR
THREE CHANNEL POWER-AMPLIFIER

1. General

1.00 The system may be called a three channel power-amplifier for a wind tunnel electromagnetic sypport system. The electromagnetic support will be used to produce forces along three orthogonal axes to freely suspend an aerodynamic model in a wind tunnel. To do this, three cryogenic coil sets will be used to produce magnetic fields to produce the support forces. Due to the large force capability of the support, the response time required and the size of the tunnel cross section, a large amount of energy is required. Since the coils themselves will have a zero or negligible resistance, due to cryogenic cooling, the energy supplied to the magnetic field can and must be retrieved. The power involved except for losses in the system is purely reactive.

1.01 Three separately controlled (electrically isolated) power-amplifiers to act as current sources to supply three separate loads.

1.02 Each amplifier must have two operating modes.

(a) A linear mode in the desired current range.
(b) A saturated mode, where maximum voltage is applied to the load to change the current in a minimum period of time.

1.03 The power-amplifiers shall be designed, fabricated and installed.

1.04 Plans for any preinstallation construction at our site shall be furnished in time for the construction to be completed.

1.05 Test data, operating instructions, maintenance instructions, and circuit schematics shall be provided with equipment.

1.06 The system is expected to be maintainable and we would anticipate long life of the equipment.

1.07 In all respects not covered by these specifications, the design fabrication and installation shall be in accordance with normal standard practices.

2. Construction

2.01 Hook-up wire shall have the type of insulation and shall be of a size suitable for the circuit current and voltage conditions and the temperature environment. Wire smaller than No. 22 gauge shall not be used. Wire subject to hinged action shall be of the stranded type. Color coding or some other appropriate means shall be used to identify each lead.

2.02 Terminal strips and connectors with at least 10 percent space shall be provided with ready access.

2.03 Components (relays, circuit breakers, etc.) shall not be used as terminals.

2.04 Equipment mounting and fastening bolts shall be readily accessible so that equipment can be easily maintained without the necessity of removing parts and assemblies or the use of special tools.

3. Safety and Hazards

3.01 The design of the equipment shall be such that personnel shall not be exposed to any safety hazards and equipment damage shall not occur during the installation, operation, and maintenance service.

3.02 Safety provisions should be made so that no damage to system or injury to operator will be caused in case of:
1) Short circuit output
2) Open circuit output
3) Input transients

4. Environment

4.01 The amplifier shall operate in a reliable manner in an ambient temperature range of 0 degrees C to 50 degrees C (forced air cooling may be used).

4.02 There shall be no more Radio frequency interference than is consistent with commercially accepted standards.

4.03 The system must operate continuously at maximum current for a ten-minute period, after which a rest period of several hours will occur.

4.04 The acoustic noise of the equipment shall not be objectional and should be in conformance with the environmental requirements of the equipment.

5. Power Input

5.01 A power source for the load will be a 34.5 KV ± 5% power line. The line must be maintained within ± 1/2% under all conditions. The impedance of the three phase line is given on a 10MVA base. Frequency is 60 Hertz.

$$R = 0.592\% \qquad X = 2.94\%$$

5.02 An on-off switch shall be provided for start-up and shut-down of the equipment. This shall include an on-off indicating light.

5.03 Provisions must be made for disconnecting the 34.5 KV line.

5.04 Panel meters shall be provided to read secondary voltages and currents.

6. Control Inputs

6.01 The current output of the amplifier must be proportional to a control voltage of ± 7 volts. The linearity must be at least 1%.

Control Voltage	Current Output
+ 7 Volts	350 Amperes
0 Volts	175 Amperes
- 7 Volts	0 Amperes

6.02 When the ± 7 volt control voltage exceeds its limits, the amplifier must go into a saturated mode.

> + 7 Volts	gives full rectification
< - 7 Volts	gives full inversion

6.03 This control terminal input impedance shall not be less than 1000 ohms.

6.04 The system bandwidth must be better than 100 hertz with a resistive load.

7. Control Outputs

7.01 A control voltage that is proportional to the load current must be made available. (In the approximate range of 0 to 10 volts.) The output impedance shall be not greater than 1000 ohms.

7.02 A control voltage that is proportional to the triggering angle of the power SCR's must be made availab.e (In the approximate range of 0 to 10 volts)

7.03 Six synchronizing outputs, with pulses occurring simultaneously with the power SCR trigger pulses,shall be made available.

7.04 All control outputs shall be easily accessible and marked accordingly.

8. Load Current Output

8.01 The load is inductance of not more than approximately 8.0 millihenries. The resistance of the lead coil will be negligible due to cryogenic cooling. The system as installed must take lead resistances into consideration.

8.02 The output current must be variable between 0 and 350 amperes with a nominal operating point of 175 amperes. Note that, due to the nature of the load, only enough voltage to make up the internal and lead losses of the system is needed when the current remains unchanged.

8.03 The system must be capable of changing the load current from 0 to 350 amperes or from 350 to 0 amperes in a period not exceeding 16×10^{-3} seconds. There shall be no delay when the current is at its maximum or minimum values. The system must be capable of going from 0 to 350 amperes and back again in 32×10^{-3} seconds.

8.04 Current ripple must be limited to within 5% of the nominal (175 amperes) current.

8.05 The value of output voltage shall not exceed approximately 600 volts. This value is somewhat flexible and may be changed through consultation with us.

Note: The calculations were made under the following conditions using the relation:

$$V = L \frac{di}{dt}$$

(1) Assume a 6 phase SCR star with output voltage being changed by varying the triggering angle of the SCR's.

(2) The worst case starts with maximum current and voltage and desires to reduce the current to zero just after an SCR is turned on.

This is an explanation note and it is not meant to specify a method of synthesis.

8.06 Panel meters shall be provided on the control panel to indicate the load voltage and current.

DISTRIBUTION LIST

Copy No.	
1-10	National Aeronautics & Space Administration Office of University Affairs, Cody Y Washington, D. C. 20546 Attn: Technical Report Officer
11-12	Mr. Robert A. Kilgore General Dynamics Branch National Aeronautics and Space Administration Langley Station Hampton, Virginia
13-15	H. M. Parker
16	R. A. Lowry
17-18	R. N. Zapata
19-20	G. B. Matthews
21	F. E. Moss
22	R. A. Smoak
23	I. D. Jacobson
24	D. S. Wood
25-26	University Library, Attn: Dr. R. W. Frantz
27-33	RLES Files